TRANSLATION NO. 69-5

PHYSICAL PROPERTIES OF REMOLDED COHESIVE SOILS

(UBER DIE FESTIGKEITSEIGENSCHAFTEN GESTORTER BINDIGER BODEN)

by

Dr. M. Juul Hvorslev

DANMARKS NATURVIDENSKABELIGE SAMFUND
INGENIORVIDENSKABELIGE SKRIFTER A-Nr. 45
Copenhagen 1937

June 1969

U. S. Army Engineer Waterways Experiment Station
CORPS OF ENGINEERS
Vicksburg, Mississippi

TRANSLATION NO. 69-5

PHYSICAL PROPERTIES OF REMOLDED COHESIVE SOILS

(UBER DIE FESTIGKEITSEIGENSCHAFTEN GESTORTER BINDIGER BODEN)

by

Dr. M. Juul Hvorslev

DANMARKS NATURVIDENSKABELIGE SAMFUND
INGENIORVIDENSKABELIGE SKRIFTER A-Nr. 45
Copenhagen 1937

June 1969

U. S. Army Engineer Waterways Experiment Station
CORPS OF ENGINEERS
Vicksburg, Mississippi

ARMY-MRC VICKSBURG, MISS.

PREFACE

This thesis was translated from the German by Mr. Jan C. Van Tienhoven, Research Center, U. S. Army Engineer Waterways Experiment Station.

Translation service for the Corps of Engineers is maintained as a continuing feature of Item 900, "Research Center Operations," of the Corps of Engineers Engineering Studies program.

There have been many inquiries about a possible translation of this thesis in recent years, generated by interest in the early development of soil mechanics and by the many references to and quotations from the thesis in soil mechanics literature. Partial translations have been made from time to time, both in England and the United States; but these translations were for private use and were not publicly available.

The thesis formed the basis for the paper, "Physical Components of the Shear Strength of Saturated Clays," presented at the ASCE Research Conference on Shear Strength of Cohesive Soils, which was held at the University of Colorado in 1960. However, inquiries about translation of the original German version of the thesis have not decreased since publication of the Proceedings of the above-mentioned conference. Certain passages have been clarified in footnotes or by reference to other publications. The original symbols have been retained, which in some cases are different from those currently used; a few definitions of symbols have been modified in accordance with current usage.

CONTENTS

PHYSICAL PROPERTIES OF REMOLDED COHESIVE SOILS

by

Dr. M. Juul Hvorslev

FOREWORD

The economical design of the portion of a structure located above the ground, with observance of the prescribed factor of safety, is based upon accurate knowledge of the strength properties of the building materials used. By the same token, the physical properties of the natural types of soil and their behavior at failure must be known for the design of a structure's foundation and evaluation of the factor of safety. In this respect, our present knowledge of the failure conditions is, among other matters, still incomplete, particularly insofar as undisturbed cohesive soils are concerned. The accurate determination of the failure conditions of such soils is beset with numerous difficulties. These difficulties must be attributed partly to shortcomings in the test procedures and testing equipment, but particularly to the fact that the physical properties of undisturbed soils differ slightly from each other, even in similar soil layers. To this must be added the disturbance of the original soil structure by the sampling operation and by the preparation of test specimens.

It seems expedient that investigations for determining the failure conditions first be made with remolded, thoroughly mixed soil material, which can be produced in a more homogeneous condition in the amounts required than that prevailing in natural, undisturbed soils. For tests with remolded soils, it is possible to make specimens of any desired shape and with any degree of consolidation, and the effects of the various testing methods and devices upon the results are more easily determined. The results of the investigations of remolded soils cannot be applied directly to the undisturbed condition, to be sure; however, knowledge of the results is a prerequisite for the evaluation of test data on undisturbed soils and signifies a step toward the clarification of the physical properties.

Furthermore, the failure conditions obtained for remolded soil material apply to all such practical cases where structures are built in or upon disturbed soils.

However, in many cases it is not the failure conditions that determine the safety of a structure but the settlements produced by a change in stress prior to failure. In some soils these settlements are affected by a slow plastic flow before failure. In other cases it is also necessary to know the possible changes in the physical properties after failure, in addition to the failure conditions. On the basis of observations made at various structures, Terzaghi frequently called attention to the significance of this slow plastic flow before failure and to the temporary or permanent decrease in the shearing resistance after failure, and recommended that these phenomena be taken into account.

Despite the fact that numerous test results concerning the shear and compressive strengths of remolded soils already exist, they cannot be fully explained by the failure conditions previously proposed. Thus far only a few test results have been published relative to the slow, plastic flow phenomena before failure and the change in the shearing resistance after failure. For the most part this must be attributed to the fact that the conventional shear devices are not suited for such investigations because the effective cross section of the specimen and hence the stress condition change during the test.

The aforementioned voids in our knowledge prompted the present study which deals with the following problems:

1. Thorough investigations concerning the shearing resistance of two clayey soils, of very different character, by means of Krey's shear apparatus and Terzaghi's shear boxes, with special consideration of the relationship between cohesion and void ratio.
2. Design of a new shear apparatus (ring shear apparatus) which makes it possible to determine the plastic flow and the change in shearing resistance after failure, and to investigate the effect of cyclic loading.
3. Investigations with the ring shear apparatus.

Since both the principles of the testing equipment and the test procedure have a very pronounced influence on the test results, these effects were thoroughly investigated. Furthermore, various tests were made in addition to the conventional physical soil tests to determine the effect of the structure and of the thixotropic properties of soils.

The tests were carried out in the Laboratory for Soil Mechanics of the Vienna Institute of Technology. Reports of some test results were sent to the International Conference on Soil Mechanics and Foundation Engineering, June 22 to 26, 1936, at Harvard University, Cambridge, Mass. These test results were published as abstracts in the Proceedings of this conference. At the same time the author submitted a more complete report concerning the test results and the conclusions derived therefrom to the Vienna Institute of Technology in the form of a technical doctoral dissertation, and was awarded the degree on the basis thereof. The present publication is based upon this dissertation and was supplemented by the results of tests completed during the spring of 1936.

The author considers it a pleasant duty to thank the Vienna Institute of Technology for the hospitality extended to him and for permission to enter the examination for obtaining the Doctor's degree. He expresses his heartfelt thanks to Professor K. von Terzaghi for the invaluable suggestions received during the lectures and also during personal discussions concerning the research field involved, and further for the extensive assistance rendered in defraying the cost of construction of new testing equipment. Finally, the author also wishes to thank Dr. O. K. Fröhlich, who was a deputy for Professor von Terzaghi at the Vienna Institute of Technology during the 1935-1936 term, for his kindness in facilitating the research, and the assistants in the Laboratory for Soil Mechanics, Engineer K. Kienzl, Dr. H. Borowicka, Dr. F. Schaffernak, Engineer O. Schwarz, and Dr. W. Steinbrenner, for their continual and friendly readiness to be of assistance.

Copenhagen, March 1937

M. Juul Hvorslev

BLANK PAGE

I. PHYSICAL BASES OF THE TESTS

1. Some of the physical properties that distinguish cohesive soils from other building materials have a special significance for the test conditions in shear and compression tests and for the practical evaluation of the test results. Frequently, however, the effect of these properties is but partly taken into consideration. These properties will be discussed briefly below.

Formation and Structure of Cohesive Soils

2. Soils are coarse to colloidal, disperse systems of solid, liquid, and gaseous phases. Cohesive soils are generally understood to be clays and loams, i.e., a predominantly two-phase system consisting of fine mineral grains and water. However, common cohesive soils frequently contain a small amount of air and, in many cases, also organic admixtures in both the undisturbed and in the remolded condition. These admixtures may exert a considerable influence upon the properties of the soil.

In contrast to cohesionless soils, cohesive soils are characterized by their cohesion, plasticity, and slight internal friction. Under certain conditions, fine-grained, moist sands also seem to have a cohesion, but this cohesion is only apparent. It is caused by the surface forces of the water (capillary pressure) or by the pore-water flow. On the other hand, if all external forces including capillary and flow pressures are disregarded, cohesive soils show a certain amount of intrinsic pressure, depending upon the degree of consolidation. This intrinsic pressure produces a shearing resistance independent of external forces, which is called the true cohesion.

3. These properties of cohesive soils originate chiefly from the amount of colloidal, flaky mineral particles with a stratified lattice structure contained in the soil and from the bipolar molecules of the liquid phase, in this case, water (Atterberg (2), Terzaghi (45), Goldschmidt (23) and others). Because of the cations at the surfaces of the lattice structure, these flaky mineral particles have the ability to bind

relatively large amounts of the bipolar water molecules and to arrange these molecules in systematic order. But when the liquid with bipolar molecules is exchanged for another one that has molecules which do not possess a pronounced polarity, the above-mentioned properties of cohesive soils disappear, as shown by Goldschmidt (23). The investigations carried out by various researchers in recent years have led to the conclusion that a certain group of minerals, the so-called clay minerals, are highly capable of binding water. According to Endell and Hoffmann (17, 42), the minerals of the montmorillonite group can also absorb water molecules within the crystal lattice. However, the water bonded to the surface of the crystals is primarily responsible for the special properties of clay. The water-binding capacity of the clay particles depends largely upon the cations at the crystal surface. When the existing cations are exchanged for other ones, the water-binding capacity and hence the properties of the soil also change (Winterkorn (54)).

However, the real nature of this water-binding process and the origin of cohesion are not fully understood at present and are outside the scope of this work. To explain the processes occurring during compression and shear tests, the mechanical concept (Terzaghi (51), Brenner (6)) is, for the time being, sufficient in most cases. According to this concept, the particles, particularly those of the clay minerals, are surrounded by relatively dense water films that show increasing density and viscosity at decreasing distance from the solid material, so that the water molecules close to the solid material eventually possess the properties of a solid matter. When these water films or force fields overlap, an intrinsic pressure develops, the magnitude of which depends upon the extent of the overlapping. The more the particles deviate from the spherical shape and the smaller they are, the greater is the total surface and hence the influence of the water films. The shorter the distance between the particles becomes, the greater is the overlapping of water films and thereby also the intrinsic pressures.

Because of the water films, the small particles are not in direct contact with each other, and since the water molecules are arranged with their axes at right angles to the surfaces of the lattice structure, the

friction becomes less (Terzaghi (50)). Whether the overall shearing resistance decreases or increases with respect to certain external forces depends upon the decrease in friction and upon the magnitude of the resultant intrinsic pressure in proportion to the external forces.

Besides the clay minerals, the type, shape, and grain size of the noncolloidal components obviously also affect the properties of the soil. The elastic deformation is very considerably increased by admixtures of flaky or rodlike mineral components as shown by Terzaghi (50) and Gilboy (22). A very large increase in the water-binding capacity and of the thixotropic changes in strength mentioned later can be produced by small quantities of organic matter, particularly humus.

4. The microstructure of the soil originating from sedimentation depends largely upon the type of cations adsorbed at the crystal surface of the clay particles. Clay particles that are saturated with univalent cations (Na) favor the development of a granular soil structure, whereas clay particles with bivalent (Ca) or trivalent (Al, Fe) cations frequently form flocs or ball together with larger mineral particles to form crumbs or granules (Endell (42)). Sedimentation of flocs frequently produces a loose honeycomb structure (Terzaghi (45)) or, in combination with coarser mineral grains, still more complicated types of structures (Casagrande (11)) which are characterized by the fact that the voids may be much larger than the individual grains. It may also occur that large voids, formed by framework of the coarser mineral grains, are filled with soft clay.

As a result of sedimentation and later geological depositions and displacements, a stratification of the soil occurs in most cases. Particularly the flaky particles are oriented in definite directions. When such a soil is thoroughly remolded, the structure becomes disturbed, and while all flocs and crumbs are probably not broken down into their small particles, it may nevertheless be assumed that the flaky particles do not have a preferred orientation in a thoroughly remolded soil. From an elastic standpoint the material, on the whole, can be regarded as homogeneous and isotropic. However, when such a remolded soil is reconsolidated, a rearrangement of the flaky particles occurs in such a manner

that the flakes orient themselves with their faces perpendicular to the major principal stress. Hence the material can no longer be considered isotropic. This stratification of remolded and reconsolidated soils can be verified by permeability and compression tests and also in the following simple manner.

5. A remolded clay specimen is reconsolidated in a confined compression test at a pressure of 4 to 5 kg/cm^2. After the specimen is air-dried, two thin slices, one cut parallel and the other perpendicular to the direction of pressure, are placed in water. As shown in figs. 1A and 1B, the clay slakes in layers or flakes perpendicular to the direction of the consolidation pressure. However, if a ball is formed from soft, thoroughly remolded clay and slowly air-dried, a slaking test with a slice cut arbitrarily from it will not show any preferred direction of the fissures (fig. 1C). The above-mentioned figures show the results of tests with Vienna clay, a clayey marl rich in silt; but also in clay soils that consist almost entirely of colloidal mineral particles, a preferred orientation of these particles can be detected by slaking tests. Fig. 1D shows the result of such a test with Little Belt clay.

The direction of the original consolidation pressure could also be observed in undisturbed clay soils by means of slaking tests. The slaking phenomena of two undisturbed clays are shown in figs. 2A and 2B. From each of the dried specimens of these soils, obtained by borings, two equally large, thin slices were cut parallel and perpendicular to the axis of the borehole and placed in water. As shown by the figures, the direction of the consolidation pressure is evidenced not only by the fissures but also by the deformations: the left specimen has become thicker and the right one wider, i.e., the deformation occurs chiefly in the direction of the original consolidation pressure. This can be used for determining the direction of the consolidation pressure, even if there are no oriented fissures. Fig. 2C shows the slaking phenomena of a brittle, crumbly clayey marl. Despite the fact that no distinct fissures have been formed, the direction of the consolidation pressure can be estimated from the fact that the right specimen has become wider than the left one.

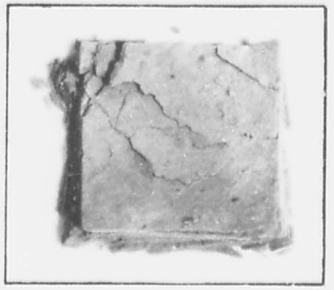

Pressure perpendicular to plane of picture

A

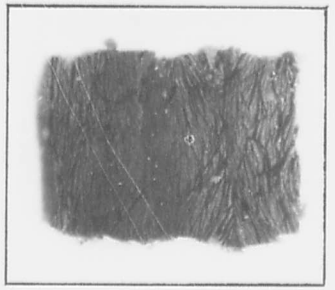

Pressure parallel to plane of picture

B

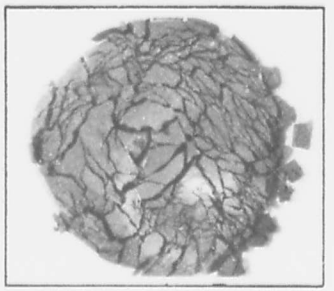

Uniform pressure in all directions

C

Vienna clay

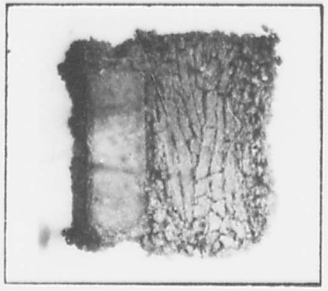

D

Little Belt clay

D

Direction of pressure:

Left: perpendicular to plane of picture

Right: parallel to plane of picture

Fig. 1. Slaking of thin slices of thoroughly remolded reconsolidated clays in water

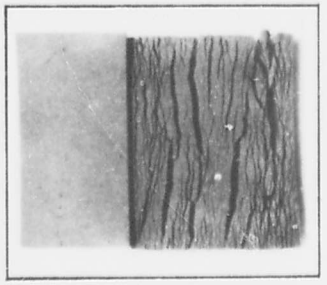

Silty marl, Mannersdorf
A

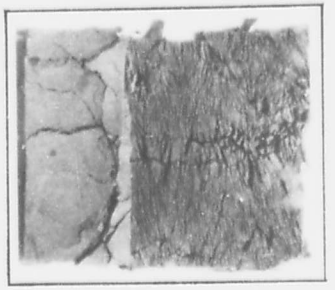

Vienna clay, Reichsbrücke
B

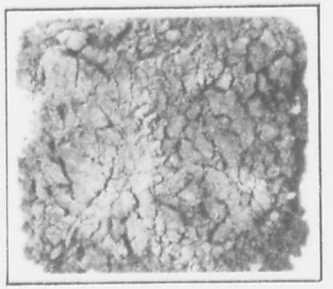

Crumbly clayey marl
C

Direction of pressure:

Left: perpendicular to plane of picture
Right: parallel to plane of picture

Fig. 2. Slaking of thin slices of undisturbed cohesive soils in water

Thixotropic Changes and Viscosity

6. A content of a few percent of colloidal matter is frequently sufficient to give the soil some properties characteristic for colloids (Freundlich (20)). Two of these special properties of colloids, namely thixotropy and anomalous or structural viscosity, will be briefly discussed here. The term thixotropy designates the isothermal transformation from sol to gel, at which a sol solidified to a gel is transformed to a sol by a purely mechanical means, for example remolding by vibration or plastic displacements, whereupon it solidifies again to a gel during the subsequent state of rest. For many gels this process is not entirely reversible. In most clays the liquefaction produced by remolding is not complete. Through remolding or plastic flow the material loses only part of its strength which is slowly recovered after the remolding process has ceased. In some clays this recovery of the strength appears to be incomplete. In any case, the process is a very slow one. To explain the physical processes during thixotropic changes, various theories have been advanced; however, none of them seem to be conclusive and entirely satisfactory (Freundlich (20)). Without entering into the physical processes proper, a thixotropic change can be regarded as a temporary disarrangement of the water films around the small particles discussed earlier.

Both gels and clays offer some resistance to a thixotropic loss of strength which must first be overcome by external forces. This resistance depends not only upon the character of the colloidal particles and the dissolved salts but also upon the concentration in the case of gels and upon the water content in that of clays, and further upon the manner in which the remolding occurs. Thus it appears that clays are particularly sensitive to pure shear stresses and the large angular displacements connected therewith. Also the orientation of the particles with respect to the direction of displacement has a considerable effect upon the thixotropic loss of strength. The solidification period of gels or, in the case of clays, the time required for the recovery of the strength, depends upon the water content and particularly upon the dissolved salts (Freundlich (20), Ruth von Terzaghi (52)).

Many cohesive soils are called sensitive in the undisturbed state, i.e., the strength of the soil decreases considerably as a result of remolding, such as occurs during pile driving. In soils with a pronounced framework structure, this decrease in strength is explained by a disturbance of the framework (Terzaghi (48) and Casagrande (11)). However, part of the decrease in strength is probably caused by pure thixotropic disturbances. In sensitive, cohesive soils with a simpler structure, the thixotropic disturbance might constitute the main cause of the decrease in strength. If piles are driven in such soils, it has been observed that the bearing capacity of the piles increases with time after the driving operation has ceased.

7. In many cohesive soils a slow, plastic flow occurs even at fairly low stresses (Terzaghi (49)). As will be shown in Chapter VI, the velocity gradient of this slow plastic flow increases up to the failure point approximately proportional to the increase in stress. At failure and the thixotropic loss of strength of the material connected therewith, the velocity gradient of the plastic flow is increased manyfold. The changes in the velocity gradient are no longer proportional to the stress changes. Here the variable or abnormal viscosity (also called "structure viscosity") becomes manifest (Freundlich (19)). Adhering to the concept "viscosity," it can be said that the coefficient of viscosity η depends upon the velocity gradient in the sense that the coefficient of viscosity usually decreases with increasing velocity gradient. The coefficient of viscosity also seems to be dependent upon the preceding maximum velocity gradient and upon the time elapsed after this maximum velocity has been attained. These observations indicate that a direct connection exists between the abnormal viscosity and the thixotropic loss of strength, i.e., when the velocity of the plastic flow increases, the liquefaction of a thixotropic gel or the decrease in strength of the clay also becomes more pronounced.

Pore-Water Pressure and Effective Stresses

8. The total normal stress acting on any sectional plane in a cohesive soil is partly absorbed by the solid phase and partly by the liquid

phase. The difference σ' between the total normal stress σ and the hydrostatic pressure p_h in free pore water is called the effective normal stress at the sectional plane under consideration. This can be written:

$$\sigma = \sigma' + p_h \tag{1a}$$

and since p_h is equal in all directions, it follows that:

$$\tau = \tau' \tag{1b}$$

in which τ is the total and τ' the effective shear stress. The effective stresses are also considered to be the stresses transmitted by the solid phase alone. Mathematically speaking, however, they apply to the total sectional plane and not to the actual sectional plane of the solid substance.

The tests of many researchers relative to shear and compressive strength of cohesive soils have shown that the changes in shape and volume as well as the failure conditions of such materials depend almost exclusively on the effective stresses σ'. If these stresses remain constant, the effect of a change in the hydrostatic pressure of the pore water can be disregarded (see fig. 32B). Thorough tests to verify this basic law were recently performed by Rendulic (37).

9. When the total stresses are changed by external forces, the hydrostatic pressure in the pore water will change at the same time. The latter change is a function of the existing effective stress condition and of the state of consolidation of the soil produced by all earlier effective stress conditions. If the soil has the opportunity to discharge or absorb water, the change in the pore-water pressure will be equalized in the course of time. The laws according to which this stress equalization occurs are given by Terzaghi in the theory of hydrodynamic stress phenomena (45). The methods for the practical application of this theory were worked out by Terzaghi and Fröhlich (53).

At present, the changes in the pore-water pressure, the so-called zero isochrones, occurring immediately after the changes in stress, can

only be determined in an approximate manner and for simple cases. In many practical problems the failure conditions are therefore determined as a function of the total stresses σ. Obviously, the failure conditions determined in this manner are only valid for the stress condition prevailing during the test, but this stress condition usually differs substantially from that which exists in the foundation soil. Hence, in order to obtain failure conditions which are valid in all cases, it is necessary to determine the effective stresses σ' not only for the test but also for the practical application.

10. In the stress computation, it should not be forgotten that the elastic properties, particularly Poisson's ratio or the coefficient of earth pressure at rest ζ, introduced by Terzaghi (45), are different in the solid and liquid phases of the soil. It is therefore necessary to compute σ' and p_h separately wherever possible, and to determine σ from their sum. However, at vertical loading of the surface, the total perpendicular stresses σ_z in the foundation soil can be determined directly by means of the conventional formulas or graphical procedures, since these stresses are independent of Poisson's ratio. On the other hand, the total horizontal stresses must be computed with the aid of equation (1).

11. In most cases, the computation of the effective stresses and of the hydrodynamic stress equalization (Terzaghi (53)), as well as the determination of the failure conditions of the soil, becomes clearer and simpler if the hydrostatic excess or negative pressure of the pore water and the unit weight of the soil less the uplift (also called the apparent unit weight) is introduced.

The pore-water pressures

$$p_n = h\gamma_w \qquad (\gamma_w = 1) \tag{2}$$

corresponding to the static pressure heads h (fig. 3) are called the natural pore-water pressures. The excess or negative pressure p_u of the pore water is then:

$$p_u = p_h - p_n \tag{3}$$

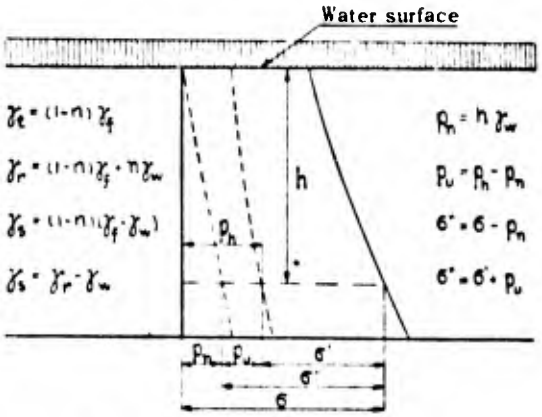

Fig. 3. Stresses and unit weights

If the total unit weight of the water-saturated soil is

$$\gamma_r = (1 - n)\gamma_f + n\gamma_w \tag{4a}$$

then the apparent unit weight is

$$\gamma_s = (1 - n)(\gamma_f - \gamma_w) = \gamma_r - \gamma_w \tag{4b}$$

in which n is the porosity, γ_f the unit weight of the solid phase, and γ_w the unit weight of the water ($\gamma_w = 1$).*

If γ_s is introduced in the stress computations instead of γ_r and the total stresses thus obtained are designated as σ'' and τ'', then according to equation (4b):

$$\sigma = \sigma'' + h\gamma_w$$

$$\tau = \tau''$$

and further, according to equation (3):

$$\sigma'' = \sigma' + p_u \tag{5a}$$

$$\tau'' = \tau' \tag{5b}$$

---

* Translator/author note: This refers to the metric system and use of gram and centimeter.

At $p_u = 0$ a complete equalization of the hydrodynamic stresses exists, and $\sigma' = \sigma''$.

12. If a capillary pressure p_k acts upon the soil surface, then

$$p_u = -p_k \tag{6a}$$

and in the event that the capillary pressure acts in all directions and alone, then the active normal stress will also be:

$$\sigma' = p_k \tag{6b}$$

However, if the capillary pressure acts in one direction only, equation (6b) is valid for this direction alone. The stresses in other directions depend upon the boundary conditions and the elastic properties of the soil.

When a flow with a hydraulic gradient i occurs in the soil, a flow pressure $i\gamma_w$ is produced. This flow pressure can be regarded as an inertial force acting upon the solid phase in the direction of flow (Terzaghi (45)). The total flow pressure Δp_s produced over a distance ΔL is:

$$\Delta p_s = i \cdot \Delta L \cdot \gamma_w = \Delta h \cdot \gamma_w \tag{7}$$

or equal to the loss Δp_u of excess pressure of the pore water. When the flow occurs in vertical direction only, the effect of the flow pressure upon the vertical, active stress is taken into account simply by the introduction of the values of p_u determined by the hydraulic gradients (isochrones of the hydrostatic pressures of the pore water) in equation (5).

Changes in Volume Caused by a Change in Stresses

13. While solid materials show chiefly changes in shape and only small changes in volume at a change in the stress condition, soils and particularly cohesive soils frequently exhibit relatively large changes in volume. However, at a time immediately after the change in stress the

changes in shape are greater than the changes in volume, even in soils saturated with water (two-phase systems). But at the same time a change in the pore-water pressure occurs, as mentioned before. If the soil has the opportunity to discharge or absorb water, or if differences develop in the excess pressure p_u of the pore water in the soil, a flow and, in the course of time, a change in the water content and in the total volume of the soil will develop.

It is necessary to know these changes in volume, not only for the accurate evaluation of strength tests but also for the practical application of the test results. In the case of cohesive soils it is also necessary to know the pertinent changes in the pore-water pressure at arbitrary changes in an arbitrary triaxial stress condition. At present our knowledge relative to this matter is still very incomplete. Although investigations of this problem are in progress (Ehrenberg (42), Bernatzik (3), Rendulic (36, 37, 38), Samsioe (39), and Kjellman (27)), sufficient test data which can be used for deriving the basic equations have not yet been published. These volume changes have only been investigated to an adequate extent in tests without lateral deformation (consolidometer tests), fig. 5. In such tests there is no way of controlling the lateral stresses, and their magnitude can only be determined approximately.

14. The result of such a compression test with a remolded soil and with an initial water content larger than the liquid limit is illustrated in fig. 6A. The active vertical stress or the consolidation pressure is called p and the corresponding lateral pressure is $p_s = \zeta p$, in which ζ is the coefficient of earth pressure at rest. The changes in volume are shown as changes in the void ratio ϵ (volume of the voids/volume of the solid phase), the porosity n (volume of the voids/total volume), and the water content w (weight of the water/weight of the solid phase), fig. 4:

$$\epsilon = \frac{n}{1 - n} = w \frac{\gamma_f}{\gamma_w} \qquad (\gamma_w = 1) \tag{8}$$

The voids are here assumed to be entirely filled with water (no air content). The conditions of consolidation corresponding to the virgin

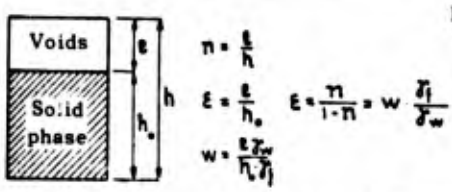

Fig. 4. Porosity, void-ratio, water content

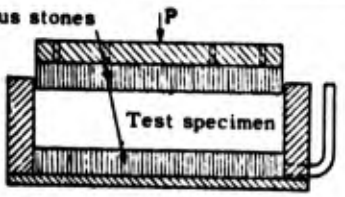

Fig. 5. Consolidation test

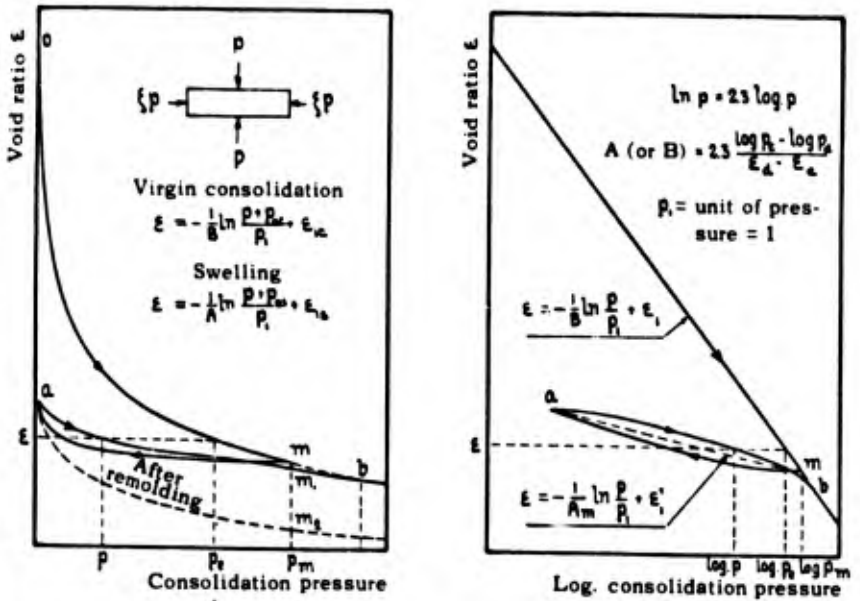

Fig. 6. Pressure-void ratio diagram

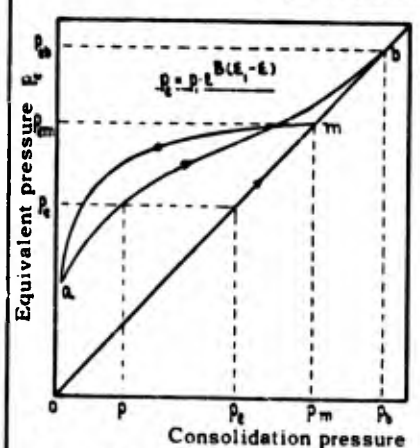

Fig. 6C. Equivalent consolidation pressures

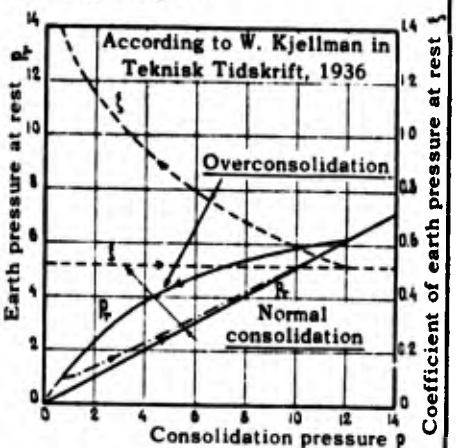

Fig. 6D. Earth pressure at rest for sand

consolidation curve o-m-b (main curve) are called "normal consolidation" and those of the relief or rebound curve m-a and of the reconsolidation curve a-b are called, respectively, "simple overconsolidation" and "cyclic overconsolidation."

According to Terzaghi (45, 35), the virgin consolidation curves are approximately represented by the equation:

$$\epsilon = -\frac{1}{B} \ln \frac{(p + p_{0c})}{p_1} + \epsilon_{1c} \qquad (9)$$

in which p_{0c} = constant (initial pressure), p_1 = unit of pressure, ϵ_{1c} (constant) = void ratio for the total pressure $p + p_{0c} = p_1$, and in which B is a dimensionless constant called coefficient of consolidation.

The rebound curve m-a is approximately represented by a similar equation, likewise according to Terzaghi:

$$\epsilon = -\frac{1}{A} \ln \frac{(p + p_{0s})}{p_1} + \epsilon_{1s} \qquad (10)$$

A, p_{0s}, p_1, and ϵ_{1s} have the same meanings as above. A is the coefficient of swelling. For cohesive soils the initial and final pressures p_{0c} and p_{0s} are usually so small that they may be disregarded.

Hence if ln p or log p is substituted for p in the pressure-void ratio diagram, then consolidation and unloading diagrams are represented by slightly curved lines that can approximately be replaced by straight lines (fig. 6B and figs. 15 and 16).

The reconsolidation curve a-b usually consists of two transition curves and a main section that can be represented in a similar manner by equations (9) and (10).

15. The position of the unloading and reloading curves (ϵ_{1s} in equation (10)) is given by the reversal pressure p_m. This pressure also seems to affect the values A and p_{0s}. As p_m increases, A decreases (figs. 15 and 16). In many soils the position and shape of the virgin consolidation curves are somewhat affected by the initial void ratio and by the process of loading. The larger the initial void ratio and the slower the rate of load increase, the higher the curves will lie (Langer (30)).

Hence the various coefficients and constants in equations (9) and (10) cannot be considered as true material constants.

When, during the consolidation process, a remolded soil specimen again is remolded, or even when it is but slightly disturbed by bending, the curves of the pressure-void ratio diagram, a-m_2 in fig. 6A, will lie considerably lower, i.e., an additional consolidation caused by the disturbance is obtained. This fact was first observed by Jürgenson (26), who explains the additional consolidation as a disturbance of the framework formed by the mineral particles.

For the loading process of the consolidation used in conventional shear tests and for the testing materials used in this study, equation (9) with $p_{0c} = 0$ can be applied with sufficient accuracy. Since this equation will henceforth be used very frequently, ϵ_{1c} will be replaced by ϵ_1 for the sake of simplicity, with the result that:

$$\epsilon = -\frac{1}{B} \ln \frac{p}{p_1} + \epsilon_1 \qquad (p_1 = 1) \tag{11}$$

16. The stress condition of the soil during the consolidation tests discussed above is given by the principal pressures p , ζp , ζp . During the virgin consolidation o-m-b the coefficient of earth pressure at rest ζ appears to be constant. On the other hand, the value of ζ appears to be increasing steadily during the unloading m-a. During the reloading a-b it decreases fairly rapidly down to the original value for the virgin consolidation. Samsiöe (39, 40) proposed a working hypothesis of these variations in ζ . However, the conditions have not been sufficiently clarified by tests. Thus far, only one series of tests has been published, namely for sand (fig. 6D) (Kjellman (27)).

17. Another very significant difference between solid materials and cohesive soils is that cohesive soils not only experience changes in shape but also in volume when they are subjected to a pure shear stress. Casagrande (14) and Jürgenson (26) showed that naturally consolidated cohesive soils experience a considerable reduction in volume during a shear test. In this paper it is demonstrated that the volume of highly overconsolidated cohesive soils increases during such a test. Jürgenson (26) attributed

this change in volume at pure shear stress to a mechanical rearrangement of the soil particles. However, it is possible that these changes in volume are partly caused by the thixotropic disturbance of the equilibrium of the internal and external forces. Furthermore, a pure shear stress may be regarded as the increase of a principal stress plus the numerically equal decrease of another principal stress. In natural or slightly overconsolidated cohesive soils, the increase in stress causes a reduction in volume. This reduction is greater than the increase in volume caused by the numerically equal decrease of the other principal stress. The final result is therefore a reduction in volume. In highly overconsolidated cohesive soils the reduction in volume is, on the contrary, less than the corresponding increase in volume (figs. 15 and 16).

These changes in volume are very significant for the evaluation of the results of shear tests, since the cohesion of the soil is changed as a result thereof. Moreover, the fact that during a shear test changes in volume occur leads to the conclusion that a temporary excess or negative pressure develops in the pore water, even during application of pure shear.

Equivalent Consolidation Pressure

18. Both the analytical expression and the graphical representation of the influence of the void ratio upon the physical properties are facilitated by the introduction of the equivalent consolidation pressure, or more briefly the equivalent pressure, i.e., the pressure p_e on the virgin consolidation curve (o-m-b in fig. 6A) that corresponds to the prevailing void ratio of the soil or, according to equation (11):

$$p_e = p_1 e^{B(\epsilon_1 - \epsilon)} \qquad (p_1 = 1) \tag{12}$$

This form of representation has been used previously by Terzaghi and Janiczek (50) for evaluating the results of compression tests without lateral deformation.

Furthermore, the ratio n_c between the equivalent pressure p_e and

the actual consolidation pressure p' will be designated as degree of overconsolidation:

$$n_c = \frac{p_e}{p} \tag{13}$$

When the void ratios are replaced by the corresponding equivalent pressures, by use of the relationships between ε and p represented in fig. 6A, a diagram like that shown in fig. 6C is obtained. For normally consolidated soils $p_e = p$ and $n_c = 1$, but for simple or cyclic overconsolidated soils $n_c > 1$.

19. The equivalent pressure defined above refers to the pressure-void ratio diagram for compression without lateral deformation. This is expedient inasmuch as the stress conditions in the consolidometer are almost identical with those in the shear devices. In general, it would usually be more logical to refer the equivalent pressures to a pressure-void ratio diagram for equal pressure in all directions and to substitute such compression tests for consolidometer tests. In this manner it would be possible to eliminate the hard-to-define lateral pressures during unloading, as well as various frictional effects. However, before such a test method can be used in practice, the present testing devices must be simplified and improved to a considerable extent.

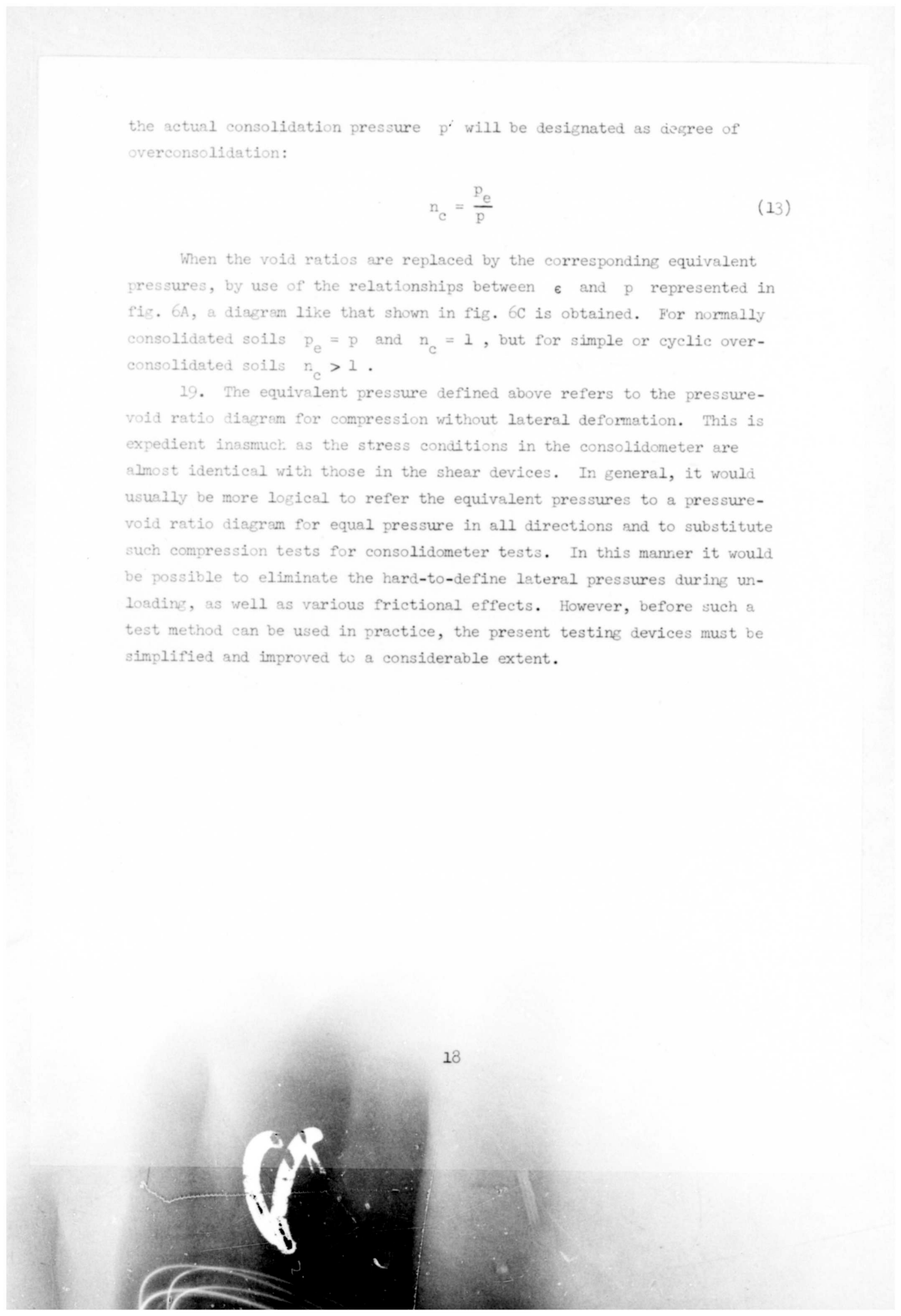

II. CURRENTLY AVAILABLE THEORIES FOR FAILURE OF SOILS

Flow and Failure Phenomena

20. As mentioned before, a slow, plastic flow may start at relatively low stresses in many cohesive soils. After each load increment, the displacement velocity reaches a maximum value, whereupon it decreases to a stationary value. A rapid, plastic flow begins after the last load increment before failure. The displacement velocity again increases until it attains a maximum value, but will no longer decrease provided stresses corresponding to the effective cross section remain constant. The start of a rapid, plastic flow must be regarded as the beginning of failure.

In many clays, particularly those in a normally consolidated condition, a temporary, more rapid plastic flow may start at a few load increments before failure and is caused by a rearrangement of the grains. However, the velocity of flow decreases again after a certain displacement has been attained.

As will be shown in this study, during failure and after a given displacement the cohesion decreases to a fraction of its original value. When the plastic flow is halted, or even when the rate of flow is reduced by a decrease in stress, the lost cohesion will be partly or fully recovered in the course of time.

In order to distinguish between conditions of flow and of failure, Fröhlich (21) uses as a decisive criterion that the cohesion must be zero after true failure. In the case of cohesive soils, this condition will probably be fulfilled on rare occasions only. However, since a considerable decrease in the cohesion occurs after the start of rapid, plastic flow, a stress condition leading to the occurrence of rapid, plastic flow will henceforth be called "failure condition." By the same token, a stress condition that signifies the beginning of slow, plastic flow will be called "flow condition." The shear stresses in the plane of failure corresponding to these two stress conditions were respectively called "shearing resistance" and "bond resistance" by Terzaghi (49). These designations will also be used in this paper.

21. Until a few years ago, the published results of shear tests with cohesive soils showed large scatterings and contradictions, with respect not only to the cohesion but also to the angle of internal friction and to the angle of inclination of the planes of failure determined by compression tests. These contradictions in the test results were mainly caused by the fact that the influence of the pore-water pressure was not recognized or taken into account. Incomplete consolidation by a vertical load frequently leads to erroneous results. When shear tests are carried out too rapidly, the pore-water pressure has a decisive effect because in such tests an equalization of changes in the pore-water pressure caused by the deformations is not possible. The results of investigations by Krey, Terzaghi, Casagrande, and Jürgenson demonstrated the great influence of the equalization of the pore-water pressures, not only during consolidation but also during the shear test. Thereby it also became possible to obtain more definitive coefficients for determining the shearing resistance of cohesive soils.

Coulomb's Failure Condition

22. The earliest failure condition for cohesive soils is the one by Coulomb. It is expressed as follows:

$$s = \mu p + c \qquad \text{or} \qquad s = p \tan \phi + c \tag{14}$$

where s is the shearing resistance and p the effective stress normal to the failure surface. $\mu = \tan \phi$ is called the coefficient and ϕ the angle of internal friction; c is designated as the cohesion. This failure condition is graphically represented in fig. 7. The straight line a-b is called the line of shearing resistance. If in equation (14) ϕ and c are constants, independent of the direction of the failure surface, then it follows from the failure condition that the major principal stress forms an angle of

$$\alpha = 45 - \frac{\phi}{2} \qquad \text{(see fig. 8)} \tag{15}$$

with the plane of failure. For the case $c = 0$, the shear line o-m in fig. 7 and the following failure condition are obtained:

$$s = \mu_s p \qquad \text{or} \qquad s = p \tan \phi_s \tag{16}$$

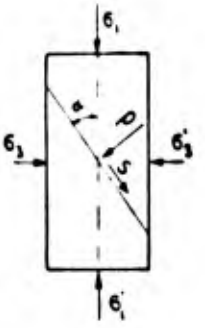

Fig. 8. Inclination of planes of failure

The failure condition expressed by equation (16) applies to both cohesionless soils and normally consolidated clays. The coefficient μ_s was given the subscript s since it has been known for a long time that it does not represent the true coefficient of internal friction in cohesive soils, but only an apparent one. The same applies to ϕ_s. The validity of this contention arises from the fact that, in one and the same soil, the shearing resistance line o-m as well as a-b can be obtained by merely changing the consolidation procedure, whereas angle α and hence the values of ϕ computed from equation (15) remain constant in all cases.

23. For the stress conditions at failure determined by equation (14) the Mohr stress diagram can be drawn by means of equation (15), as shown in fig. 10. Coulomb's shearing resistance line is identical with the envelope of Mohr's circles and represents Mohr's curve of failure. Coulomb's failure condition can now be expressed by the effective principal stresses with the aid of Mohr's diagram:

$$\sigma_1' - \sigma_3' = 2 \sin \phi \left[\frac{c}{\tan \phi} + \frac{1}{2} (\sigma_1' + \sigma_3') \right] \tag{17a}$$

or, with $p_i = \frac{c}{\tan \phi}$, where p_i is a measure of the intrinsic pressure,

$$\sigma_1' - \sigma_3' = 2 \sin \phi \left[p_i + \frac{1}{2} (\sigma_1' + \sigma_3') \right] \tag{17b}$$

Equation (17b) is known as Mohr's failure condition, but in this case it is only a general expression for Coulomb's failure condition. Both equations presuppose that the intermediate principal stress does not affect the failure condition.

If the cohesion c becomes equal to zero, equation (17a) yields:

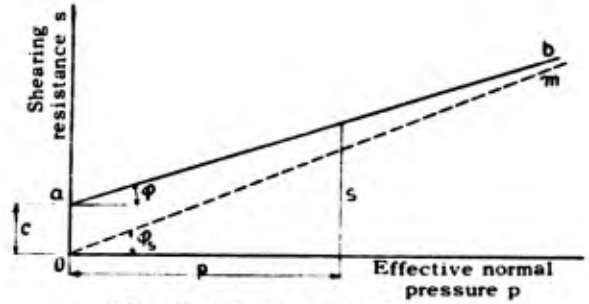

Fig. 7. Coulomb's failure condition

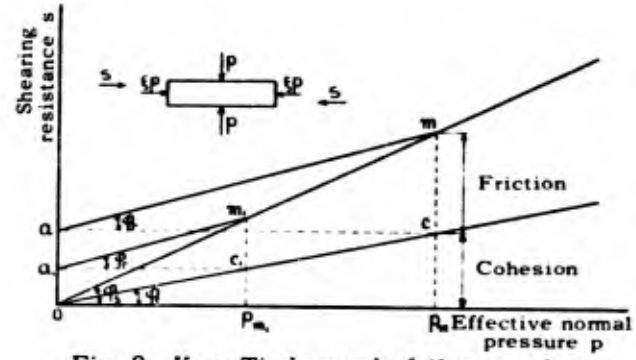

Fig. 9. Krey-Tiedemann's failure condition

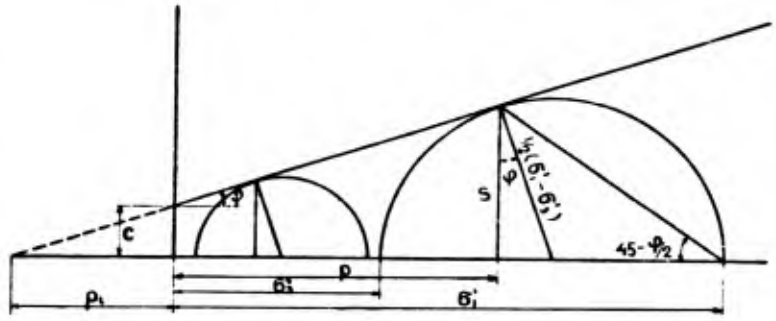

Fig. 10. Coulomb's failure condition in form of Mohr's diagram

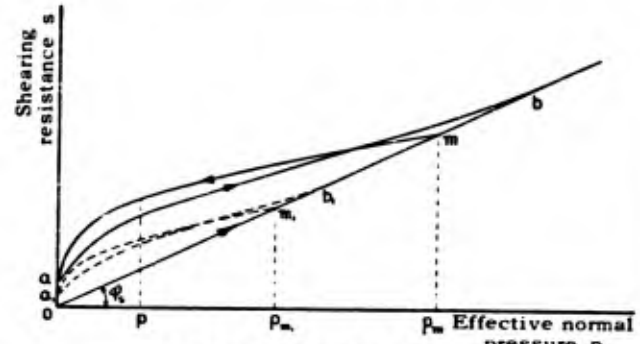

Fig. 11. Hysteresis loop of the shearing resistance

$$\frac{\sigma_1' - \sigma_3'}{\sigma_1' + \sigma_3'} = \sin \phi \qquad (17c)$$

This special case is known as Rankine's failure condition for cohesionless soils. As will be shown later, this failure condition can often also be used for normally consolidated clays with a sufficient degree of accuracy, even though in this case $\phi = \phi_s$ does not correspond to the angle of effective internal friction.

Krey-Tiedemann's Failure Condition

24. It has long since been known that, for a given remolded soil, the cohesion c is not a constant but depends upon the state of consolidation and upon the test procedure. Thus Krey determined a large number of shearing resistance lines for one and the same soil by means of shear tests (28, 29).

In conjunction with Krey's studies, Tiedemann (41, 42) established the following failure condition through tests conducted at the Prussian Laboratory for Hydraulic Research and Marine Engineering:

$$s = \mu_r p + \mu_c p_m = p \cdot \tan \phi_r + p_m \cdot \tan \phi_c \qquad (18)$$

in which p is the consolidation pressure prevailing at the moment of shear failure (effective consolidation pressure normal to the shear plane) and p_m the maximum consolidation pressure at which the soil was previously consolidated, whereas μ_r and μ_c are respectively called coefficient of friction and of cohesion.

The test procedure for determining these coefficients is illustrated in fig. 9, where o-m_1-m is the shearing resistance line of naturally consolidated specimens, and a-m, a_1-m_1 the shearing resistance line of simple overconsolidated specimens. According to this concept, angle ϕ_r represents the true angle of internal friction, also in the case of a normally consolidated soil. In this manner one of the deficiencies of

Coulomb's failure condition is eliminated and a significant improvement achieved.*

The Hysteresis Loop of the Shearing Resistance

25. According to Terzaghi (47, 50), the shearing resistances of a series of clay specimens, for which the relation between void ratio and consolidated pressure corresponds to the curves o-m-a-b in fig. 6A, form the hysteresis loop o-m-a-b shown in fig. 11. This demonstrates first, that at a given final consolidation and normal pressure p and at the same maximum consolidation pressure p_m various values of the shearing resistance are obtained for simple or cyclic overconsolidated specimens, and secondly, that the shearing resistance lines for simple overconsolidated soils are not straight but show a curvature which increases as p decreases.

26. Terzaghi and Janiczek also conducted tests with clay specimens in the normally consolidated and simple overconsolidated state (50). As shown in fig. 12, the resulting values of the compressive strength were plotted as a function of the earlier defined equivalent pressures (p_e) and yielded straight lines passing through the origin, both for specimens in the normally consolidated state and for those that were fully unloaded after preconsolidation (point a in fig. 6A).

The compressive strength line a_1-i_1 corresponds to the total shearing resistance at normal consolidation, whereas line d_1'-m_1' indicates the residual shearing resistance after unloading. From this Terzaghi concludes that part of the shearing resistance caused by consolidation is irreversible and appears as cohesion during unloading, and further that, in each type of soil, this cohesion amounts to a definite fraction of the full shearing resistance at normal consolidation. Since this cohesion was determined in tests with specimens whose state of consolidation corresponds to complete unloading, it should not be confused with Krey-Tiedemann's

---

* Translator/author note: This testing procedure does not fully agree with that described by Tiedemann in 1937; see further discussion, Hvorslev, 1960, page 176.

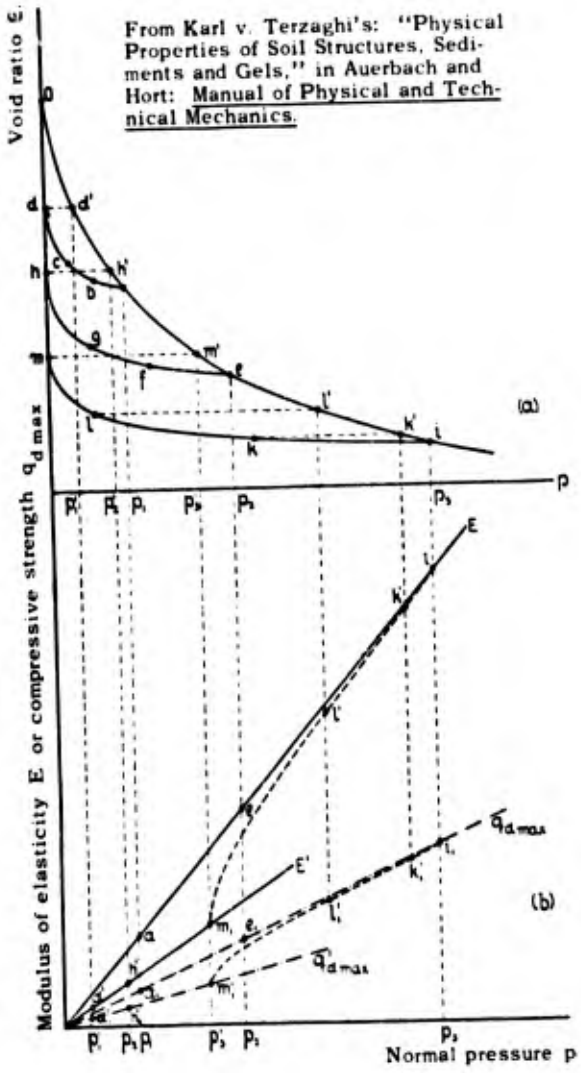

Fig. 12. Terzaghi-Janiczek's compression tests

cohesion, determined by substituting straight lines for the shearing resistance lines.

Other conclusions that can be drawn from the Terzaghi-Janiczek test will be discussed later.

General Considerations

27. Krey-Tiedemann's failure condition is based on the assumption that the cohesion depends solely upon the maximum normal pressure occurring at any time, and remains constant during the unloading process. As

mentioned before, this assumption is contradicted by the hysteresis loop of the shearing resistance. Also, the values ϕ_s and ϕ_r of the angle of internal friction, determined by Coulomb's or Krey-Tiedemann's procedure for cohesive soils, are much higher than the values determined from compression tests and from equation (15). This discrepancy must be attributed to the fact that none of the aforementioned procedures takes into account that the variation in the void ratio occurring during the shear test greatly affects the cohesion.

A comparison of the hysteresis loop for shearing resistance with a hysteresis loop for the pressure-void ratio diagram corresponding to the same consolidation procedure, particularly when this loop is represented by means of equivalent pressures as in fig. 6C, gives rise to the hypothesis that the cohesion depends chiefly upon the void ratio.

One of the main objectives of this study is to investigate whether such a relationship between cohesion and void ratio exists, and whether it will lead to a failure condition that corresponds more satisfactorily to the test results than the failure conditions formulated thus far.

III. MATERIALS USED IN TESTS

Vienna Clay

28. In the great majority of the tests, so-called Vienna or Baden clay was used. This is a blue-gray, stiff, marine clay from the Miocene, occurring in the region around Vienna. It contains a large amount of silt and approximately 13 percent calcium carbonate.

The laboratory had at its disposal a large, mechanically mixed supply of this clay from which smaller quantities, ranging from 15 to 20 liters, were taken as needed and prepared for testing. Despite the uniformity of this soil and the careful mixing and remolding, it proved to be extremely difficult to fully homogenize a major amount thereof and particularly to keep it in an unchanged and homogeneous condition over a considerable period of time. The physical and elastic properties of the homogenized soil would change slightly with time. Also, layers would develop that differed somewhat with respect to these properties. Even though the variations were small (maximum deviations for the shearing resistance: 4 to 5 percent) they complicated the general evaluation of the tests and rendered it particularly difficult to accurately determine the sources of error in the testing devices and the effect of various test procedures. They made it necessary to perform many control tests and repetitions, and on several occasions they prevented a test series from being carried out as planned. For this reason the results of tests made with various smaller batches could only be compared on the basis of their trends but not directly by numerical values.

Little Belt Clay

29. In order to verify the general validity of the results obtained in tests with Vienna clay, a smaller series of tests was made with Little Belt clay. This material was made available by the courtesy of the Danish State Railroads on recommendation of Professor A. Engelund. This soil is an extremely fine, plastic clay, more than 75 percent (dry weight) of its

mineral components being present in colloidal form. In the undisturbed condition and when taken from deeper strata, it is very stiff and has a blue-gray color. In contact with the air its color changes rather rapidly as a result of the oxidation of the iron compounds and it becomes gray-brown to reddish.

This clay, which in places attains a thickness of more than 100 meters, occurs most frequently in the vicinity of the Little Belt, and the soil used here was taken near the ground surface at the steep coast "Rø gle Klint." Little Belt clay is closely related to the English "London clay" and to the French "argile plastique" insofar as its structure and physical properties are concerned, and it also originates from the same geological epoch (Paleocene-Eocene). A very thorough investigation and a comparison of the physical properties of Little Belt clay with those of London clay were made by Mrs. E. L. Mertz in connection with the construction of the bridge across the Little Belt (31). However, since the physical properties of the deposit are not the same everywhere, the specimen used here was subjected not only to shear tests but also to all other standard tests. Also, in the case of this soil, difficulties were encountered in performance of the tests because of the slight changes in physical properties, which probably were caused by oxidation.

Grain-Size Distribution and Atterberg Limits

30. The grain-size distribution was determined by the hydrometer method of Boujoucos-Casagrande (12). The results are graphically represented in fig. 13. In this figure, the mean unit weights of the mineral grains and the Atterberg limits of the water content (in percent of the dry material) are also shown. The fluctuations of these limits refer to the use of various small batches. In general, the lower limiting values were predominant.

31. The test procedure is also important. If the liquid limits are determined by means of Casagrande's liquid limit device (10), a higher liquid limit is obtained when the initial water content is greater than the liquid limit and the clay mixture is prepared a few hours before the test than when the initial water content is lower than the liquid limit or the

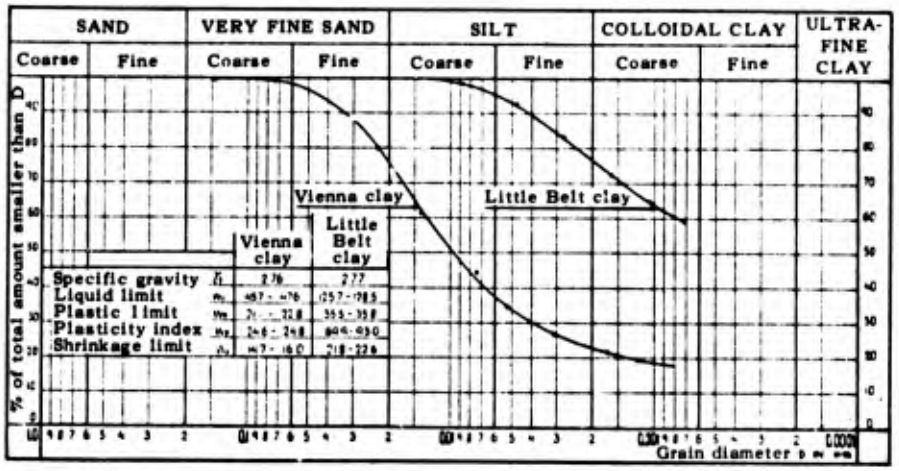

Fig. 13. Grain-size distribution curves

clay mixture is prepared just before the test (fig. 14). In the case of Vienna clay, the effect of the test procedure is slight and amounts to about one percent in terms of the water content, but in the case of Little Belt clay the difference in results obtained by the two procedures varies between 7 and 8 percent in terms of the water content. These results indicate that attainment of equilibrium between the newly added water and the clay minerals requires a certain amount of time. The liquid limits shown in fig. 13 were obtained in tests with an initial water content above the liquid limit.

32. The results of shrinkage limit tests are affected by the water content during specimen preparation and by the rate of drying. This is clearly indicated by the results of the shrinkage limit tests with Vienna clay shown in the following table.

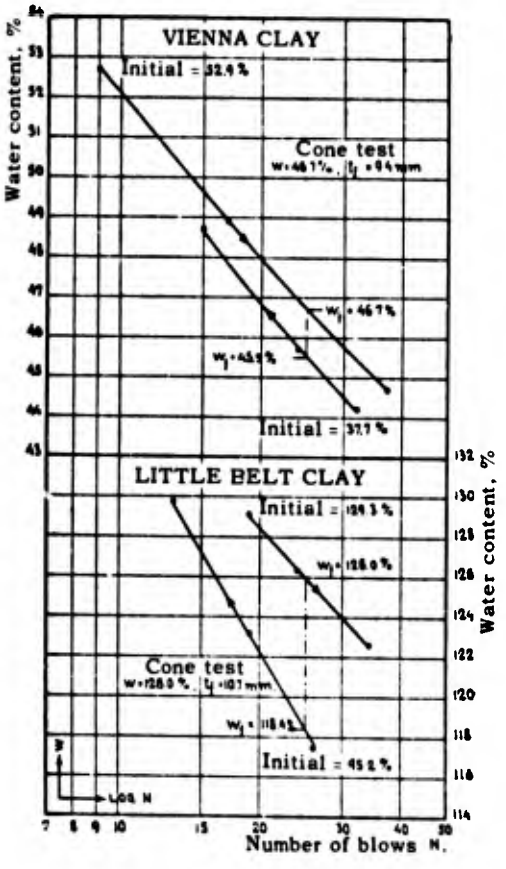

Fig. 14. Effect of initial water content at liquid limit determinations

Table 1

Results of Shrinkage Limits Tests with Vienna Clay

Test Procedure	Initial Water Content, %	Shrinkage Limit, %
Specimen placed immediately in drying oven	45	18.4
Specimen first dried in open air (4 days)	45	17.1
Specimen first dried under bell jar (12 days)	45	16.0
Specimen first dried in open air (7 days)	25 to 30	14.7

The fact that a higher shrinkage limit is obtained when the specimen is rapidly dried is probably caused by the formation of a dry, outer shell that prevents the escape of air bubbles and shrinkage of the core. Similar tests could not be made with Little Belt clay, since test specimens of this clay develop numerous fissures, also at the surface, when subjected to rapid drying. The shrinkage limits shown in fig. 13 were obtained from specimens that were remolded close to the plastic limit and subsequently dried slowly.

Permeability, Consolidation, and Earth Pressure at Rest

33. The results of consolidation tests by means of Terzaghi's consolidometer and the pertinent direct permeability determinations are plotted in figs. 15 and 16 in a simple logarithmic representation (ϵ, log p). The tests were carried out in a normalized manner, i.e., each load increment caused former pressure to be doubled or halved. The time interval between load increments amounted to approximately 24 hours. This period is not entirely sufficient to achieve a complete equalization of the hydrodynamic stresses and to halt the settlements or swellings. However, the resulting errors are small and of minor significance as compared with other sources of error (see below).

The virgin consolidation curve of Vienna clay is almost a straight line. It complies with equation (11), whereas in the case of Little Belt clay the line begins to show a curvature at a pressure as low as 2.0 kg/cm^2

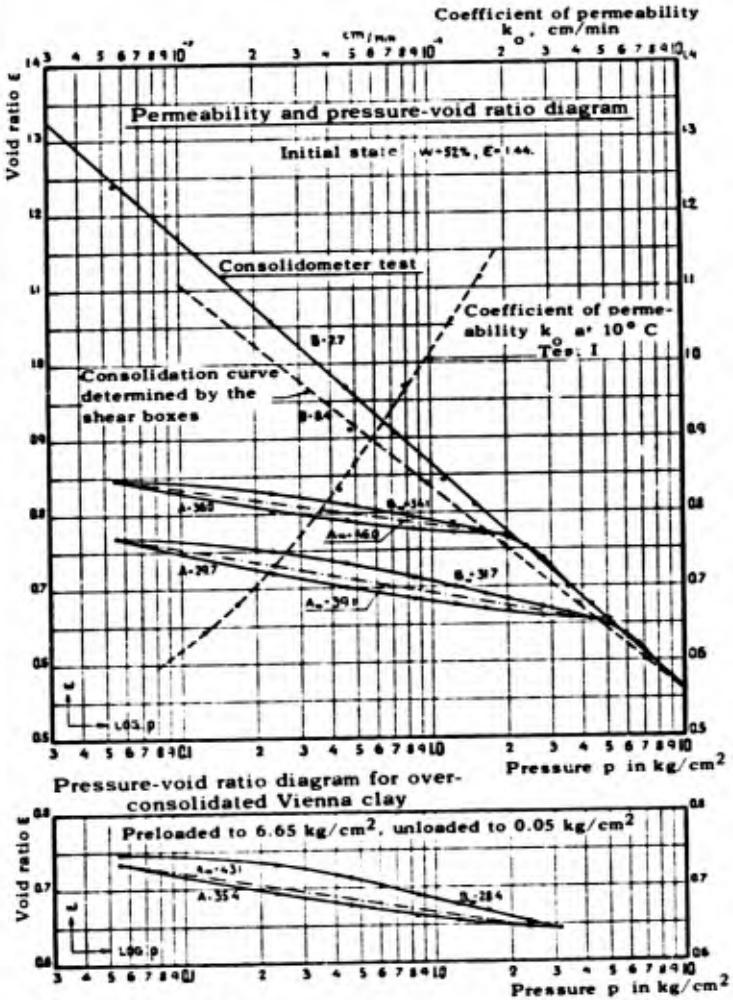

Fig. 15. Confined consolidation, Vienna clay

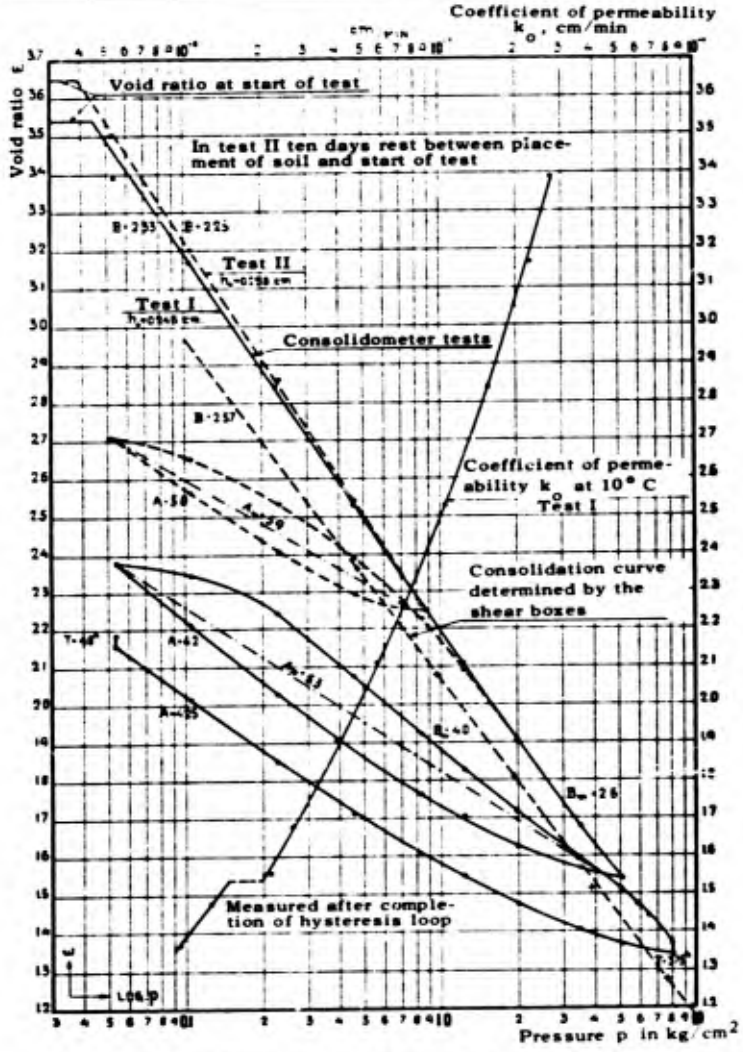

Fig. 16. Confined consolidation, Little Belt clay

and the curvature increases with the pressure p. The transition curve between the reconsolidation curves and the virgin consolidation curves should be noted. Here the soil is momentarily slightly underconsolidated or $n_c < 1$.

The swelling and reconsolidation curves show fairly strong curvatures. The values of A and B_w indicated in the figures only correspond to such portions of the curves that can approximately be replaced by straight lines. The values A_m correspond to the mean inclinations of the hysteresis loops. As the reversal pressure (p_m in fig. 6A) increases, the inclinations of the hysteresis loops increase and the coefficients A_m decrease.

34. During the consolidation of specimens for shear tests, the load increase is considerably faster than in conventional consolidometer tests. In addition, the effect of lateral friction is different, first, because the proportion between thickness and cross section of the specimen is not the same and second, because in shear boxes the effect of lateral friction is reduced since the walls are lined with greased filter paper.

Therefore, in order to obtain a reliable basis for the computation of the equivalent pressures p_e in the shear tests, consolidation tests with shear boxes were carried out in addition to consolidometer tests. A series of specimens was consolidated in the shear boxes at various loads with exactly the same loading procedure as that used in preparation of specimens for shear tests, i.e., the full load was applied within one or two days and this load was maintained for a period of five to seven days. After the consolidation was completed the water contents of these specimens were determined without a preceding shear test.

The pressure-void ratio curves obtained in this case are also shown in figs. 15 and 16. In order to facilitate their use for the determination of the equivalent pressures in shear tests, these curves are also plotted in fig. 17 as pressure-water content curves. As can be seen from figs. 15 and 16, the curves determined with the aid of the shear boxes lie lower than those obtained by means of the consolidometer. They respond almost exactly to equation (11) until pressures of approximately 10 kg/cm^2 are attained. From then on the lines begin to show a slight curvature in this case also.

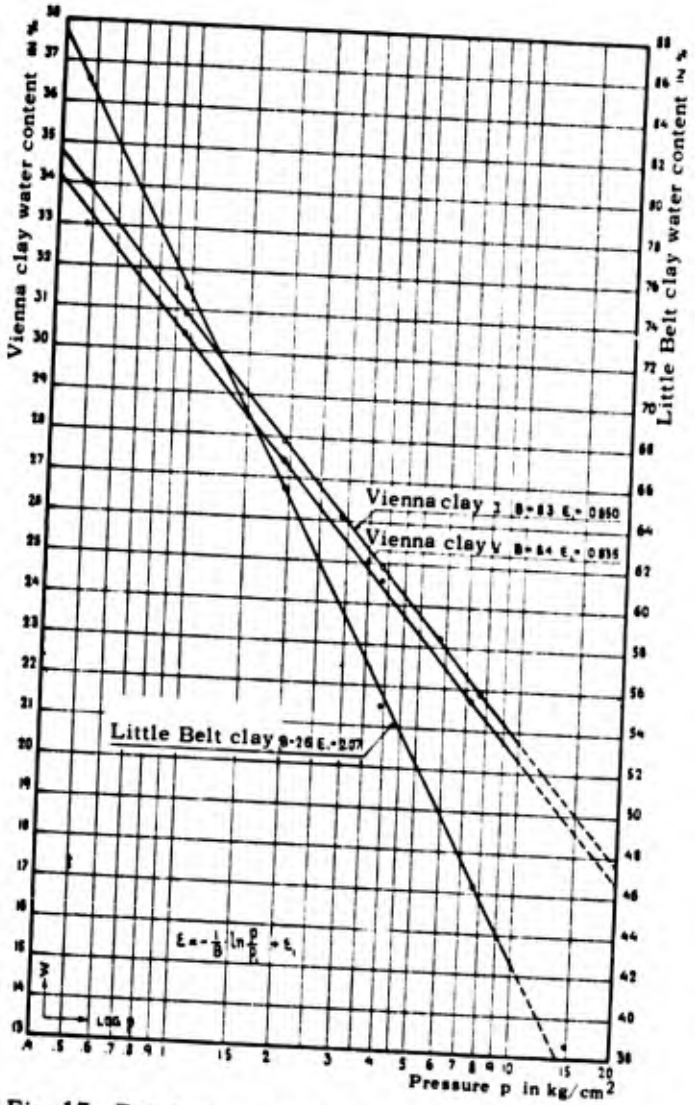

Fig. 17. Pressure-water content diagram determined with the shear boxes

The values of B and ϵ_1, obtained through the two test methods, are shown in table 2.

Table 2

Coefficients of Consolidation

Consolidation in	Vienna Clay V		Little Belt Clay	
	B	ϵ_1	B	ϵ_1
Consolidometer	7.7	0.866	2.3	2.25
Shear boxes	8.4	0.835	2.6	2.07

35. In order to determine the coefficient of earth pressure at rest ζ for Vienna clay, the material was first consolidated in the shear boxes (fig. 22) at a steadily increasing load up to various normal pressures p (normal consolidation). The total frictional force between the frame of the shear box and the test specimen inclosed in greased filter paper was determined by raising the frame after the consolidation was completed. The influence of zero friction could be eliminated by means of parallel tests with different specimen thicknesses, and the following equation for the friction S_r as a function of p was obtained:

$$S_r = 2.24\ h\ p \text{ kg (h in cm)} \tag{19a}$$

in which p is the specimen thickness above the base of the shear box, or since the circumference of the specimen is 40 cm, the frictional force per unit area is:

$$s_r = \frac{2.24h}{40h}\ p = 0.056\ p \text{ kg/cm}^2 \tag{19b}$$

The coefficient of friction between bronze and the wet filter paper coated with vaseline varies from $\mu_F = 0.065$ to $\mu_F = 0.103$, depending upon the test conditions and the velocity of displacement. Assuming a mean value $\mu_F = 0.084$,

$$\zeta = \frac{0.556}{0.084} = 0.67 \tag{20}$$

However, because of the variations of μ_F, this result should only be considered as an approximation.

A few values of S_r at decreasing normal pressure (simple overconsolidation) were also determined. However, because of scattering in the test results, it was impossible to determine definite relations. It was only possible to determine that ζ steadily increases with decreasing normal pressure (see fig. 6D and Kjellman (27)).

The earth pressure at rest for Little Belt clay was not determined because there was not enough material for making the pertinent tests. Its

value was estimated to be $\zeta = 0.75$ in computation of corrections of results of the shear tests.

Thixotropic Properties

36. The thixotropic properties of Vienna clay were first investigated by determining the Casagrande flow curves. After thorough remolding, the specimen was placed in the bowl of the liquid limit device and the groove was made. The bowl then was placed under a water-sealed bell jar, and after a certain rest period T (one minute to 120 hours), the number of blows N required for closing the groove was determined. Since it is almost impossible to conduct all tests with the same water content and to keep it constant during the rest period, the complete flow curves were determined for the various rest periods. These curves are plotted in fig. 18.

With these curves the relationship between rest period and number of blows can easily be determined for any constant water content. These relationships are represented by the curves in fig. 19. Logs N_T/N_1 are plotted as abscissas and logs T as ordinates. N_1 corresponds to the rest period T = 1 minute. The lines for lower values of T are slightly curved. However, they show an increasing curvature in downward direction as the values of T increase, particularly at lesser water contents, whereas a curvature would be expected in upward direction. These phenomena may depend more on the test method and on the development of a surface layer with increased strength than on the actual relationship between the rest period and the inner strength of the clay. The number of blows N is a function not only of the strength of the clay, but also of its viscosity and of the friction between clay and metal bowl. To this must be added the effect of the thixotropic disturbance caused by the blows and the fact that small clay particles in the groove dry out during prolonged rest periods, thus increasing the frictional resistance between clay and bowl.

37. In order to avoid these deficiencies in determination of the strength by means of a liquid limit device and to check the results

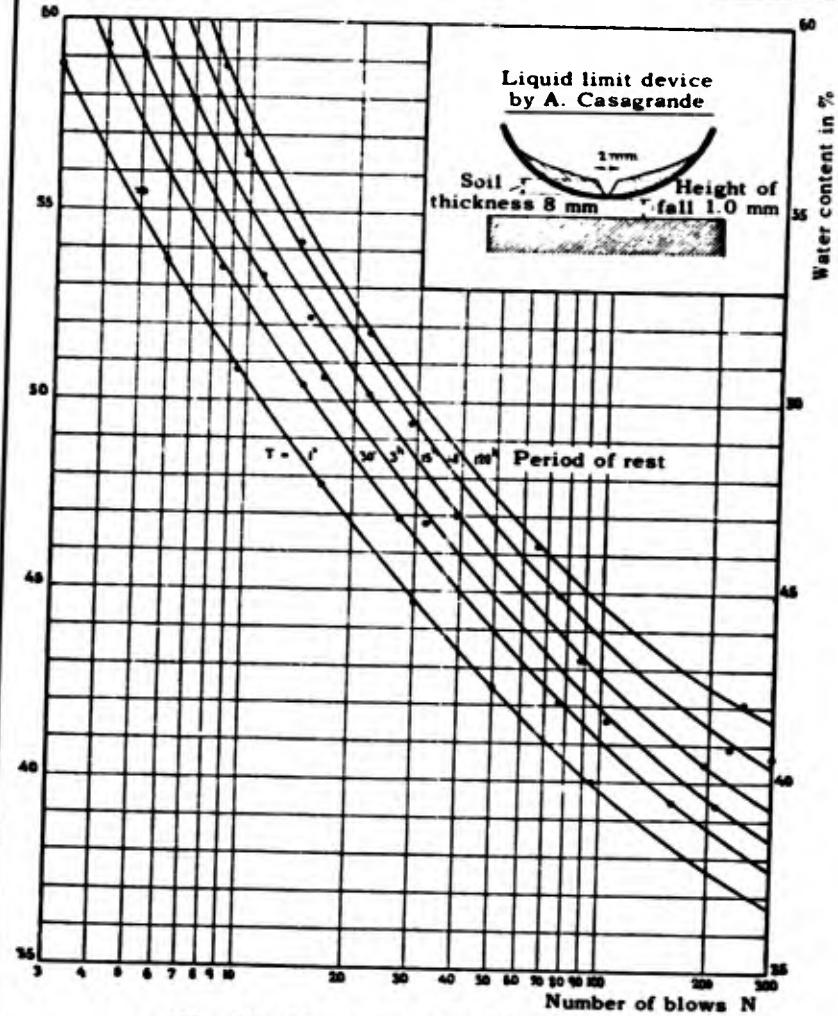

Fig. 18. Determination of flow-index curves for ascertaining the strength recovery of a remolded Vienna clay as a function of time

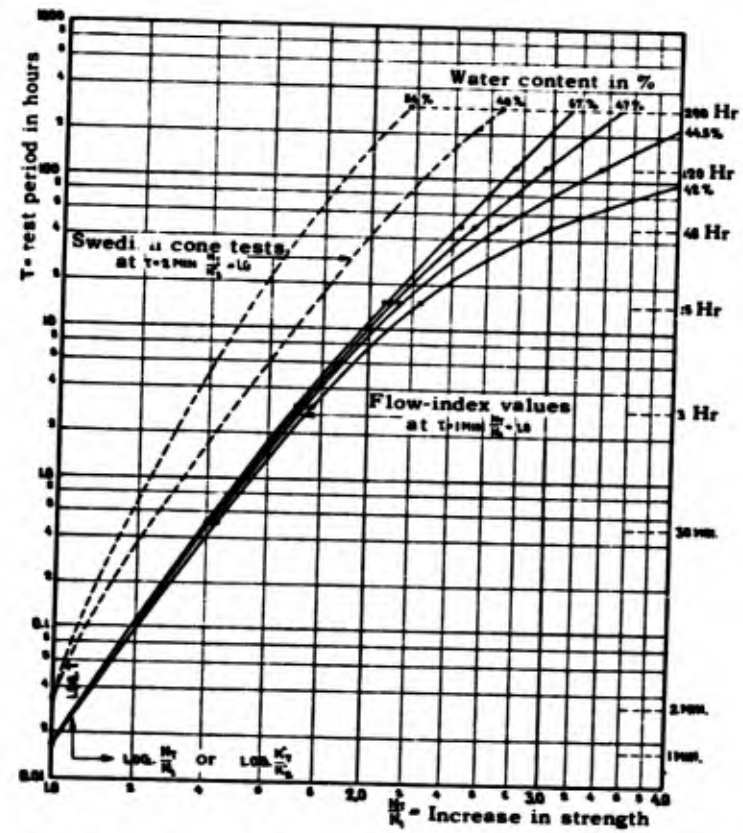

Fig. 19. Strength recovery of a remolded Vienna clay as a function of time

obtained, the thixotropic recovery of strength was also investigated by means of the Swedish cone device (fig. 20A), not only for Vienna clay but also for Little Belt clay. Dr. Ruth von Terzaghi has previously made similar investigations with various other soils (52).

After having been thoroughly remolded, the material was placed in a cylindrical bowl and its surface smoothed, whereupon the penetration depth t of a free-falling cone weighing 60 g and having an angle $2\alpha = 60^\circ$ was measured. Before the test, the cone is so placed that the point touches the surface of the soil. Hence the height of fall is also t. The test was repeated after several rest periods T (2 minutes to 290 hours). The water content of the specimen at the point of penetration of the cone was determined after each test. Between tests the bowl with the soil was placed under a water-sealed bell jar in order to prevent evaporation. However, it is not possible to keep the water content entirely constant during prolonged rest periods. For that reason a series of tests was made with soils of various water contents, as in the case of flow-index determinations.

38. With the weight of the cone Q and the depth of penetration t, the mean pressure q upon the contact surface between the cone and the horizontal surface of the soil is:

$$q = \frac{Q}{\pi t^2 \tan^2 30^\circ} = \frac{3}{\pi} \frac{Q}{t^2} \qquad (21)$$

Prandtl's theory (34) suggests, first, that q probably is independent of the weight of the cone and the corresponding value of t, and, secondly, that q is a function only of the strength or the shearing resistance of the material. However, it should be noted that Prandtl's theory is valid for the two-dimensional stress condition only, whereas the spatial problem has not yet been solved. Moreover, the cone angle 2α corresponds only on rare occasions to the effective angle or friction ϕ of the soil ($2\alpha = 90 - \phi$), and the friction between the soil and the smooth cone is at variance with the internal friction of the soil. And lastly, soils do not obey the same physical laws as the conventional plastic construction materials.

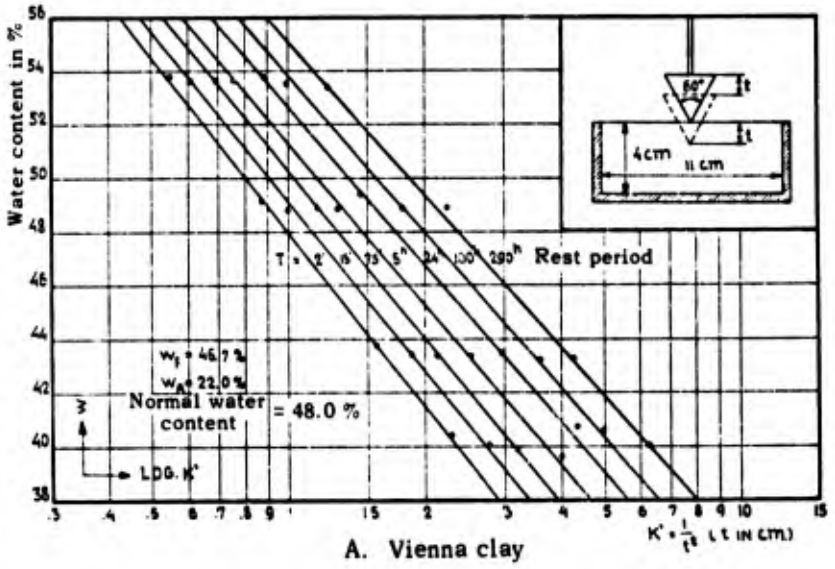

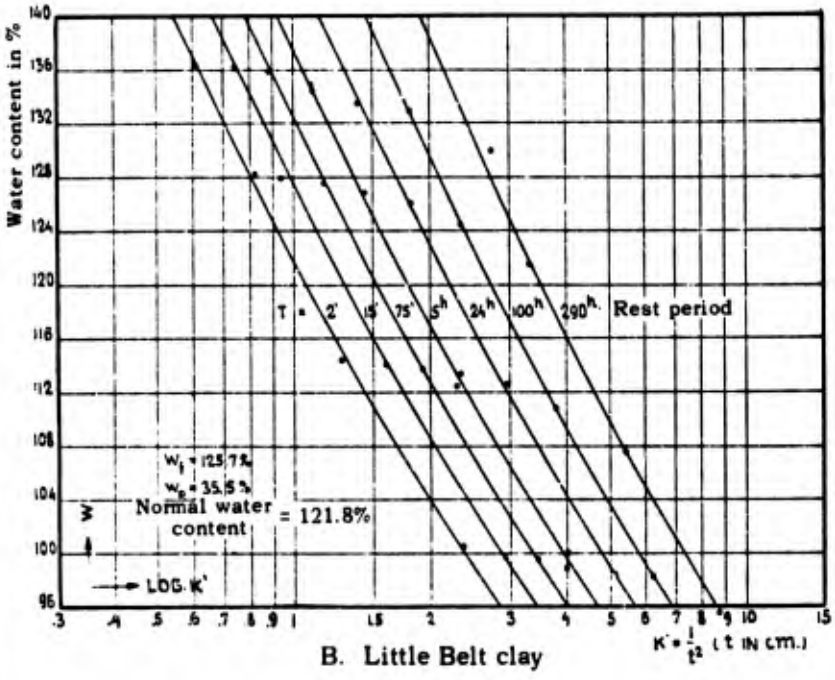

Fig. 20. Swedish cone tests for determining the strength recovery of remolded clay soils as a function of time

The investigations of several researchers showed that, at various values of the cone load Q, the ratio Q/t^2 is constant for some soils (Terzaghi (46), Buisman (9)), whereas for other soils the value Q/t^2 may be assumed constant only for minor changes of Q and t (Geotechnical Committee of the Swedish Railroads (43), Terzaghi (46), Bretting (7)). In order to circumvent these difficulties, the cone load K (consistency factor), at which the depth of penetration $t = 1$ cm, was designated as a measure of the strength of the soil.

Heretofore the relationship between q or K and the strength or the shearing resistance of the soil was chiefly determined by comparisons with the unconfined compressive strengths. An approximate linear relationship was found for many soils (46), (9), (43), (7). However, in the case of other soils such a relationship could only be established for smaller values of q or K. Above all, the coefficients in the linear relationship vary for different soil groups.

Better test results would doubtless be obtained by loading a balanced rough cone relatively slowly by means of weights or springs until a penetration depth $t = 1$ cm is reached. In this manner the impact effect of the falling cone would be eliminated and the consistency factor K would be measured directly.

For the present tests, which are only concerned with comparisons between various shear strengths s of the same soils, and where the weight Q of the cone is constant, the shear strength can be expressed by:

$$s = c_k \cdot \frac{1}{t^2} \tag{22}$$

in which c_k is assumed to be constant for a given soil and within certain boundary values of s and t. With

$$\frac{1}{t^2} = K' \tag{23}$$

and two specimens with shear strengths s_a and s_b and the corresponding penetration depths t_a and t_b there results:

$$\frac{s_a}{s_b} = \frac{K'_a}{K'_b} \qquad (24)$$

However, until more accurate investigations are available concerning the validity range of equation (22), equation (24) may be considered sufficiently accurate only for minor differences between s_a and s_b or, respectively, K'_a and K'_b.

39. The test results are shown in figs. 20A and 20B. The values log K' were plotted as abscissas and the water contents w as ordinates. The curves corresponding to the various rest periods form a family of almost parallel straight lines in the case of Vienna clay and a family of slightly curved lines in that of Little Belt clay. From these curves the values of T and K' corresponding to the various constant water contents are now derived, as in the case of the flow-index determinations. The curves obtained in this manner are represented in fig. 21. The rest period, corresponding to the first cone test of each test series, was estimated to be two minutes. The corresponding values of K' are designated as K'_2. In fig. 21 the values log K'_T/K'_2 are plotted as abscissas, and the values log T as ordinates. Slightly curved lines, the curvature of which increases somewhat with T, are obtained in this case also. This increasing curvature is probably caused partly by the formation of a soil surface layer with greater strength, and partly by the circumstance that the difference

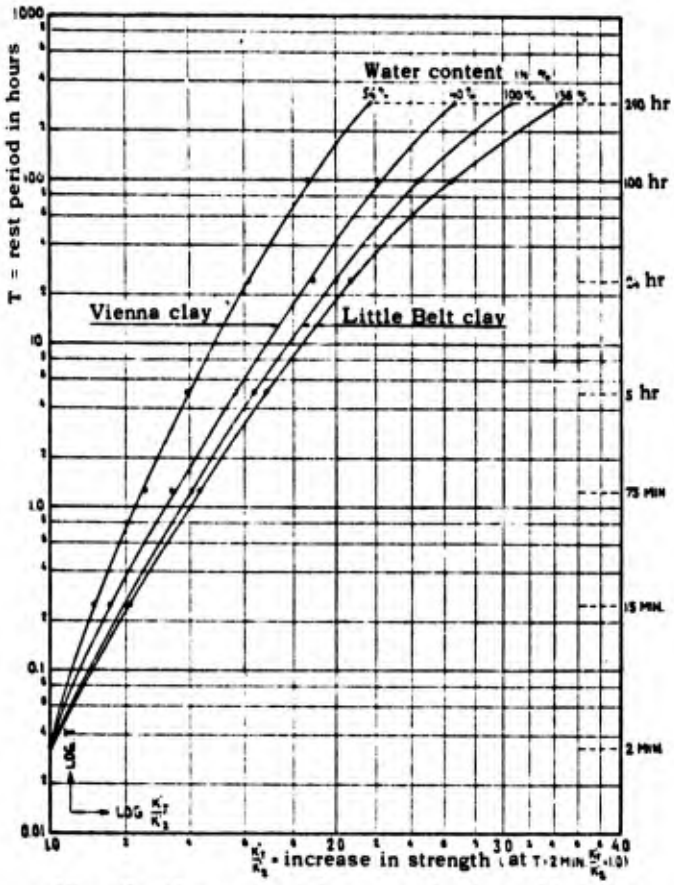

Fig. 21. Recovery of the strength of remolded clay soils as a function of time

between K'_T and K'_2 becomes so great that K'_T/K'_2 no longer indicates the actual increase in strength s_T/s_2 .

The curves for Vienna clay are also plotted in fig. 19 (dashed lines). Since the increases in strength determined by the liquid limit device are based on the rest period T = 1 minute, but those of the cone tests on T = 2 minutes, the latter curves must be shifted to the right for the purpose of comparison. As shown in fig. 19, the values of the increase in strength obtained from the cone tests are considerably lower at higher values of T than those determined by means of the liquid limit devices.

The results of these tests will be discussed further in the section on "Changes in the Shearing Resistance After Failure" and will be compared with a few results obtained by means of shear tests.

40. The curves in figs. 20A and 20B, also yield the values of the Swedish "Finlekstal" (according to Terzaghi (45): normal water content), i.e., the water content w_n at which the depth of penetration of a cone with a 60° angle and a weight of 60 g is equal to 1 cm (K' = 1). Furthermore, the values of t corresponding to the liquid limits w_f can be determined. These values and the corresponding values for two other soils, determined by Engineer Per Alenius (1), are shown in table 3.

Table 3

Comparison Between Liquid Limit and "Finlekstal"

	Liquid Limit		"Finlekstal"	
	w_f, %	t_f, mm	w_n, %	t_n, mm
Vienna clay	46.7	9.4	48.0	10.0
Little Belt clay	126.0	10.7	121.8	10.0
Halikko clay	7[illegible]	~12	68	10.0
Havel clay	49	~9	~51	10.0

Thus, Alenius's statement that the liquid limits and "Finlekstal" are almost identical also holds good for Vienna clay and Little Belt clay.

41. Heretofore the investigations concerning the effects of thixotropic disturbances were almost exclusively limited to changes in strength or viscosity. However, it would seem natural to assume that such a

thixotropic disturbance can also affect the permeability of the material. To clarify this problem, several tests were made with Vienna clay in order to determine the coefficient of permeability k_o as a function of the rest period after remolding. For these tests Terzaghi's consolidometer was used as a permeameter. In order to eliminate the effect of direct external forces, the dowel pin of the piston was not pulled out.

The tests showed that the value of the coefficient of permeability k_o immediately after remolding is a multiple of the normal values of k_o corresponding to the existing void ratio. The value of k_o decreases fairly rapidly with time, however, and in the course of 5 or 6 hours k_o again assumes its normal value. This phenomenon is partly caused by the seepage pressure and the subsequent consolidation of the specimen and discharge of the pore water. The effect of the formation of a relatively impervious surface film was investigated by tests with various specimen thicknesses. It was found to be very small in this case. Attempts were then made to determine the effect of the seepage pressure, partly by various test procedures and partly by means of computations according to the formulas proposed by Terzaghi-Frölich (53). This is difficult, however, without a more complete knowledge of the effect of thixotropic disturbances on the coefficients of consolidation and of swelling. Moreover, the effect of small inaccuracies in the devices, particularly in the fitting of the porous stones, may be very considerable.

For this reason, more accurate data concerning possible changes in the permeability caused by thixotropic disturbances cannot be furnished without further tests and improved equipment.

IV. THE TESTING DEVICES

Krey's Shear Apparatus with Terzaghi's Shear Boxes

42. The shearing resistance at failure was determined, except in a few control tests, by means of the Krey shear apparatus (29, 41, 42) with the improved shear box by Terzaghi.

The shear box with part of the shear apparatus is shown in figs. 22 and 23. The overall arrangement of Krey's shear apparatus as well as the preliminary consolidation devices and the ring shear apparatus, to be discussed later, are illustrated in fig. 24. The shear box consists of a

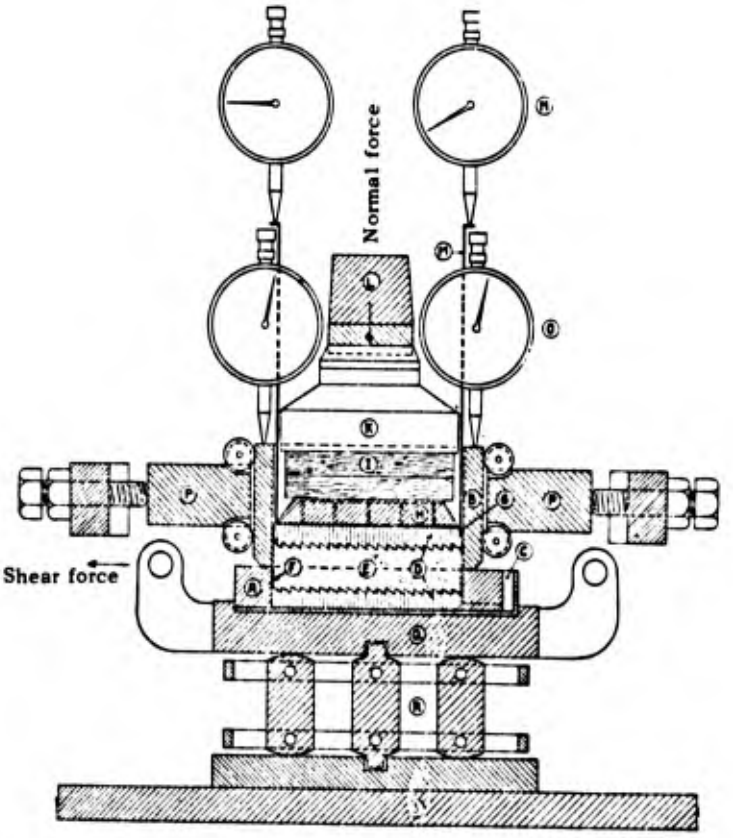

A Shear box base
B Shear box frame
C Water outlet
D Dentated porous stones
E Soil test specimen
F Greased filter paper
G Cotton wadding
H Perforated pressure plate
I Wood inserts
K Piston with steel knife edge
L Load lever
M Sheet metal inlay with gage stops
N Gages indicating vertical motion of sample
O Gages indicating vertical motion of frame
P Guide bars with ball bearings
Q Sliding base
R Rocker bearing
S Supporting bench

Fig. 22. Krey's shear apparatus with Terzaghi's shear box

Fig. 23. Terzaghi's shear box

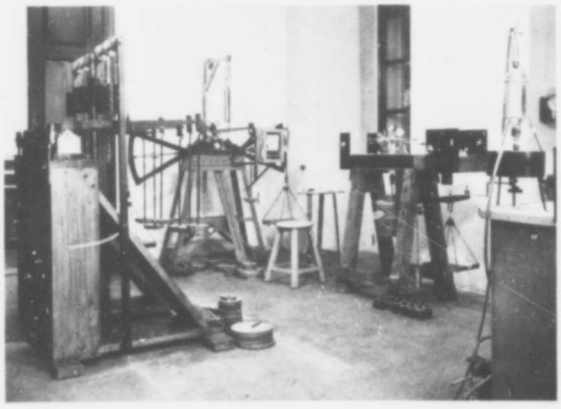

Fig. 24. Preliminary consolidation devices, Krey's shear apparatus, ring shear apparatus

lower part A that fits tightly in a recess of sliding carriage Q, and an upper part or frame B. Test specimen E is held between two dentated, porous stones D, one of which is firmly secured in the lower part, whereas the other is ground somewhat obliquely on three sides in order to prevent its becoming wedged in the frame. The vertical normal pressure is transmitted to the upper stone D through pressure lever L, piston K, and inserts I and H. The shear load is exerted on sliding carriage Q via two balanced sector levers (fig. 24) at the exact level of the shear plane. At shear failure, the sliding carriage and the lower portion of the shear box are shifted to the left in a horizontal direction, whereas the frame is held by the guide bars in such a manner that it can move in a vertical direction only.

The inner walls of the shear box are lubricated with vaseline in the area of contact with the specimen and are lined with filter paper. This serves the following purposes: first, the friction between frame and soil is reduced; second, the dewatering of the soil is accelerated, and third, the filter paper prevents the clay from being squeezed out. In the event that clay is forced out between the frame and the base of the shear box, the measured changes in the thickness of the test specimen no longer correspond to volume changes of the soil. However, the use of filter paper has the disadvantage that it causes an apparent increase in the shearing resistance of the soil.

The change in the thickness of the test specimen during the shear test usually increases somewhat from left to right (figs. 22 and 25) as a result of compressive deformation of the soil and friction between the upper stone and the front wall of the frame; hence it must be measured with the aid of two gages (N). In tests with highly overconsolidated soils, the frame experiences a slight upward movement which is measured by means of gages O. The horizontal motions of the sliding base are measured by a gage not shown in fig. 22, and in addition they are automatically registered on a recording drum, magnified tenfold.

The shear boxes are usually fastened in the shear device after the soil has been consolidated in a preliminary consolidation apparatus, and 12 hours before the start of the shear test. This procedure increases the

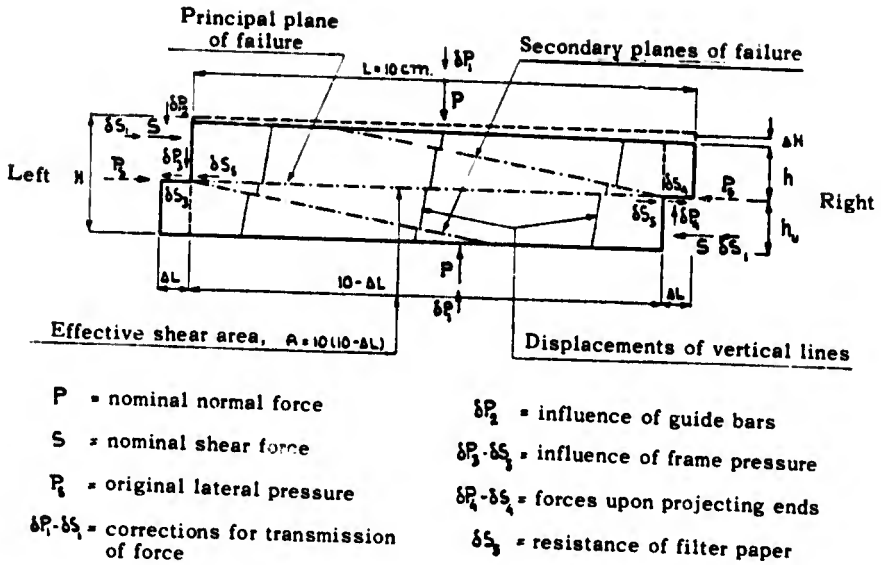

Fig. 25. Shear test specimen. Displacements and external forces

effectiveness of the shear device but has the disadvantage that the test specimen must be completely unloaded during the transfer.

Corrections for the External Forces

43. During the shear test, various additional normal and shear forces occur in the shear device and in the shear box as a result of displacements and internal friction. Moreover, the effective cross section of the specimen is reduced. The first problem is to determine these additional forces and thus the normal and shear forces actually existing in the effective shear plane $L\ (L - \Delta L)$ in fig. 25. L is the lateral length of the originally quadratic shear plane.

The separation and determination of these frequently very small forces required many carefully conducted tests and was complicated by inevitable small deviations in the test results. The corrections largely depend upon the state of consolidation of the specimen and upon the test procedure. Moreover, some of the individual corrections vary from one shear box to another. For this reason, simplified correction formulas cannot be given. The differences between the nominal mean stresses, P/L^2 and S/L^2, and the corrected mean stresses:

$$\frac{P + \Sigma\delta P}{L(L - \Delta L)} \quad \text{and} \quad \frac{S + \Sigma\delta S}{L(L - \Delta L)}$$

usually amount to only a few percent, except when the stresses themselves are very small.

Deformations of the Test Specimen

44. The internal displacements of the test specimen and the location of the planes of failure were investigated by the coloring of thin, vertical zones in the soil. A general illustration of the internal and external displacements of the test specimen is given in fig. 25. The form of the internal displacements changes considerably with the test procedure and the state of consolidation of the specimen, as illustrated in fig. 26. Figs. 26A, 26B, and 26C show that, at the moment of failure, the displacements are fairly uniform over the greater part of the cross section. The oblique planes of failure do not develop until the more rapid plastic flow has progressed to some extent. They are probably caused by local elimination of the lateral pressure ($p_s = \zeta p$) and the consequent squeezing out of clay by the vertical load. These inclined planes of failure apparently do not affect the overall strength of the specimen and do not as a rule occur in the case of rapid tests (fig. 26F) or tests with highly overconsolidated soils (fig. 26H).

45. At the moment of failure, the two-thirds portion of the middle cross sections does not, as a rule, exhibit any irregular deformations, whereas, at the ends of the specimen, the displacements are concentrated in the principal shear zone. Because of the lateral friction, such a concentration of the displacements also occurs to a lesser extent on the sides (parallel to the direction of shear) of the specimen (fig. 26J). Coloring of vertical zones revealed that this concentration of the displacements occurs over a width of 5 to 7 mm only (fig. 26E).

In places where the displacements are concentrated in the shear zone, early failure and a consequent reduction in the shearing resistance occur. For this reason, the mean shear stress at failure is somewhat lower than the actual maximum stress, i.e., than the peak shearing resistance. The

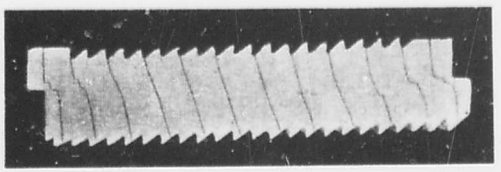

Center $p = 2$ $T_s = 88$ $H = 2.0$ $\Delta L = 3.5$ $\Delta L' = 4.0$

A

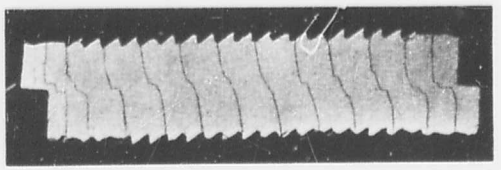

Center $p = 2$ $T_s = 76$ $H = 2.0$ $\Delta L = 4.0$ $\Delta L' = 6.1$

D

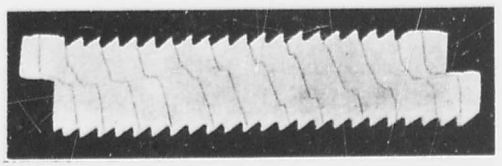

Center $p = 2$ $T_s = 89$ $H = 1.9$ $\Delta L = 4.5$ $\Delta L' = 8.5$

B

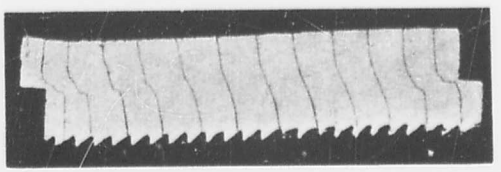

Side $p = 2$ $T_s = 76$ $H = 2.0$ $\Delta L = 4.0$ $\Delta L' = 6.1$

E

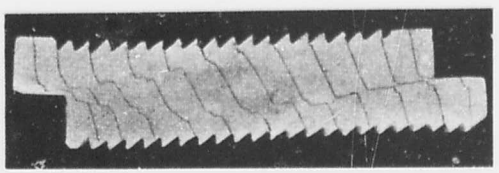

Center $p = 2$ $T_s = 84$ $H = 2.0$ $\Delta L = 3.7$ $\Delta L' = 13.0$

C

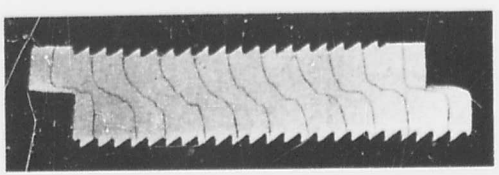

Center $p = 2$ $T_s = 3$ $H = 2.0$ $\Delta L = 4.7$ $\Delta L' = 13.0$

F

Fig. 26

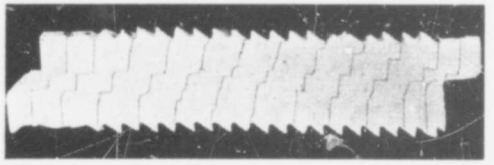

Center p = 5·0·1 T_s = 460 H = 1.9 ΔL = 4.8 $\Delta L'$ = 9.0

G

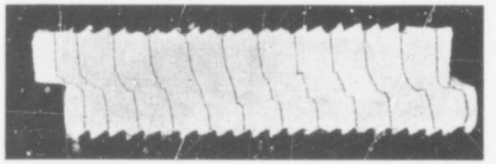

Center p = 5·0·½ T_s = 3 H = 2.2 ΔL = 4.5 $\Delta L'$ = 10.0

I

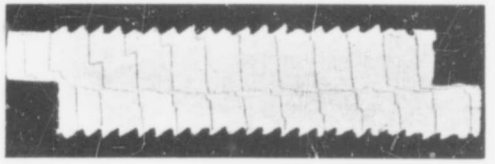

Center p = 5·0·½ T_s = 390 H = 2.2 ΔL = 4.0 $\Delta L'$ = 13.0

H

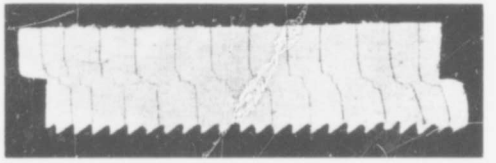

Side p = 5·0·½ T_s = 3 H = 2.2 ΔL = 4.5 $\Delta L'$ = 10.0

J

p = normal stress in kg/cm^2
T_s = equivalent duration of shear test in minutes
H = specimen thickness in cm

ΔL = displacement at failure in mm
$\Delta L'$ = displacement at end of test in mm

Fig. 26. Internal deformations of the shear test specimen.
Vienna clay in Terzaghi's shear boxes

extent of the zone of concentration can be estimated from the displacement diagrams (fig. 26), while the reduction in shearing resistance in these zones can be estimated by means of the stress-strain curves for shear, shown later. These considerations indicated that, for the soils investigated here, the mean shear stress at failure is only a few percent (3 to 5 percent) smaller than the actual maximum stress.

This conclusion is also confirmed by the observation that, in the case of slow shear tests, the thickness of the test specimen has no appreciable effect on the values obtained for the shearing resistance when this thickness ranges from 0.4 to 4.0 cm.. The values of the shearing resistance reported hereafter are the mean shear stresses corresponding to the corrected external forces at the moment of failure.

Effect of the Dentation of the Porous Stones

46. At very small thicknesses of the test specimen, the teeth of the porous stones may affect the actual shearing resistance of the specimen. In order to investigate this possibility, consolidation tests with Vienna clay and porous stones having 2-cm-high teeth were undertaken first. The internal displacements and states of consolidation were investigated by means of colored zones (fig. 27) and water content determinations (fig. 28). These two procedures revealed arching between the teeth and particularly the development of a zone of increased strength at the tips of the teeth. Fig. 28 shows that the equivalent pressure at the bottom of the teeth is only one-tenth of the equivalent pressure at their tips, and that the latter pressure is approximately 70 percent higher than the mean equivalent pressure. However, a fairly uniform pressure distribution is encountered at a height of about one-half the distance between the teeth above their tips.

47. Slow shear tests were then performed using the stones shown in fig. 22 (height of teeth 2.6 mm, distance between teeth 4.6 mm). In these tests the shear plane was set 1 mm above the teeth of the lower stone, and the total thickness of the specimen amounted to 1.4 cm. Shearing was performed in the direction of the teeth as well as in the opposite direction.

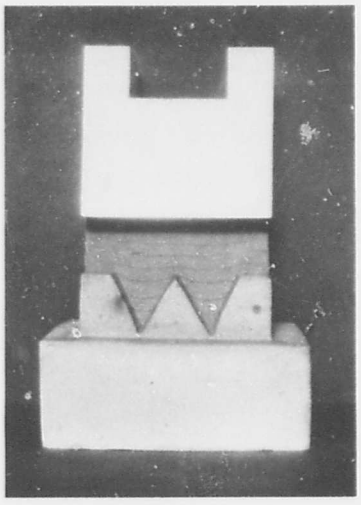

A. Test arrangement (frame removed)

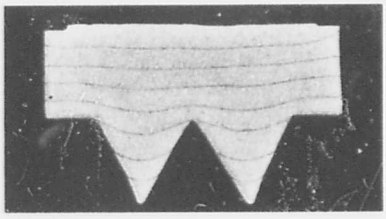

B. Horizontal layers

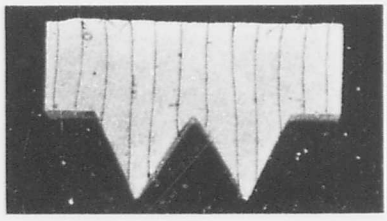

C. Vertical layers

Fig. 27. Effect of dentation. Model test with Vienna clay

Directly measured water content for Vienna clay at a normal pressure of 7.0 kg/cm^2

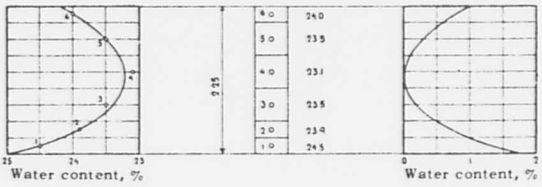

Correction curve obtained for the absorption of water during dismantling

Comparative test with pressure plates without teeth

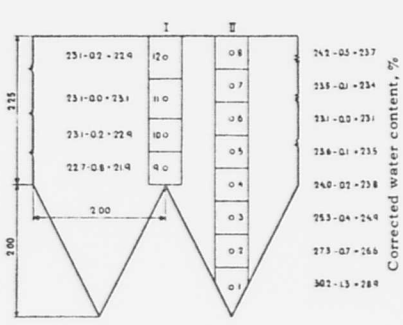

Division of the specimen

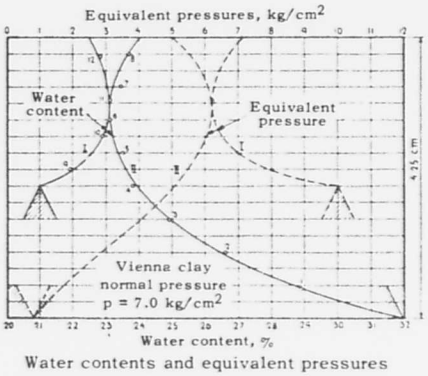

Water contents and equivalent pressures

Fig. 28. Model tests for determining the consolidation in the vicinity of the teeth

The tests revealed that the surface of failure does not lie in the shear plane but 2 to 3 mm above the teeth (fig. 29), and that the direction of the teeth has no influence on the test results. Furthermore, tests with normally consolidated soils gave the same values of the shearing resistance as those obtained in tests with 2.4-cm-thick specimens and with the shear plane at the center; on the other hand, values obtained for strongly overconsolidated soils were from 5 to 8 percent lower.

This result was of great significance for design of the ring shear apparatus described in the appendix, since in this apparatus shear failure may occur just below the teeth of the piston.

48. Finally the dentated porous stones were replaced by rough, porous stones, both coarse-grained and fine-grained. When the shear plane was set at 1 mm above the stones, the tests with the coarse-grained stones yielded the same values of the shearing resistance as those with dentated stones, whereas the tests with fine-grained stones yielded somewhat lower values in a few cases. As can be seen in fig. 30, the failure surface lies 1 to 2 mm above the stone when coarse-grained stones are used, but shear occurs in some places along the surface of the stone when fine-grained stones are used.

The Ring Shear Apparatus

49. A torsion apparatus for test specimens with an annular cross section was used to investigate the changes in the shearing resistance after failure as well as the slow plastic flow before failure. The design and calibration of this apparatus is described in detail in the appendix.

A. Displacement against the direction of the teeth

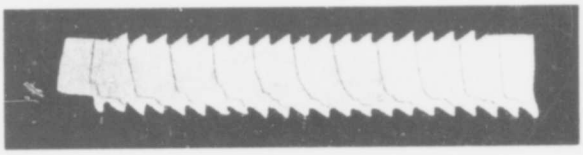

B. Displacement in the direction of the teeth

Fig. 29. Shearing just above the teeth

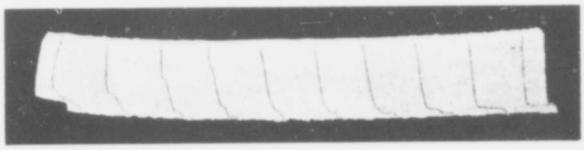

A. Coarse-grained stone

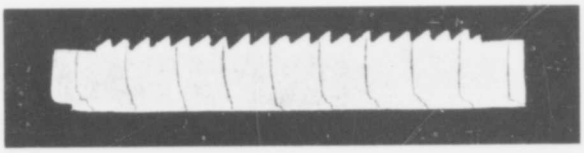

B. Fine-grained stone

Fig. 30. Shearing just above rough, porous stones

V. TESTING PROCEDURES

Preparation of Test Specimens

50. During the homogenization, the large stocks of test material mentioned earlier were prepared with a water content slightly above the liquid limit. In order to counteract the thixotropic increase in strength that had occurred in the course of time, the required quantity was thoroughly remolded just before placing it in the shear boxes.

For tests with normally consolidated soils, the specimens were consolidated during 7 to 10 days in the preliminary consolidation devices under various pressures ranging from 0.5 to 5.0 kg/cm^2, whereupon they were subjected to shear in the shear apparatus under the same vertical pressure. For simple overconsolidation, the specimens were first consolidated during 7 to 10 days under a pressure of 5.0 kg/cm^2, unloaded to between 0.2 and 5.0 kg/cm^2, and allowed to swell for a period of 7 days before the shear test was performed under the same pressure. This consolidation process is designated as (5-p-p) for the sake of simplicity. It must be emphasized that the shear test should not be started until the process of swelling as well as consolidation is fully completed. If the negative pressure in the pore water caused by the unloading operation is not entirely equalized, a flow will occur from the outside to the inside, and the corresponding seepage pressure will act as an additional effective normal pressure on the shear plane. During cyclic overconsolidation, the soil was first reconsolidated under a pressure of 5 kg/cm^2, completely unloaded to zero, and allowed to swell for seven days, after which it was again consolidated for another seven days under a pressure ranging from 0.2 to 5 kg/cm^2, and eventually subjected to shear under this pressure. This consolidation process is designated as (5-0-p). A few specimens that were only preloaded with 2.0 kg/cm^2 instead of 5.0 kg/cm^2 are designated by (2-p-p) and (2-0-p) in the diagrams.

This relatively long duration of the consolidation process was chosen in order to eliminate the effect of minor differences in time.

Approximately 12 hours before the start of the shear test the test

specimen was unloaded, the shear box was fastened in the shear apparatus, and the specimen was reloaded as soon as possible. During the entire consolidation process and also during the shear operation, the space between piston and frame as well as the drain (C in fig. 22) was filled with water in order to prevent desiccation or the development of a capillary pressure.

The Shear Test

51. As mentioned before, Casagrande and Albert (14) have shown that, in normally consolidated soils, a fairly large decrease in the water content occurs during the shearing process. As a result, a temporary hydrostatic excess pressure develops in the pore water which causes a reduction in the effective normal pressures. In the course of time this reduction is again equalized when the pore water is forced out. Since this process requires considerable time because of the low permeability of clay, the value of the shearing resistance depends to a large extent on the duration of the shear test.

This effect was investigated by Casagrande and Jürgenson (26) for normally consolidated soils. The author of this paper made similar investigations and extended them to soils in the overconsolidated state. In addition, the effect of the specimen thickness and of the various test arrangements was investigated. During these tests, the load increments ΔS of the shear load amounted to approximately 2 percent of the ultimate load, while during the shearing process the time interval ΔT of the load increment differed not only in the case of the individual tests but also during slow tests. In this manner it was possible to obtain an almost full equalization of the pore-water pressures and yet to complete the shear test within one day. Fig. 31 shows a typical load-time diagram for shear tests with Vienna clay. The tests made in this manner will henceforth be called standard tests, whereas tests of considerably longer duration will be designated as long-duration tests.

52. The effect of the actual shear test duration T depends on the shape of the load-time curve. Hence in order to be able to compare tests

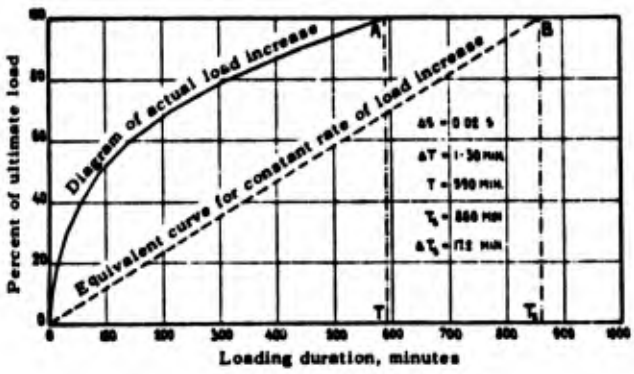

Fig. 31. Loading diagram and equivalent test duration

with dissimilar load-time curves with each other, the equivalent shear test duration T_s was introduced. The latter was obtained from the condition that the areas OAT and OBT_s in fig. 31 be equal to each other. T_s corresponds to a total shear time for which, at constant load increments and time intervals, the excess pore-water pressures attain the same degree of equalization as in the case of the actual shear time T .

Fig. 32 shows the results of the tests concerning the effect of T_s upon the shearing resistance. In accordance with earlier investigations of Casagrande and Jürgenson, the shearing resistance of normally consolidated soils increases with T_s . However, while the specimen thickness appears to have but little effect upon the results of very rapid and very slow shear tests, the effect of the specimen thickness is very pronounced for intermediate values of T_s . The tests also revealed that, in the case of highly overconsolidated soils, the shearing resistance decreases with T_s . As will be shown later, an increase instead of a decrease of the void ratio occurs during the test in this case, which implies a temporary underpressure in the pore water with corresponding increase of the effective pressures. The equalization of this underpressure causes part of the decrease in shearing resistance with T_s , whereas another part may be attributed to the effect of the viscosity.

53. The influence of a partial or complete prevention of the water content adjustments in the shear zone is demonstrated by the following

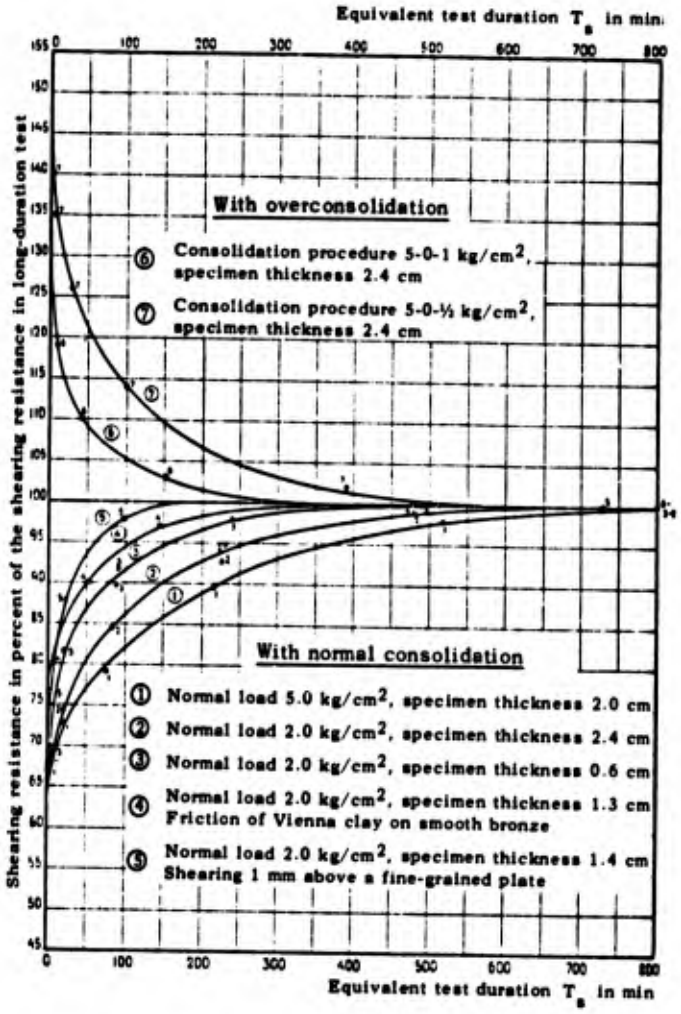

Fig. 32. Relationship between shearing resistance, duration of shear test, and the test arrangement for Vienna clay

results of some tests performed in the spring of 1933 by the author together with Engineer K. Kienzl at the suggestion of Professor Terzaghi.

First, three specimens of homogenized Vienna clay were normally consolidated under the pressures of 1, 2, and 3 kg/cm^2. After the consolidation was completed, shear tests were performed with constant load increments, $\Delta S = 1/40\ p$ (in which p is the total normal pressure), and constant time intervals $\Delta T_s = 1$ min were used. The equivalent shear test duration is then equal to the total duration or $T_s = 40\ s/p$. The shearing resistances obtained and the corresponding water contents of the shear zone at the moment of failure are represented by curves A-B and C-D in

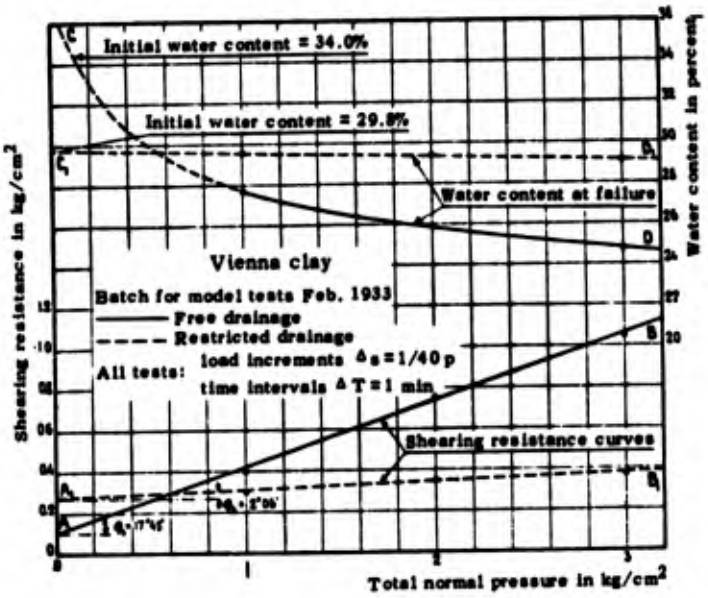

Fig. 32B. Shear tests with restricted drainage of the specimen

fig. 32B. At full equalization of the excess pore-water pressures produced by shear stresses, the shearing resistance curve of this normally consolidated Vienna clay goes through the point of origin and has an angle of inclination ϕ_s of approximately 25°.

The above-mentioned tests yielded $\phi_s = 17°45'$, and the shearing resistance curve intersects the ordinate axis at point A. The decrease of the angle of the apparent internal friction from 25° to 17°45' is caused by an incomplete equalization of the excess pore-water pressures. The development of the apparent cohesion O-A may be explained by the circumstance that, at increasing consolidation pressure p, the permeability and, in this case, also T_s, decrease (T_s = 16, 15, and 14 min). The greater p is, then the smaller the partial equalization of the excess pore-water pressure and also s/p. This results in a slightly curved shearing resistance line which in this case is replaced by the straight line A-B. The values of the cohesion and of the angle of internal friction obtained from such shear tests therefore have nothing to do with the true values of these strength coefficients.

When the water content of the soil is kept completely constant

during both shear test and consolidation procedure, all changes in the external normal pressure are absorbed by the pore water because of the rigid side walls of the shear box. The effective normal pressure is then unaffected by the external normal pressure and depends only on the water content or the capillary pressure of the test material when it is placed in the shear box. In this case a horizontal shearing resistance line should be obtained.

During performance of such tests the porous stones (D in fig. 22) were replaced by dentated metal plates, and the filter paper (F in fig. 22) by a thin rubber membrane. In addition, all joints were sealed with a mixture consisting of equal parts of paraffin and colophony. The actual shear test was started approximately one hour after application of the normal load, also using $\Delta S = 1/40\ p$ and $\Delta T_s = 1$ min. The test results are represented by dashed lines A_1-B_1 and C_1-D_1, fig. 32B. Despite the careful sealing it was impossible to keep the water content completely constant. It decreases to some extent with increasing normal pressure, and the shearing resistance curve A_1-B_1 shows a corresponding inclination $\phi_s = 2^\circ 06'$. It is possible that the shearing resistance curve may have a slight inclination even though the water content remains completely constant. When the specimen contains small air bubbles, these bubbles may permit a partial equalization of the excess pore-water pressures without a change in the total water content because of their high compressibility. This possibility exists particularly in the case of overconsolidated or undisturbed soils in which the volume changes caused by the pressure variations are relatively small.

Effect of Thickness of the Test Specimen

54. As mentioned before, the specimen thickness does not appear to affect (within certain limits) the values obtained for the shearing resistance, provided a complete equalization of the hydrodynamic pressures in the pore water occurs. Since the smaller the specimen thickness is, the more rapidly this equalization takes place, it appears to be expedient to keep the specimen as thin as possible. However, it must be

borne in mind that the soil specimen absorbs a small but not inconsiderable amount of water during dismantling after the shear test is completed. This is clearly indicated by the upper curves in fig. 28. Therefore, the water content in the plane of failure may also be affected in the case of thin specimens. Hence, in order to obtain reliable values for the water content in the zone of failure at the instant of failure, the specimen must have a certain minimum thickness. This lower limit of the specimen thickness depends upon the state of consolidation of the soil as well as on the corresponding permeability.

In the tests with Vienna clay, discussed in the following sections, the thickness of the test specimens varied from 2.0 to 2.4 cm and in tests with Little Belt clay, from 1.8 to 2.0 cm. However, the water content can be determined with a sufficient degree of accuracy even in the case of specimens ranging in thickness from 1.5 to 2.0 cm, depending on the material and its state of consolidation. Nevertheless, there is then danger that the water content in the zone of failure may be affected when the dismantling of the shear box and the cutting out of small sections of the test specimen are not carried out smoothly and rapidly.

55. The distribution of the shear stresses along the vertical cross section of the test specimen depends on the latter's thickness. As a result, the relation (k_e) between the mean change in the void ratio of the specimen as a whole and the change in the void ratio in the zone of failure becomes a function of the specimen thickness, i.e., for a given state of consolidation of the specimen, the corresponding settlement or rise of the specimen surface during the shear test is a function of its thickness.

For the Terzaghi shear box in which the frame is not raised, curve O-A in fig. 33A shows the relation between the total settlement ΔH and the specimen thickness H in the case of Vienna clay in the normally consolidated state and a normal pressure $p = 2.0\ kg/cm^2$. This curve is used for reducing the total settlements observed in shear tests with various specimen thicknesses to those for a single thickness. The formulas derived in fig. 33A for the coefficient k_e and the effective specimen thickness will be explained later. The settlements of the specimen surface in other experimental arrangements and testing devices

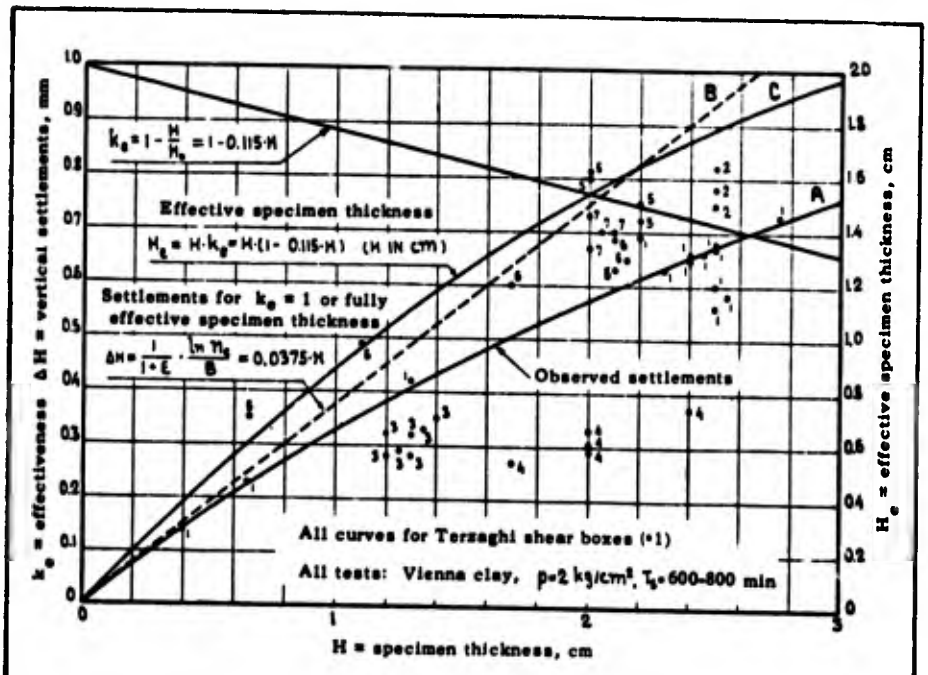

A. Vertical settlements

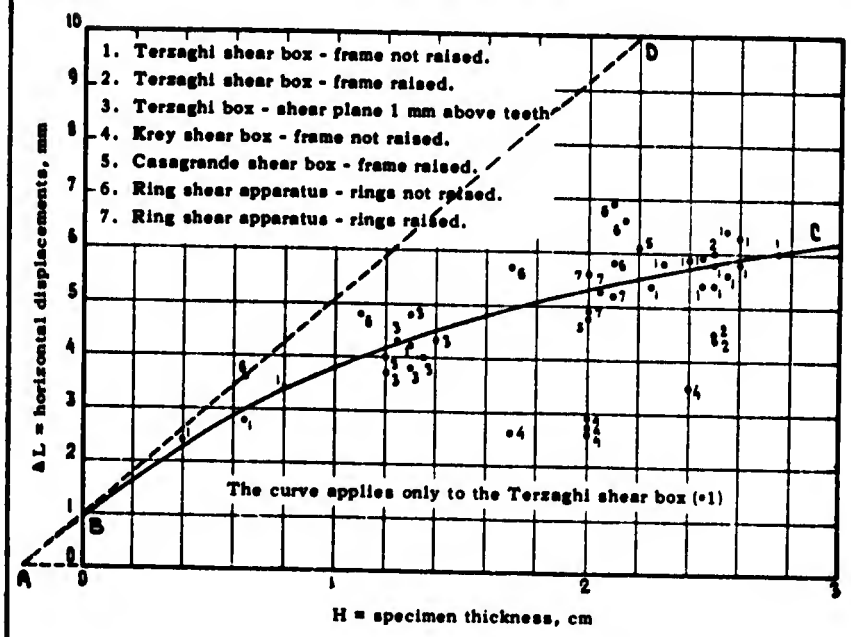

B. Horizontal displacements

Fig. 33. Effect of specimen thickness and test arrangement

are also included. They show that a specimen is subject to major settlements when the frame is raised. This is caused by the clay being forced out between the raised frame and the base of the shear box. On the other hand, smaller settlements occur in both the Terzaghi and Krey shear boxes when the specimen is sheared off just above the teeth.

56. In fig. 33B the horizontal displacements (ΔL in fig. 25) corresponding to the settlements are plotted. Since the values of the displacements at the moment of failure cannot be defined accurately, the displacement values corresponding to a shear stress of 98 percent of the failure stress were used. Curve A-B-C refers to the Terzaghi shear box in which the frame is not raised. In this case the curve does not pass through the origin, but intersects the axis of abscissas at A. The thickness O-A = 0.25 cm probably represents the effect of the material between the teeth of the porous stones.

The effective specimen thickness is $H_e = (H + 0.25)\, k_e$, in which k_e is the relation between the ordinates of curve A-B-C and of tangent A-D. These values of k_e differ from the values of k_e corresponding to the settlements and should only be considered as approximations since the location of tangent A-D is uncertain and cannot be verified by determining the water content as in the case of settlements.

The fairly large scattering of the test results shown in figs. 33A and 33B within the individual test series is partly caused by the fact that different small batches were used for the test specimens, and partly by plastic flow just before failure.

Determination of the Water Content

57. Immediately after failure the shear box is dismantled as rapidly as possible. A 2-cm-wide and 3-mm-thick strip is cut from the zone of failure, subdivided into five sections, and weighed (fig. 34). The dry weight is determined after the small sections have been dried for 24 hours at a temperature of 105° Centigrade. The slight increase in the water content caused by water absorption at the ends of the specimen is taken into account (see fig. 28), and the mean water content in the zone of failure

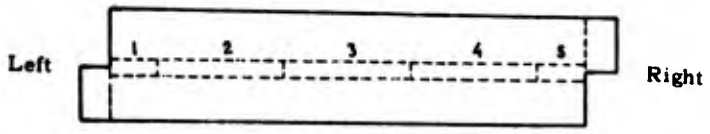

Fig. 34. Cutting out small sections for determining water content

is computed. In standard tests the water content usually decreases somewhat from left to right (fig. 34), but in tests where the specimen is sheared off just above the teeth it increases in that direction.

In the case of long-duration tests, the void ratios of the zone of failure corresponding to the individual load increments can be computed from the direct settlement measurements and by means of the curves and formulas shown in fig. 33.

VI. DEFORMATIONS BEFORE FAILURE

Deformations Occurring During Standard Tests

58. Typical stress-deformation curves for shear tests with Krey's shear apparatus and Terzaghi's shear boxes in conjunction with the loading process shown in fig. 31 (standard tests) are plotted in fig. 35. The oblique settlement and swelling of the specimen surface caused by lateral friction and compressive deformation are clearly noticeable. Similar curves, taken from corresponding tests with the ring shear apparatus, are shown in fig. 36 and in the appendix.

The shape of these curves is, of course, affected by the loading procedure. This applies particularly to the shapes of the settlement and swelling curves, when the corresponding volume changes cannot occur because of the initially fairly rapid load increase. As illustrated in fig. 36, for this loading procedure the displacement curves ΔL appear to correspond approximately to the equation

$$\tau = \beta_1 \Delta L^m$$

and for the ring shear apparatus to:

$$\tau = \beta_2 \theta^m$$

up to the vicinity of failure. Assuming that a linear relation exists between ΔL or θ, on the one hand, and the shear strain γ, the following equation applies:

$$\tau = \beta \gamma^m \qquad (25)$$

Since the coefficients of the relation between ΔL or θ and γ cannot be determined with a sufficient degree of accuracy, the coefficients β in equation (25) cannot yet be computed. On the other hand, the exponents m can easily be determined from the curves in fig. 36. In the case of

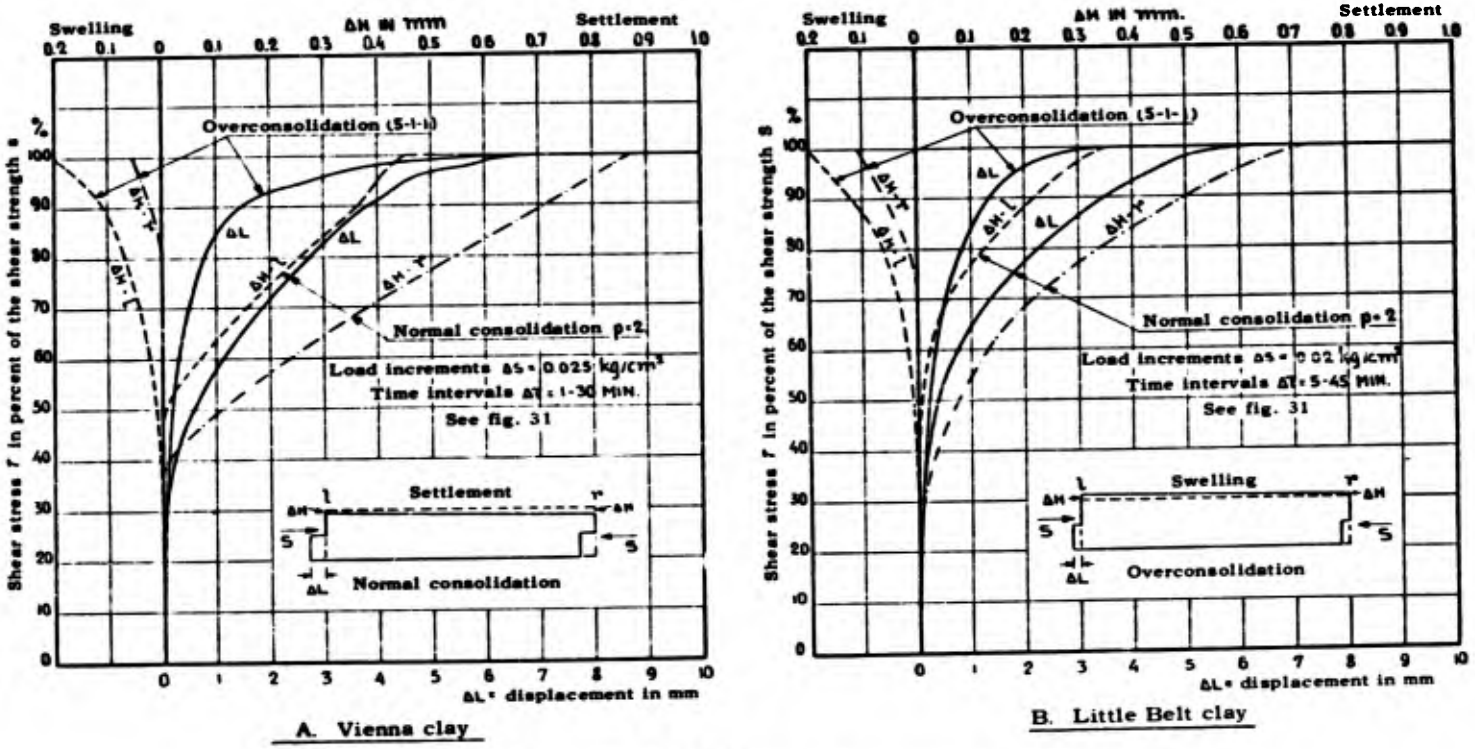

Fig. 35. Deformations of the test specimen during shear test

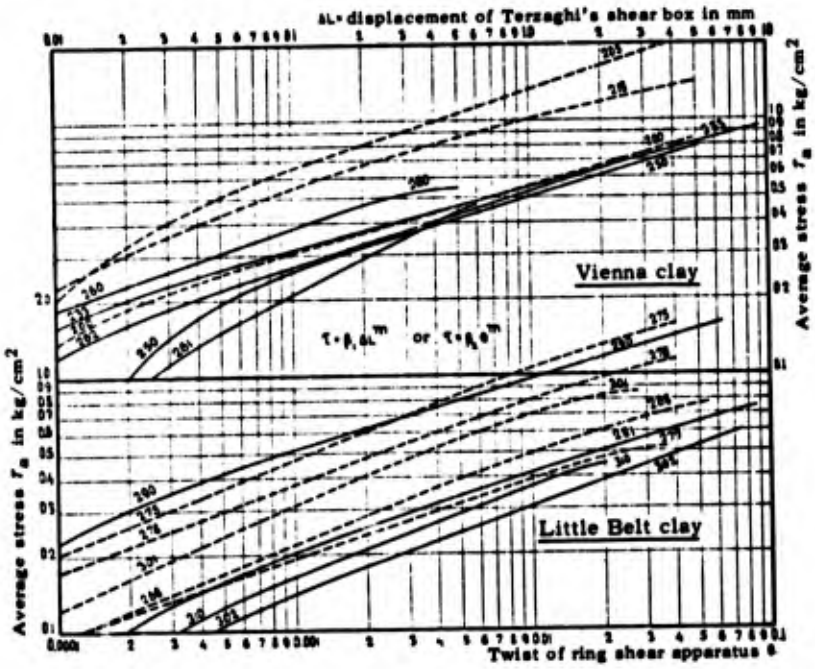

Vienna clay

No.	p	τ_s	h	m
280	2	664'	24	0.285
285	5	834'	235	0.310
218	5-0-3	646'	24	(0.260)
233	2	1300	21	0.248
290	2	11 d	21	0.278
292	2	25 d	18	0.295
288	5-1-1	483'	20	0.316
281	5-0-1	11 d	285	0.465

d = days

Little Belt clay

No.	p	τ_s	h	m
286	2	1000'	17	(0.3711)
275	5	683'	19	(0.3561)
277	5-0-1	817	18	0.304
301	5-2-2	1072	1.78	(0.3781)
278	5-0-3	1013'	185	(0.3321)
281	2	2630'	16	(0.3081)
302	2	985'	16	0.335
290	5	1160'	14	0.275
310	5-1-1	625'	15	0.358

------- Terzaghi's shear box

——— Ring shear apparatus

Fig. 36. Stress-deformation curves for pure shear load

long-duration tests, only the central portion of the displacement curves complies with equation (25). Both at the start of a test and immediately before failure the displacements are greater than the values computed by equation (25).

Effect of Unloading and Reloading

59. A long-duration test (ΔT = 24 hours) was made in a ring shear apparatus with normally consolidated Vienna clay. In this test the soil

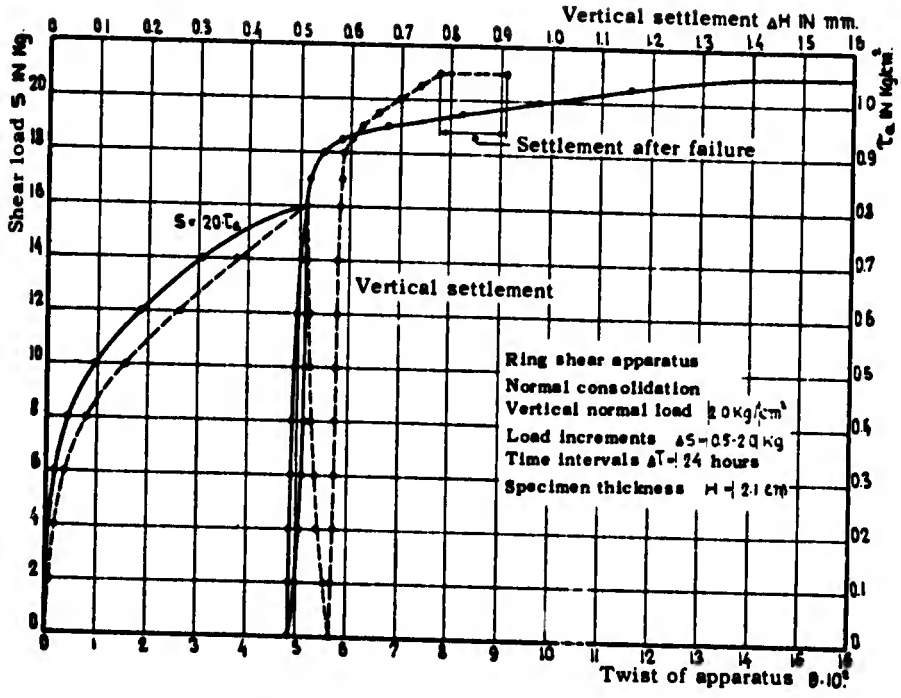

Fig. 37. Vienna clay long-duration test with hysteresis loop

specimen was fully unloaded and reloaded after 80 percent of the failure load had been reached. As may be seen in fig. 37, a reduction in the shear stress causes an interruption in the shear displacements which are not resumed until the inversion point has been exceeded considerably. The clay has become stiffer and the maximum shearing resistance has been increased approximately 5 percent by this loading procedure.

Attention is called particularly to the fact that the settlement curve has the shape of a zigzag line, whereas the displacement curve forms a complete hysteresis loop. At the start of unloading this zigzag line is almost vertical, but as τ decreases it becomes slightly curved to the right. This shape indicates that the additional settlement is not an aftereffect of the earlier shear load, but that a decrease as well as an increase of the shear stress produces an excess pore-water pressure and a decrease in the void ratio. Other tests show that, in the case of a strong overconsolidation of the soil, both an increase and a decrease of the shear stress cause a negative pressure in the pore water and an increase in the void ratio. These results indicate that part of the volume

change caused by shear stresses can be explained by the fact that such stresses actually represent an increase in one principal stress, accompanied by a numerically equal decrease of the other principal stress. The variations in volume connected therewith are different for the two stress changes.

The Slow, Plastic Flow Before Failure

60. Terzaghi (50) made unconfined compression tests to determine the starting stress and velocity of the slow, plastic flow prior to actual failure. Despite the small increase in the cross section caused by settlements, he found that, at a compressive stress of approximately 50 percent of the compressive stress at failure, these settlements continue at a very low though almost constant velocity even after half a year. In such tests it is difficult, however, to keep the water content of the specimen and hence the physical properties and the capillary pressure completely constant for such a long period. These disadvantages of compression tests are avoided when the ring shear apparatus is used. The cross section remains constant and the specimen is always under water so that the unknown and variable capillary pressure is eliminated. On the other hand, the practical performance of such investigations is rendered much more difficult because of the uninterrupted, prolonged use of the shear apparatus.

61. Fig. 38 shows the results of a somewhat shortened test with Little Belt clay in a state of strong, simple overconsolidation (5-1-1).

The time interval between the load increments was approximately 10 days. As may be seen from the time-twist curves, the velocity of the plastic flow reached a fairly constant value at the end of this time interval, even though it still decreased at a small rate.

When the velocities (represented by the tangent lines in the upper left-hand corner) are plotted against the corresponding average shear stress τ_a, a curve is obtained which indicates that the slow plastic flow starts at a shear stress $\tau_a = 0.15$ kg/cm^2 = 30 percent of the maximum value of τ_a, and that the increase in velocity of flow is approximately

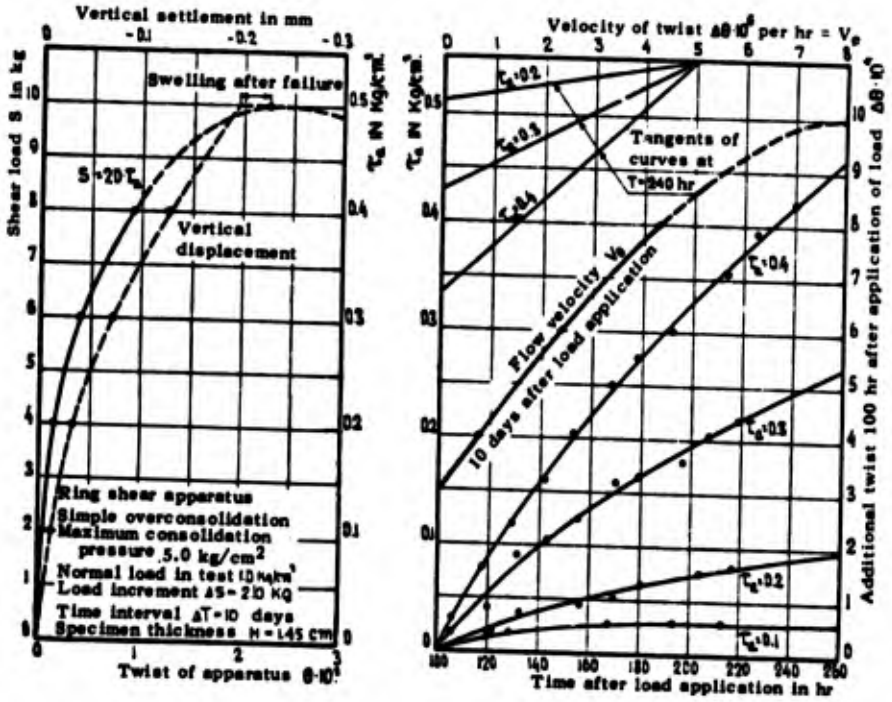

Fig. 38. Little Belt clay. Velocity of the plastic flow before failure

proportional to the increase in shear stress. Since the velocities used in the present analysis do not represent the ultimate constant velocities, the slow plastic flow actually begins at a somewhat higher value of τ_a than indicated here. The velocity of flow is here shown as a function of v_θ or the rate of increase in twist θ of the apparatus. The average velocity of the linear displacement v_a of the specimen as a whole (H = 1.45 cm) is then:

$$v_a = \frac{2}{3} v_\theta R_2 \frac{1 - n^3}{1 - n^2} = \frac{7}{9} R_2 v_\theta = 4.67\, v_\theta \qquad (26)$$

where $n = R_1/R_2$ or, for this apparatus, $n = 1/2$ and $R_2 = 6.0$ cm.

In order to obtain the average velocity v_γ of the shear strain γ, the value of coefficient k_e in equation (85) must first be determined; see appendix. Assuming that in this case the effective specimen thickness amounts to approximately 1 cm, the velocity $v_\theta 10^6 = 1$ per hour (at $\tau_a = 0.22$ kg/cm^2 or 44 percent of the shearing resistance) would mean that the points of the surfaces of a one-meter-thick specimen would be displaced approximately 1/10 mm per day.

Flow Phenomena at Failure

62. The time-displacement curves of the last load increments prior to failure, obtained from two long-duration tests with Vienna clay in the normally consolidated and the overconsolidated state, are plotted in fig. 39. These curves show that, at the next to last load increment and at normal consolidation, the maximum displacement velocity does not occur until after approximately six hours, whereupon the velocity drops to a fraction of its maximum value. In the case of overconsolidated Vienna clay, however, the maximum displacement velocity is reached shortly after the load is applied. After the last load increment is applied, the displacement velocity increases steadily until a maximum value is reached, which is a multiple of the initial velocity. However, in this case the displacement velocity does not decrease again. This condition is regarded as a sign of failure.

As shown in fig. 35A, fairly large displacements frequently occur in the case of Vienna clay at stresses ranging from 90 to 100 percent of the failure load. The occurrence of these displacements is not regarded as failure, however, since the displacement velocity decreases again after reaching a maximum value. Fig. 39 further shows that several hours may pass between the last load application and the occurrence of failure. In some cases up to 20 hours would elapse, while in others failure would occur shortly after the last load application. Taking this time interval into consideration the actual shearing resistance is estimated to be between the shear stresses corresponding to the next to last and last load increments.

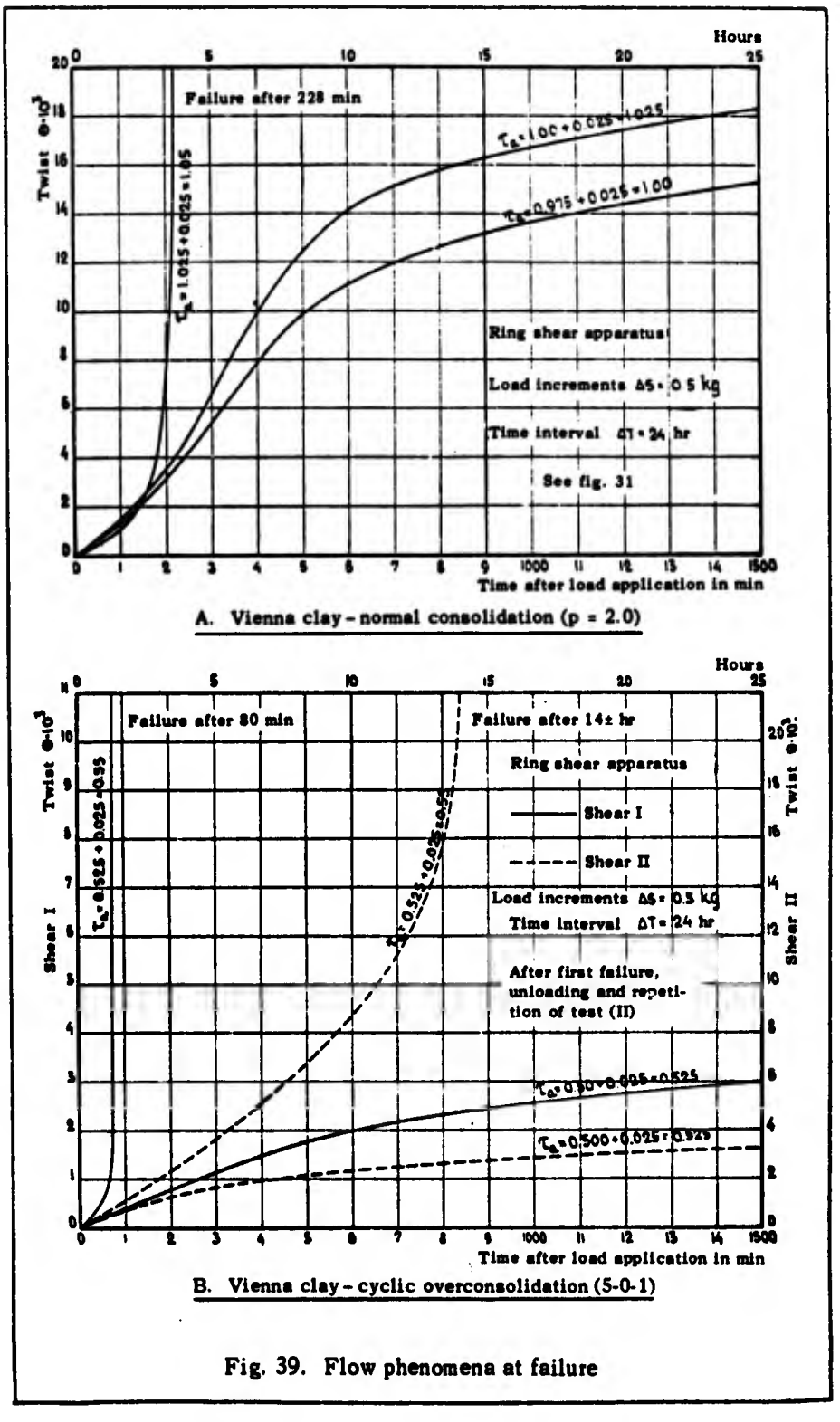

A. Vienna clay – normal consolidation (p = 2.0)

B. Vienna clay – cyclic overconsolidation (5-0-1)

Fig. 39. Flow phenomena at failure

VII: DETERMINATION OF THE FAILURE CONDITIONS

The Tests

63. The curves shown in fig. 32 yield the equivalent test duration T_s for various test conditions which assures a complete pore-pressure equalization and the true failure condition, expressed by the effective pressures, is obtained.

Accordingly, a test duration T_s from 600 to 800 minutes, depending on the state of consolidation of the specimen, and a specimen thickness $H = 2.0$ to 2.4 cm were used for Vienna clay. Because of the low permeability of Little Belt clay, the tests with this material had to be of longer duration but could be made with thinner specimens. In this case a specimen thickness from 1.8 to 2.0 cm and a test duration T_s ranging from 800 to 1600 minutes were used.*

64. The test results for Vienna clay are given in fig. 40 and for Little Belt clay in fig. 41. The shearing resistance curves are shown by the full-drawn lines in the center portion of these diagrams for various states of consolidation. Thus 0-A corresponds to normal consolidation, A-B to simple consolidation (5-p-p), and B-C to cyclic overconsolidation (5-0-p) of the material. By connecting the individual curves, the hysteresis loop of the shearing resistance curve is obtained. The water contents existing in the shear plane at the moment of failure are plotted in the upper diagram. The dashed lines for the equivalent pressure p_e were obtained on the basis of the relations between pressure and water content in fig. 17. The corresponding curves for the equivalent pressure p_e before the test (dot-dash lines) were plotted with the aid of the pressure-void ratio diagrams in figs. 15 and 16.

---

* Translator/author note: This test duration is too small for full equalization of the pore-water pressures; see Proc. ASCE Research Conference on Shear Strength of Cohesive Soils, pp 191-194, Colorado, June 1960. Changes in shear strength were very small for T_s greater than 800 minutes because the influence of a viscous component of strength counteracted that of equalization of pore-water pressures.

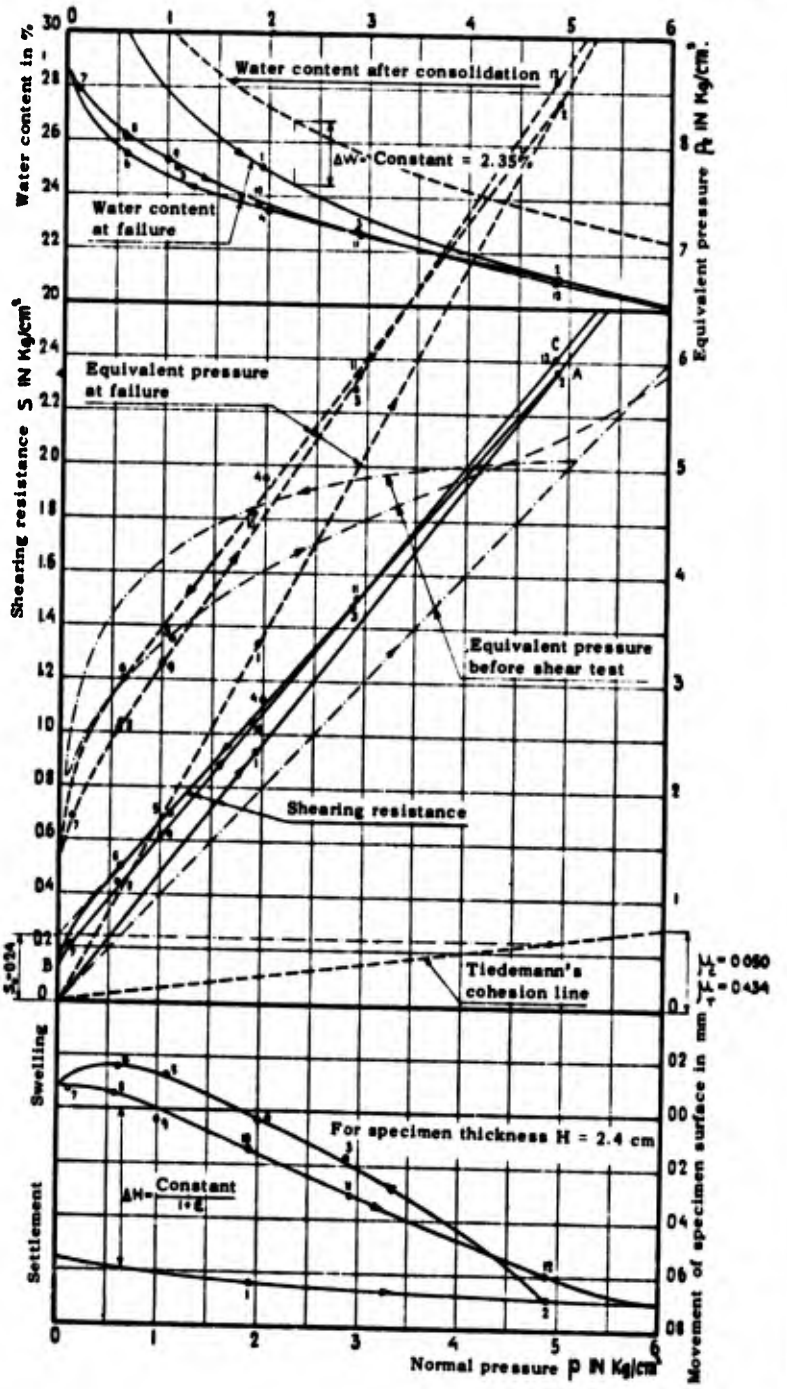

Fig. 40. Shear tests with Vienna clay V. Standard tests

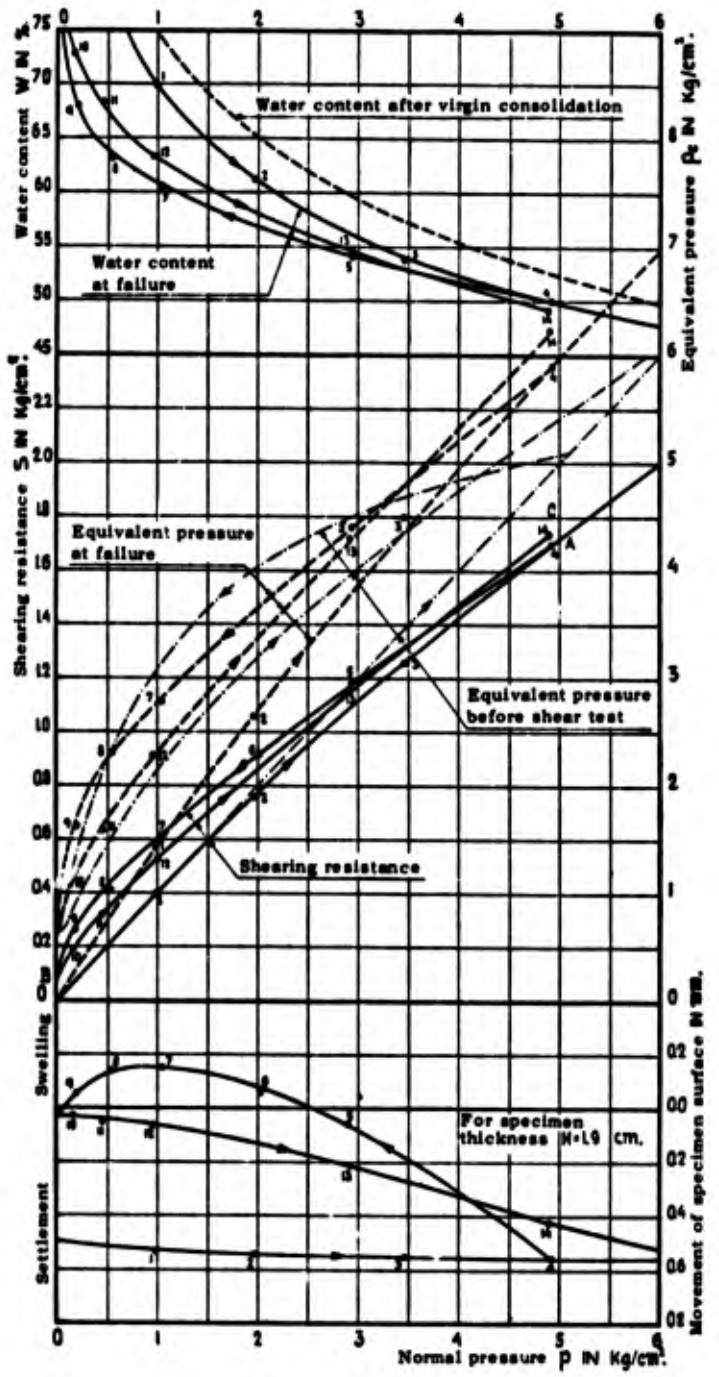

Fig. 41. Shear tests with Little Belt clay. Standard tests

Observed changes in the specimen thickness ΔH are shown in the lower diagram. For Vienna clay, these changes correspond to the specimen thickness $H = 2.4$ cm and for Little Belt clay to $H = 1.9$ cm . The curves reveal particularly that, at a given degree of overconsolidation (which differs for the two materials investigated and for simple and cyclic overconsolidation), the settlement of the specimen surface changes to a heaving as a result of swelling. Thus in strongly overconsolidated soils, a shear test causes first a negative pressure in the pore water, and subsequently an increase in volume.

The pressure p , at which the settlement of the surface becomes zero, should correspond to the value of p indicated by the intersection of the curves for equivalent pressures before and after the test. The differences observed in some cases must be attributed to the circumstance that the curves for equivalent pressures, which correspond to the state of consolidation before the test and to simple and cyclic overconsolidation, were obtained with the aid of consolidometer tests. As mentioned before, results of tests with cohesive soils are affected by the type of testing procedure used. For this reason the latter curves can, as a rule, only serve for qualitative comparison with the curves of equivalent pressures for the state of consolidation at failure. Moreover, accurate determinations of extremely small changes in the specimen thickness are very difficult to perform.

Coefficients of Coulomb's and Krey-Tiedemann's Failure Conditions

65. For Vienna clay in the normally consolidated state, the shearing resistance line (O-A in fig. 40) is, for all practical purposes, a straight line passing through the origin, i.e., according to Coulomb's failure condition, equation (16), we have:

$$\mu_s = 0.48 \qquad \text{or} \qquad \phi_s = 25^\circ 40' \tag{27}$$

For Little Belt clay in the normally consolidated state, the shearing resistance line O-A is so curved that it can be replaced by a straight

line only as a very rough approximation.

66. According to Krey-Tiedemann's failure condition, the shearing resistance lines for simple and cyclic overconsolidated soils are supposed to be identical and to form a straight line. Figs. 40 and 41 show that this is not the case. However, for Vienna clay, curves A-B and B-C can be replaced by straight lines (except for small values of p). Thereby the following coefficients are obtained for this failure condition:

Table 4

	μ_r	μ_c	ϕ_r	ϕ_c
Simple overconsolidation	0.434	0.050	28°28'	2°52'
Cyclic overconsolidation	0.460	0.034	24°43'	1°57'

The difference between the coefficients is fairly small. Hence the mean values can be used with a sufficient degree of accuracy for practical problems. Corresponding coefficients were not computed for Little Belt clay since in this case it is no longer warranted to replace the curves by straight lines. This simplification can only be permitted as a very rough approximation or for a specific stress interval.

A New Failure Condition

67. It follows from figs. 40 and 41 that the shape of the equivalent pressure curves is entirely similar to that of the lines for shearing resistance at failure. This fact leads to postulation of the following general failure condition:

$$s = \mu_o p + \kappa p_e \tag{28}$$

μ_o will be called the coefficient of effective internal friction and κ the coefficient of effective cohesion. Equation (29) can also be written

$$\frac{s}{p_e} = \mu_o \frac{p}{p_e} + \kappa \qquad (29)$$

If the ratio s/p_e is regarded as the specific shearing resistance and p/p_e as the specific normal pressure, equation (29) is identical with Coulomb's failure condition. In this case the points with coordinates p/p_e and s/p_e should lie in a straight line forming an angle ϕ_o = arc tan μ_o with the horizontal, which intersects the ordinate axis at the value of κ. Fig. 42 shows that, in the case of Vienna clay, all

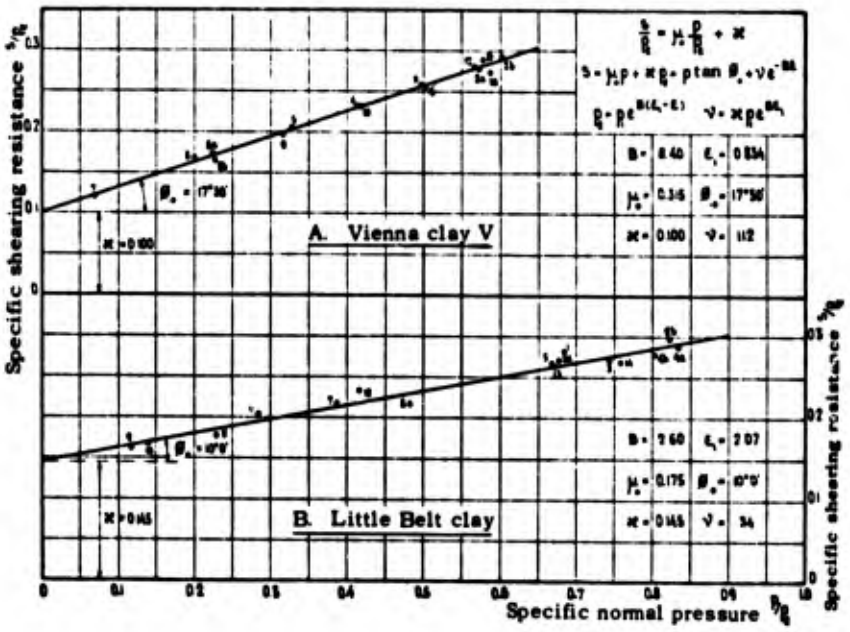

Fig. 42. Determination of the shearing resistance coefficients

points lie almost exactly in a straight line, including those that were not directly covered by the curve in the earlier diagram (fig. 40). In the case of Little Belt clay some deviations are noted, particularly in the portion corresponding to normal consolidation. However, taking the aforementioned slight differences in the physical properties of the test material into account, there is satisfactory agreement, from a practical standpoint, between the test data for the shearing resistance and the proposed failure condition.

68. On the basis of equation (12), equation (29) can be expressed as follows:

$$s = \mu_o p + \nu e^{-B\epsilon} \qquad (30)$$

in which

$$\nu = p_1 \kappa e^{B\epsilon_1} \qquad (p_1 = \text{unit of pressure} = 1) \qquad (31)$$

The shearing resistance of a cohesive soil is therefore a function of the effective normal pressure and void ratio prevailing in the shear zone at the moment of failure, and this function is independent of the preceding stress conditions.

69. This failure condition applies only to saturated cohesive soils and should only be considered as an approximation of the actual conditions, since the shearing resistance is affected by other factors besides those mentioned above. It should be pointed out particularly that the cohesion undoubtedly depends not only on the total water content but also on the ratio between the amount of bonded and free water. Until such time as the results of complementary tests become available, the proposed failure condition should not be used beyond the void-ratio zones investigated, i.e., not for very soft or very stiff soil conditions.

It must also be emphasized that the coefficients B and ϵ_1 used above are dependent upon the type of the experimental procedure. Moreover, at the moment of failure (peak strength) the shearing resistance of the soil used has already been subject to a decrease due to changes of a thixotropic nature. Finally, in conventional shear tests the shear zone and the planes of the orientation of the flaky mineral particles are parallel to each other, and it is not yet known what effect the orientation of these particles has upon the coefficient of friction and the cohesion (see Chapter IX).

70. From figs. 17 and 42 the following values are obtained for the coefficients in equations (28) and (30) and the corresponding values of ϕ_o :

Table 5

	B	ϵ_1	κ	ν	μ_o	ϕ_o
Vienna clay	8.4	0.735	0.10	112	0.315	17°30'
Little Belt clay	2.6	2.07	0.145	34	0.175	10°00'

Table 5 shows that the angle of effective internal friction ϕ_o is considerably smaller than the apparent angle of friction ϕ_s or angle ϕ_r in Krey-Tiedemann's failure condition.

Determination of the Coefficients

71. For the practical determination of values μ_o and κ it is recommended that shear tests be made with soils in the simple or cyclic overconsolidated state since, in the normally consolidated state, points $(p/p_e, s/p_e)$ lie very close together. This applies particularly to soils similar to Vienna clay where the values p/p_e and s/p_e are practically constant. Heretofore it was assumed that a pressure-void ratio diagram was available for the determination of p_e. From a theoretical standpoint such a diagram is not required for the determination of the coefficients in equation (30). In case the values s, p, and ϵ were determined for three or more values of p, and not just for the state of normal consolidation, coefficients μ_o, ν, and B can also be determined. By eliminating μ_o and ν from three equations a, b, and c, the following basic equation is obtained for B:

$$\frac{1 - n_b e^{B(\epsilon_a - \epsilon_b)}}{1 - n_c e^{B(\epsilon_a - \epsilon_c)}} = \frac{s_a - n_b s_b}{s_a - n_c s_c} \qquad (32)$$

in which

$$n_b = \frac{p_a}{p_b} \qquad \text{and} \qquad n_c = \frac{p_a}{p_c}$$

This equation can only be solved by the fairly complex method of successive approximations.

When two or more points (p, s) lie in a straight line through the origin, the following value for B is obtained directly:

$$B = - \frac{\ln p_a - \ln p_b}{\epsilon_a - \epsilon_b} \tag{33}$$

However, in this case other points (p, s) which do not lie in the straight line through the origin must also be available for the determination of μ and ν. In practice, the determination of B with the aid of shear tests on overconsolidated soils does not yield reliable values. When coefficient B is obtained through consolidation tests, coefficients μ and κ can be determined with a sufficient degree of accuracy by averaging as shown in fig. 42, despite a small scatter in ϵ_a, ϵ_b, ϵ_c, etc. On the other hand, the deviations in the small differences $(\epsilon_a - \epsilon_b)$, $(\epsilon_a - \epsilon_c)$, etc., corresponding to the above-mentioned scatter in ϵ_a, ϵ_b, ϵ_c are relatively large and cause large differences and uncertainty in the determination of B by equation (32). A simple and at the same time reliable graphical averaging method for obtaining a mean value for B, similar to that for μ_o and κ in fig. 42, has not yet been developed. As long as an appropriate procedure is not available and until testing equipment and methods have been improved, it is advisable to determine coefficient B with the aid of a pressure-void ratio diagram and to obtain this diagram through consolidation in the shear boxes.

VIII. VOLUME CHANGES CAUSED BY SHEAR AND THEIR EFFECT

Critical Void Ratio and Critical Consolidation Procedure

72. According to Casagrande (13), the deformations and volume changes of cohesionless soils subjected to shear stress can be represented by the curves shown in fig. 43A. When in a loose condition, the soil experiences a decrease in the void ratio during shear (curve C-D). The corresponding displacement curve is O-A. However, a complete failure does not occur at A, but rather a steady flow without further changes in the void ratio or the shearing resistance. When the same soil in a dense condition is subjected to shear under the same normal pressure, it first experiences an increase in the void ratio (curve E-F), whereupon sudden failure occurs at point B on the displacement curve O-B followed by a more rapid flow. There is also a decrease in the shearing resistance (curve B-A) and an additional increase in the void ratio (curve F-D). Eventually a condition is reached under which a continued flow does not cause further changes in the shearing resistance and void ratio. These ultimate values of the shearing resistance as well as the ultimate values of the void ratio are equal in both cases and therefore independent of the initial state of consolidation of the soil.

Casagrande called this ultimate value of the void ratio, ϵ_k, the critical void ratio. When the void ratio of a cohesionless soil is equal to ϵ_k, shear displacements in this soil do not cause volume changes. When the void ratio is greater than ϵ_k, displacements produce a decrease in volume or, in case the pores are filled with water, an excess pressure in the pore water. The decrease of the effective normal stresses and of the shearing resistance caused by this excess pressure may then produce slides. On the other hand, when the void ratio is smaller than ϵ_k, displacements will cause an increase in volume or an underpressure in the pore water and therewith also an increase in the effective stresses and in the shearing resistance.

73. A similar representation of the behavior of cohesive soils is given in fig. 43B. The normally consolidated soils (curves O-A-B and

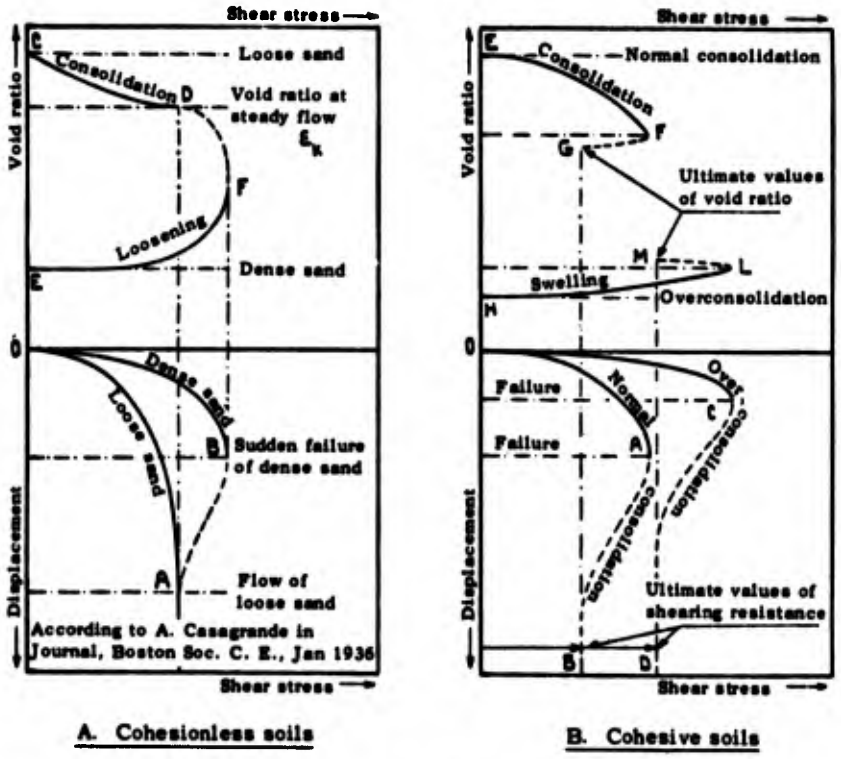

Fig. 43. Behavior of soils under shear loading

E-F-G) correspond to loose, cohesionless soils, whereas the highly overconsolidated soils (curves O-C-D and H-L-M) correspond to dense, cohesionless soils. The curves represent the results of shear tests that were made under the same vertical normal pressure p. In this case a continued displacement after failure causes a decrease in the shearing resistance, not only in overconsolidated but also in normally consolidated soils (see Chapter XII). Moreover, the ultimate values of the shearing resistance and the void ratio attained after failure are different. For this reason, cohesive soils do not have a critical void ratio with a corresponding, well-defined ultimate value of the shearing resistance.

Figs. 40 and 41 show that cohesive soils after certain consolidation procedures do not experience volume changes when subjected to shear. Therefore it may be said that, referring to the critical void ratio of cohesionless soils, cohesive soils do not have a critical void ratio but a critical consolidation procedure. In cohesive soils, any void ratio can become critical when it is produced by a critical consolidation procedure.

Volume Changes of Normally Consolidated Soils

74. As mentioned before, the shearing resistance curve of Vienna clay in the normally consolidated state is a straight line. This is also apparent in fig. 44 where the results of complementary tests which were made with a slightly different batch, however, are shown.

Before the tests, $p_e = p$, that is, points (p, p_e) lie on a straight line through the origin. The figure shows that points (p, p_e) also lie on a straight line through the origin after the test. The following equation applies to the two batches II and V at the moment of failure:

$$p_e = 1.72p$$

that is, for such normally consolidated types of soil the degree of overconsolidation at failure is constant or, in general:

$$p_e = n_c p \tag{34}$$

This equation indicates that a gradual increase of the shear stresses from zero to the maximum shearing resistance s at failure produces an additional consolidation which is equivalent to that caused by an increase of the vertical consolidation pressure by $\Delta p = (n_c - 1)p$. Since $s = \mu_s p$,

$$\Delta p = s \frac{n_c - 1}{\mu_s} \tag{35}$$

When in a confined consolidation test the vertical normal pressure is suddenly increased by Δp, the hydrostatic pressure of the pore water is initially also increased by the same amount. Since the consolidation procedure and the stress changes in a shear test are entirely different from those in consolidation tests, it may not be concluded directly that the initial excess pressure in the pore water caused by a sudden application of a shear stress s can be computed by means of equation (35). The determination of this initial excess pressure in the pore water will be discussed later in connection with rapid shear tests.

75. The change in the void ratio, Δe during a shear test is

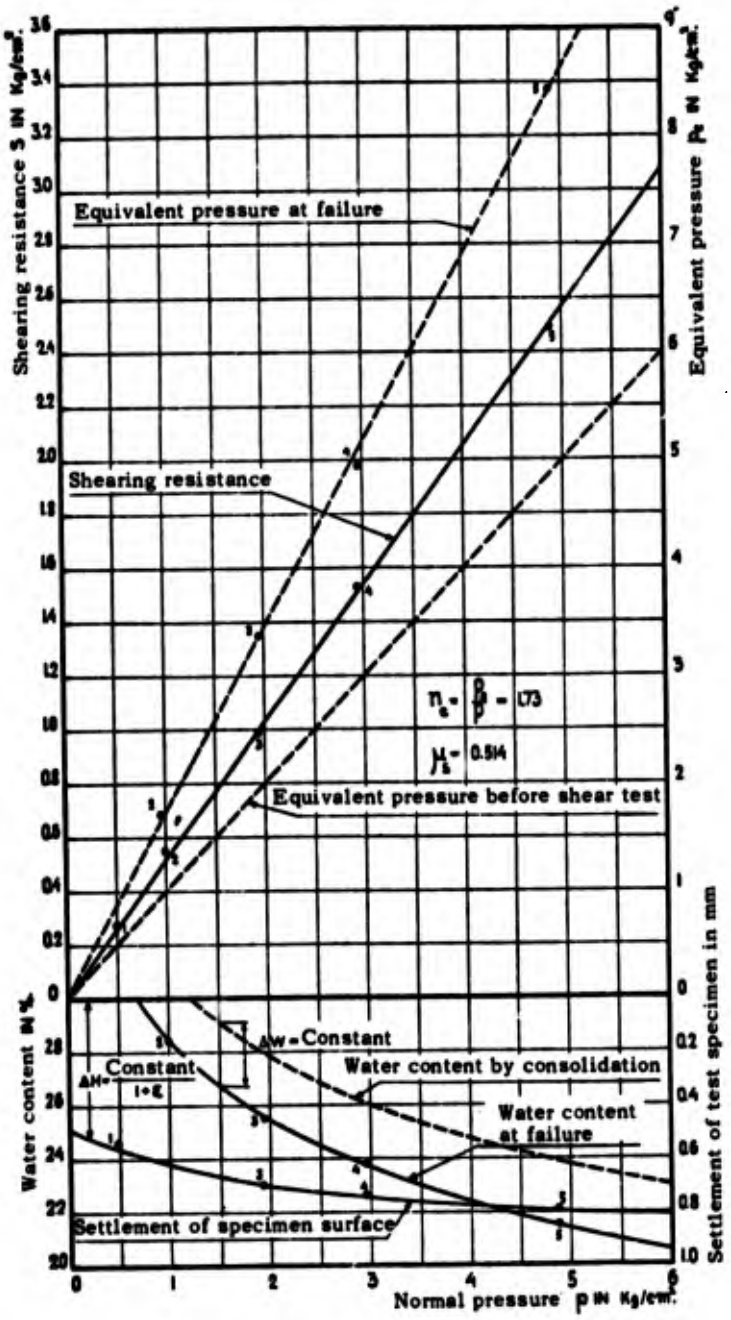

Fig. 44. Standard shear tests with normally consolidated Vienna clay II

obtained by means of equations (12) and (34), as follows:

$$e^{B(\epsilon_1-\epsilon-\Delta\epsilon)} = n_c e^{B(\epsilon_1-\epsilon)}$$

$$\Delta\epsilon = -\frac{\ln n_c}{B} \tag{36}$$

i.e., $\Delta\epsilon$ is constant for a given material.

These formulas do not apply to Little Belt clay since the line of the equivalent pressures becomes curved at failure and the degree of overconsolidation n_c is not constant.

Effective Thickness of the Test Specimen

76. From equation (36) the following value is obtained for the total change of the specimen thickness in the case of Vienna clay:

$$\Delta H = -k_e \frac{H}{1+\epsilon} \frac{\ln n_c}{B} \tag{37}$$

in which H represents the thickness and ϵ the void ratio of the soil before the shear test. The coefficient k_e depends on H and denotes the ratio between the mean variation in the void ratio for the entire specimen and the change in the void ratio directly in the failure zone. In the present tests, H, k_e, n_c, and B are constant and hence:

$$\Delta H = \frac{\text{constant}}{1+\epsilon} \tag{38}$$

77. The coefficient k_e can be determined by tests with various specimen thicknesses H. The results of tests of this type are shown in fig. 33A, where the dashed lines represent settlements computed by equation (37) and for $k_e = 1$. The ratios between the observed settlements and the corresponding settlements for $k_e = 1$ yield the k_e values for various specimen thicknesses H. For values of H up to 3 cm,

$$k_e = 1 - \frac{H}{H_o} = 1 - 0.115H \qquad (H \text{ in cm}) \tag{39}$$

and for the effective specimen thickness H_e :

$$H_e = H(1 - 0.115H) \qquad (H \text{ in cm}) \tag{40}$$

Although these equations were derived on the basis of tests with normally consolidated Vienna clay and for $p = 2.0$ kg/cm^2, they can probably also be applied to other states of consolidation and other soils (at least in an approximate manner). Furthermore, with the aid of this equation it is possible to compute the changes of the void ratio in the shear zone for an observed value of ΔH corresponding to a given load increment or a shear stress lower than that at failure.

Changes in Cohesion During the Shear Test

78. It is now possible to determine for Vienna clay in a state of normal consolidation the effect of the change in the void ratio during a shear test upon the shearing resistance. According to equation (34), equation (16) can be written as follows:

$$s = p(\mu_o + n_c\kappa) \tag{41}$$

and

$$\mu_s = \mu_o + n_c\kappa \tag{42}$$

This means that in this case the cohesion

$$c = n_c\kappa p \tag{43}$$

is also proportional to p .

Before the test, the cohesion is κp and, at the moment of failure, $\kappa p_e = n_c\kappa p$. Hence the increase in the cohesion Δc is

$$\Delta c = \kappa(n_c - 1)p \tag{44}$$

and amounts, for Vienna clay for example, to 72 percent. In the application of the test results to practical foundation problems, this increase in the cohesion during the shear test must be taken into account, since in many instances the full load is applied before the void ratio has adapted itself to the new stress conditions.

In normally consolidated Little Belt clay, the p_e line is curved in such a manner after failure that the simple rules like those obtained for Vienna clay cannot be applied. In each case the volume changes and their effect on the cohesion value must be determined from the curves. The same applies to Vienna and Little Belt clay in a simple and cyclic overconsolidated state.

79. Even though the difference between the coefficients of friction according to equations (18) and (29) (see tables 4 and 5) is conspicuous, it can be fully explained by the effect of the change in the void ratio during the test. For Vienna clay in a simple overconsolidated state (A-B in fig. 40), equation (18) is based on the assumption that the cohesion is constant and equal to 0.24 kg/cm^2 for the entire range A-B. At point A $p = 4.88$ kg/cm^2 and $s = 2.36$ kg/cm^2, hence the frictional resistance $s_r = 2.36 - 0.24 = 2.12$ kg/cm^2 and $\mu_r = 2.12/4.88 = 0.434$. According to equations (28) and (43), for $p = 4.88$ kg/cm^2 the cohesion is equal to $n_c \kappa p = 1.72 \times 0.10 \times 4.88 = 0.84$ kg/cm^2, and hence the frictional resistance $s_r = 2.36 - 0.84 = 1.52$ kg/cm^2 and $\mu_o = 0.312$.

IX. COMPRESSION TESTS AND EFFECT OF STRATIFICATION OF THE MATERIAL

Test Procedures

80. The effect of orientation of the flaky soil particles in a preferred direction, caused by the consolidation procedure, was investigated with the aid of unconfined compression tests. The small specimens used in the test were cut from larger specimens that had first been subjected to normal consolidation at 5 kg/cm^2.

As can be seen in fig. 45, the test specimens were prepared in three groups with the longitudinal axis of the specimens being either vertical, inclined under an angle of 45°, or parallel to the plane of orientation of the flaky particles. Most test specimens had a square cross section with a side length of 2 cm. This shape of the cross section permits more accurate measurement of the angle of inclination of the planes of failure; in addition, it reduces disturbance of the internal structure of the soil during specimen preparation. A small number of circular cylindrical specimens were prepared for compression tests for the purpose of comparison. The height of all test specimens was 4 cm. It would have been advantageous to work with a greater height, but the height was limited by the specimen thickness obtainable in the consolidation procedure. It is of particular importance that the end surfaces be perfectly flat, parallel to each other, and normal to the specimen axis, since the test results, especially the inclination of the planes of failure, depend greatly on the accuracy with which the specimens are prepared. During the test the specimens were protected against desiccation by a glass cylinder sealed with a rubber diaphragm (fig. 46). The individual load increments were approximately 2.5 percent of the ultimate load and the time interval between the load increments was two minutes.

In accordance with the conventional test procedure, the compressive stress was computed for the deformed cross section by means of the formula:

$$q = \frac{Q(1 - e)}{A} \qquad (45)$$

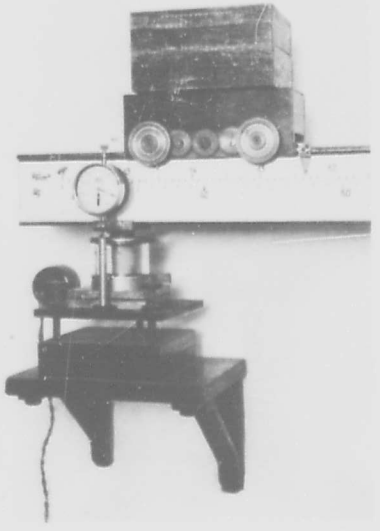

Fig. 46. Apparatus for compression tests. Unconfined compression

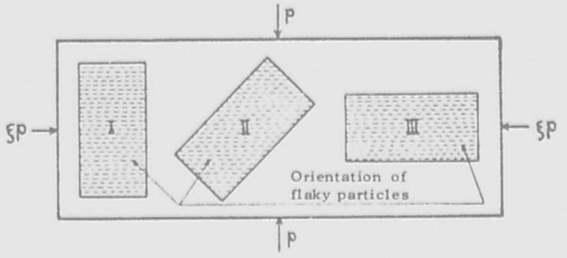

Fig. 45. Specimens for compression tests

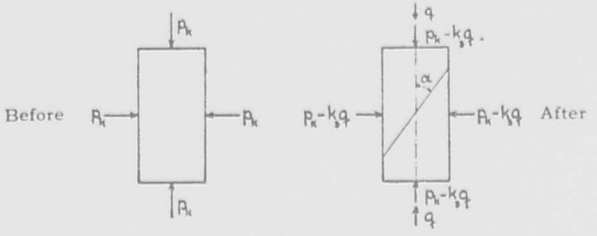

Fig. 47. Change in the capillary pressure during compression tests

in which Q is the total external load, e the longitudinal strain, and A the original cross-sectional area of the test specimen.

Capillary Pressures and Their Changes

81. Before describing the test results, it is necessary to discuss the various pertinent factors and forces. After the consolidation is completed, the large initial specimen is subjected to a state of stress given by the pressures $(p, \zeta p, \zeta p)$, where ζ is the coefficient of earth pressure at rest. The equivalent pressure p_e is equal to the vertical consolidation pressure p. Now when the specimen is removed from the shear box these pressures are replaced by the capillary pressure p_k which acts in all directions and is numerically equal to the negative pressure in the pore water $(p_u = -p_k)$. Its value lies between ζp and p, or

$$p_k = p\,[\zeta + k_1' (1 - \zeta)] = k_1 p_e \tag{46}$$

in which k_1 represents a coefficient that depends primarily on the coefficients of swelling and consolidation and on the coefficient of earth pressure at rest. The soil is now in a slightly overconsolidated state with respect to the uniform triaxial pressure p_k. This pressure p_k is therefore very sensitive to slight changes in the void ratio caused by evaporation of the pore water.

Eventually, a state of normal consolidation corresponding to the uniform triaxial pressure is reached after a certain amount of evaporation. If the void ratio and the virgin consolidation curve of the clay are known for a uniform pressure acting in all directions, p_k can be determined therefrom. As a rule, only the virgin consolidation curve for a confined compression test (consolidometer test) is known. Between the equivalent pressures p_e and p_k obtained therefrom, the following simple relationship can be obtained by theoretical considerations:

$$p_k = k_2 p_e \tag{47}$$

Here k_2 is a coefficient that depends primarily on the elastic properties of the material, but to a certain extent also on the time during which the specimen has been kept at a constant water content, inasmuch as k_2 decreases somewhat with time.

82. Now when a specimen is subjected to an axial compressive stress q (fig. 47), p_k must decrease to a value p_k' in accordance with the fact that the void ratio remains constant during the compression test (Rendulic (38)). This means that the decrease of the void ratio caused by the compressive stress q must be equal to the increase in the void ratio caused by the drop in the capillary pressure p_k :

$$p_k' = p_k - k_3 q \tag{48}$$

in which k_3 is a coefficient that depends primarily on the elastic properties of the material, namely on the coefficients of swelling and consolidation for an arbitrary change in the triaxial stress condition. If the elastic properties change with the direction of orientation of the soil particles, then k_3 also varies with the direction of q in relation to these planes of orientation. However for a given test series, the value k_3 may be considered approximately constant with a sufficient degree of accuracy, provided the direction of the compressive force with respect to the planes of orientation also remains unchanged.

When no volume changes occur in a perfectly elastic isotropic material, the sum of the three principal stresses must remain constant and $k_3 = 1/3$ is obtained. But when a decrease of the stress does not cause an increase in volume, k_3 is equal to 1. The true value of k_3 lies between these boundary values.

Compressive Strength

83. If α is the angle between the direction of pressure of q and the plane of failure, the equation for the effective normal pressure p upon this plane is:

$$p = p_k' + q \sin^2 \alpha = k_2 p_e - q(k_3 - \sin^2 \alpha) \tag{49}$$

and the shear stress s :

$$s = q \sin \alpha \cos \alpha \tag{50}$$

At failure, from equation (28):

$$s = \mu_o p + \kappa p_e$$

The introduction of p and s from equations (49) and (50), after reductions, yields:

$$\frac{q}{p_e} = \frac{k_2 \mu_o + \kappa}{\cos \alpha \sin \alpha + (k_3 - \sin^2 \alpha)\mu_o} \tag{51}$$

For an isotropic material with an angle of internal friction ϕ_o , the relationship

$$\alpha = 45 - \frac{\phi_o}{2}$$

can be used independently of variations of the value p_k . However, in case ϕ_o and κ change with the direction of the plane of failure, α depends not only on the internal friction but also on the laws governing the variation in the friction and in the cohesion. In equation (51), coefficient k_2 may be considered independent of angle β between the direction of q and the plane of orientation, whereas coefficients k_3 , μ_o , and κ and also α may vary with β . If angle β is constant for a test series, coefficients k_3 , μ_o , and κ as well as α and therewith q/p_e are also constant, provided the assumptions for equations (47) and (49) are valid.

84. Previously mentioned tests of Terzaghi and Janiczek (line a_1-i_1 in fig. 12) demonstrate that q/p_e is constant. In these tests the direction of the compressive force was normal to the direction of orientation of the flaky particles (type I, fig. 45), and the tests were made immediately after the consolidation was completed. Hence, in this case the capillary pressures must be computed in accordance with

equation (46), i.e., in equation (51) k_2 must be replaced by k_1.

85. Fig. 48 shows the results of a test series with specimens of

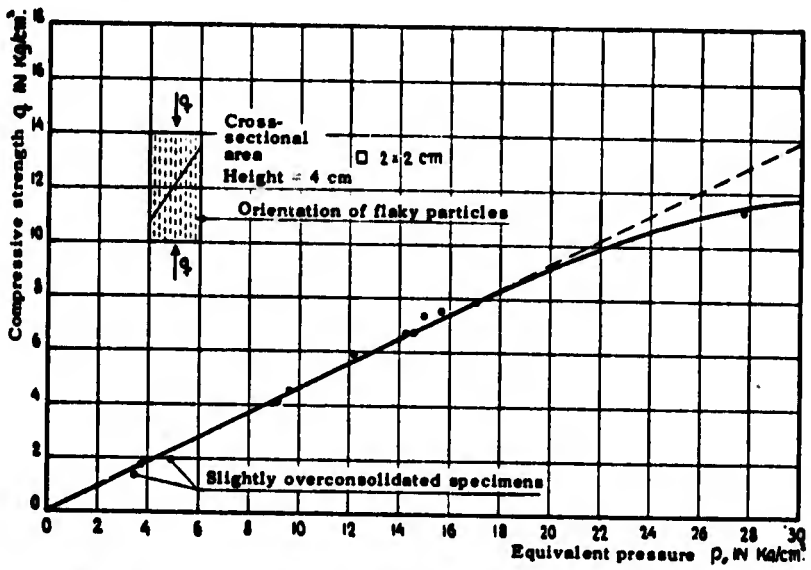

Fig. 48. Unconfined compression tests with Vienna clay II. Relationship between compressive strength and void ratio or equivalent pressure

Type III, and soil from batch II of Vienna clay. The large initial specimens were consolidated under various loads, and the test specimens were then allowed to dry somewhat, which made it possible to obtain greater differences and higher values of p_e and p_k. As can be seen in fig. 48, points (p_e, q) lie fairly close to a straight line through the point of origin to values of p_e corresponding to a void ratio near the shrinkage limit. Therefore, it can be assumed that, up to fairly high values of p_e, the ratio q/p_e is constant for a given soil and the same orientation of the soil particles with respect to the direction of the compressive force. However, this only applies when the specimens are in similar states of consolidation.

86. It follows from the above considerations that the compressive strength of a clay specimen may be affected by its stratification, not only through changes in the friction and cohesion but also through changes in the decrease of the capillary pressure, which is expressed by coefficient k_3 of equation (48). However, the ratio q/p_e can be used for comparisons of compressive strengths in cases where the void ratios of the individual specimens are at variance.

Inclination of Planes of Failure and Effect of Stratification

87. A tabular summary of the results of principal tests made with Vienna clay III, Vienna clay IX, and Little Belt clay III is shown in fig. 49. Fig. 50 shows photographs of a few specimens after dehydrating

	Vienna clay III			Vienna clay IX			Little Belt clay III		
	I	I	II	I	I	II	I	I	II
q/p_c	0.54	0.50	0.45	0.48	0.44	0.42	0.38	0.41	0.46
Relative strength	108	100	90	109	100	95	93	100	112
α	36°	36°	35°30'	(39°)	36°30'	36°	(43°)	40°15'	(42°)
$\beta = 90-2\alpha$	18°	18°	19°	(12°)	17°	18°	(4°)	9°30'	(6°)
β_o	Vienna clay I: 18°			Vienna clay V: 17°30'			Little Belt clay II: 10°		
β_r	Vienna clay I: 25°			Vienna clay V: 24°			Little Belt clay II: (17°30')		
β_s	Vienna clay I: 26°34'			Vienna clay V: 25°40'			Little Belt clay II: (20°)		

Fig. 49. Effect of stratification in compression tests

in a drying oven. From each kind of material and type of test, four specimens were made and tested. Each value in fig. 49 represents the average of the three most similar results of four tests. From the angles of inclination of the planes of failure the corresponding angles of internal friction ϕ, equation (15), were computed and compared with angles ϕ_o, ϕ_r, and ϕ_s. The soil for which the latter angles obtained was the same but did not come from the same batch. Results which lacked desirable accuracy, because of a scattering of the individual values or a curvature of the shearing resistance lines, are placed in parentheses.

Test Specimens of Type I

Compressive force normal to plane of orientation

88. With the exception of Vienna clay III, the soil specimens showed a strong and irregular transverse expansion during the test. In many instances the shear planes were indistinct, and their angle of inclination

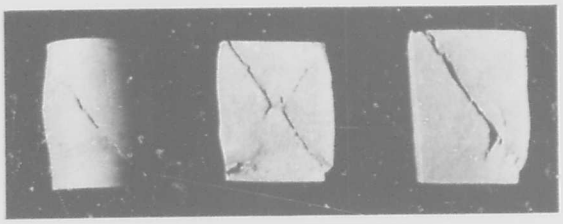

I I III

A. Vienna clay III

I II III

B. Vienna clay IX

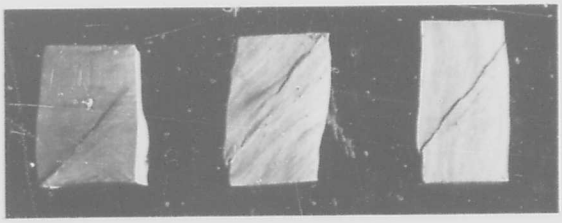

I II III

C. Little Belt clay III

Type I Type II Type III

Fig. 50. Compression test specimens after failure

appeared to be affected by the transverse expansion of the specimens and could therefore not be determined with the required accuracy. For Vienna clay of batch III the values of p_e were higher and the deformations usually smaller. The shear planes were distinct and their angles of inclination α, which differed but slightly from those of specimens of type III, could be determined with sufficient accuracy. The corresponding angles ϕ agreed almost perfectly with the angle of effective internal friction ϕ_o, whereas in the case of Vienna clay IX and Little Belt clay the angles ϕ were considerably smaller than ϕ_o. For Vienna clay the compressive strength ratio q/p_e was greater and for Little Belt clay, less than that of the specimens of types II and III. In the case of Vienna clay III, specimens of type I with a circular cross section were investigated instead of specimens of type II. They had the same angle of internal friction ϕ as the square specimens of the same type, but the value q/p_e was 8 percent higher.

Test Specimens of Type II

Compressive force at an angle of 45^o with the plane of orientation

89. The planes of failure were very distinct and almost parallel to the plane of orientation of the soil particles. Their angle of inclination α could be determined accurately and the corresponding angle ϕ was almost equal to the angle ϕ_o for both Vienna clay and Little Belt clay. In Little Belt clay there also appeared planes of failure of the second order after failure, which planes were more or less normal to the stratification plane while their angles of inclination differed substantially from those of the principal planes of failure. The angles of inclination of these planes of failure of the second order showed fairly large scattering so that the mean value $\alpha = 44^o$ is not very reliable. In addition, a general plastic flow parallel to the planes of orientation could be observed after the formation of the principal plane of failure (fig. 50C). The compressive strength of all specimens was between the values of types I and III.

Test Specimens of Type III

Compressive force parallel to the plane of orientation

90. The plane of failure was clearly recognizable, and the inclined cracks at the surface could be observed only at side faces which were normal to the planes of stratification (fig. 51A). The cracks were somewhat

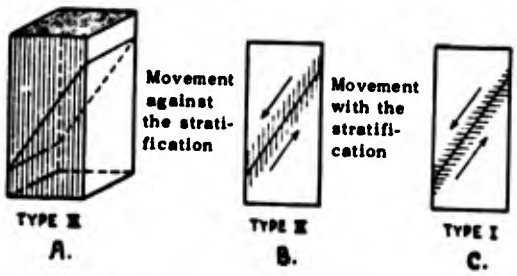

Fig. 51. Planes of failure in compression tests

serrated in most cases. In a few cases, vertical cracks could be observed at the ends (figs. 50A and 50B). This phenomenon can be explained by the fact that in this case the direction of motion in the planes of failure is against the orientation of the flaky particles, and that in type I the direction of motion is with the direction of these particles (figs. 51B and 51C). In Vienna clay the values of α were almost constant and differed but very slightly from those of type II, while in the case of Little Belt clay there were slight variations in the test results and the angles were considerably higher than those of type II. For Vienna clay, the compressive strength of specimens of type III is lower and for Little Belt clay, higher than that of types I and II.

91. In a general interpretation of the test results it is not sufficient to consider the relative compressive strength and the inclination of the planes of failure, but the direction of motion in the planes of failure and the possible variability of coefficient k_3 must also be taken into account. Since it is not known how this coefficient changes with the direction of pressure with respect to the plane of orientation, a final conclusion cannot be drawn relative to the variability of the friction and cohesion with respect to the plane of orientation of the flaky particles, especially since it appears that the effect of stratification is quite different for each particular type of soil. Furthermore, the effect of

the cross-sectional shape, of the height of the test specimen, and of the test duration upon the test results must be investigated before generally acceptable conclusions can be formulated.

The tests indicated, nevertheless, that the compressive strength may vary approximately ± 10 percent from the mean value, depending on the direction of the compressive force with respect to the plane of orientation. This mean compressive strength is obtained when the specimens are prepared and compressed in such a manner that the planes of failure become more or less parallel to the plane of orientation. In such cases distinct planes of failure with an almost constant angle of inclination α are obtained, and the corresponding angles of internal friction ϕ agree satisfactorily with the values of effective internal friction ϕ_o obtained from the shear tests.

X. GENERAL FAILURE CONDITIONS ASSUMING ISOTROPY

Failure Conditions at a Fully Adjusted Void Ratio

92. With few exceptions, all formulas and methods for determining the stress distribution in the subsoil are based on the assumption of an elasto-isotropic material and this assumption also serves generally as a basis for failure conditions. From a practical standpoint this is justified if the deviations are small and the failure condition for the direction of least resistance is used as the failure condition for all directions of the planes of failure. The various failure conditions as expressed by the total principal stresses σ or σ'', equations (1) and (5) will now be compared, assuming that an isotropic material is involved. First, consider the case in which the load is applied so slowly that the void ratio may be assumed to have adjusted itself completely to the stress conditions, i.e., the hydrostatic pressure in the pore water p_h is equal to the natural pore-water pressure p_n, and the effective stresses σ' are equal to σ''.

93. According to equations (16) and (41), the shearing resistance curve for a normally consolidated soil similar to Vienna clay is a straight line through the origin, which forms an angle ϕ_s with the axis of abscissas. According to the proposed failure condition equation (29), the true angle of internal friction is ϕ_o. Assuming isotropy, equation (15) can be used, and with the aid of angle ϕ_o, Mohr's circle of stress for all stress conditions at failure, expressed by the effective stresses p and s, can be constructed. The construction is shown in fig. 52A where the line O-B represents the shearing resistance line. Since $\phi_o < \phi_s$, Mohr's circle of stress intersects the shearing resistance line. The envelope of the circles of stress is the straight line O-B_1 which is not Mohr's failure curve, however, since the points of contact of the circles of stress and O-B_1 do not correspond to the failure condition. According to fig. 52A, the following general failure condition is obtained, expressed by the total principal stresses σ_1 and σ_3:

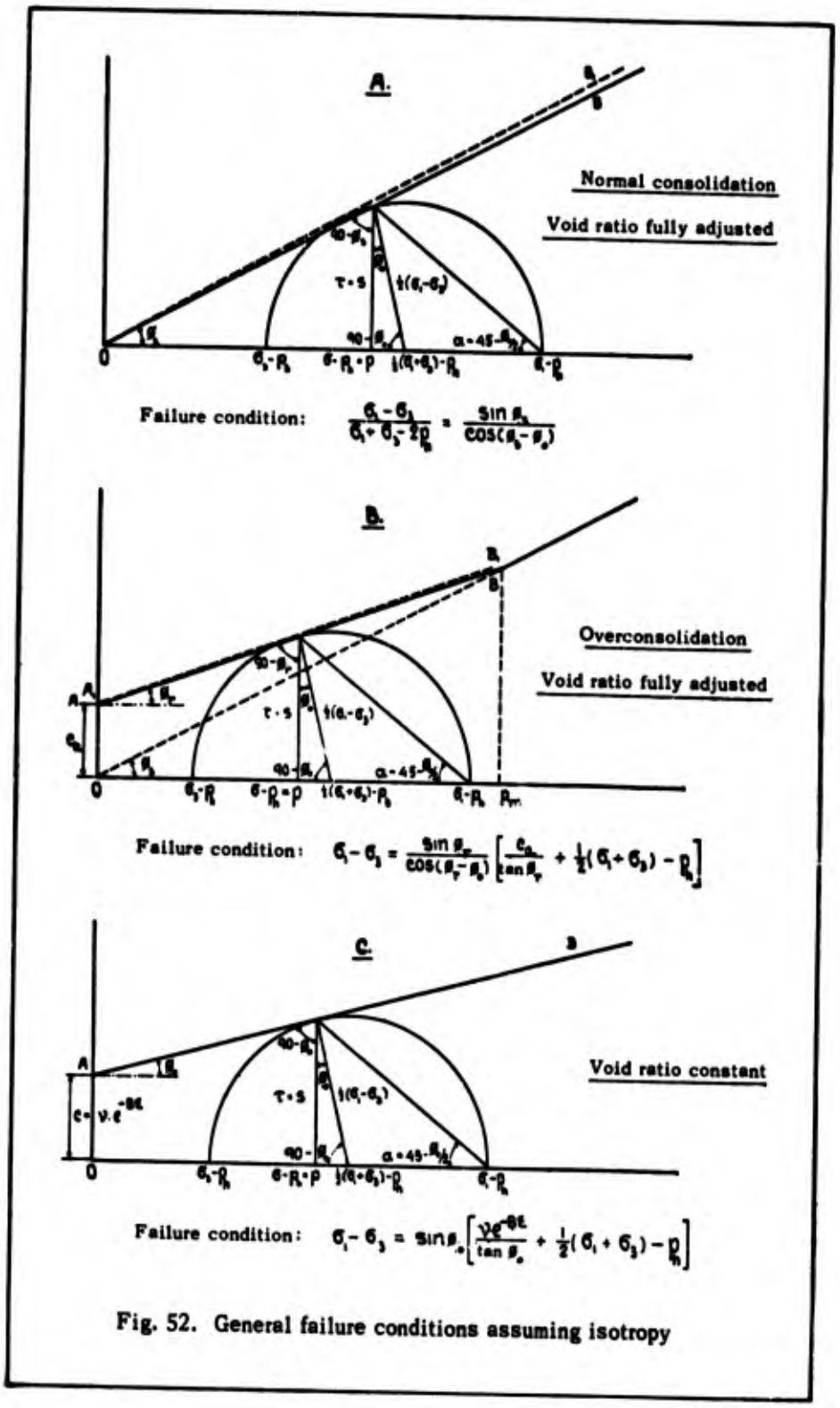

Fig. 52. General failure conditions assuming isotropy

$$\frac{\sigma_1 - \sigma_3}{\sigma_1 + \sigma_3 - 2p_h} = \frac{\sin \phi_s}{\cos (\phi_s - \phi_o)} \qquad (52a)$$

If the apparent unit weight is introduced in the stress computations instead of the actual unit weight, then $p_u = 0$ and $\sigma' = \sigma''$ or,

$$\frac{\sigma''_1 - \sigma''_3}{\sigma''_1 + \sigma''_3} = \frac{\sin \phi_s}{\cos (\phi_s - \phi_o)} \qquad (52b)$$

Since $\cos (\phi_s - \phi_o)$ can, for all practical purposes, be set equal to "one" (e.g., for Vienna clay: $\phi_s = 25^o40'$, $\phi_o = 17^o30'$, and $\cos (\phi_s - \phi_o) = \cos 8^o10' = 0.99$), Rankine's failure condition for cohesionless material is obtained with the following angle of effective internal friction ϕ_s :

$$\frac{\sigma_1 - \sigma_3}{\sigma_1 + \sigma_3 - 2p_h} = \sin \phi_s \qquad (53a)$$

or

$$\frac{\sigma''_1 - \sigma''_3}{\sigma''_1 + \sigma''_3} = \sin \phi_s \qquad (53b)$$

that is, the cohesion is assumed to be zero and the angle of internal friction is set equal to the angle of apparent internal friction.

94. Except for low values of p , the shearing resistance line can, for the same type of soil in the overconsolidated state, be replaced by a straight line like A-B in fig. 52B. This straight line forms an angle ϕ_r with the axis of abscissas and intersects the axis of ordinates at a height c_a . Provided the effective normal pressures p upon the shear plane do not exceed p_m , the following failure condition is obtained:

$$\sigma_1 - \sigma_3 = \frac{2 \sin \phi_r}{\cos (\phi_r - \phi_o)} \left[\frac{c_a}{\tan \phi_r} + \frac{1}{2} (\sigma_1 + \sigma_3) - p_h \right] \qquad (54a)$$

or by introducing the apparent unit weight:

$$\sigma_1'' - \sigma_3'' = \frac{2 \sin \phi_r}{\cos (\phi_r - \phi_o)} \left[\frac{c_a}{\tan \phi_r} + \frac{1}{2} (\sigma_1'' + \sigma_3'') \right] \tag{54b}$$

Since $\cos (\phi_r - \phi_o)$ differs even less from "one" than $\cos (\phi_s - \phi_o)$, the above equations can respectively be replaced by:

$$\sigma_1 - \sigma_3 = 2 \sin \phi_r \left[\frac{c_a}{\tan \phi_r} + \frac{1}{2} (\sigma_1 + \sigma_3) - p_h \right] \tag{55a}$$

and

$$\sigma_1'' - \sigma_3'' = 2 \sin \phi_r \left[\frac{c_a}{\tan \phi_r} + \frac{1}{2} (\sigma_1'' + \sigma_3'') \right] \tag{55b}$$

These equations represent Mohr's general failure condition, but with the coefficients determined according to the Krey-Tiedemann procedure.

In soils with a highly curved shearing resistance line, only a specific portion of these curves can be replaced by a straight line, and an apparent cohesion c_a must be introduced also for the normally consolidated state.

Failure Conditions at a Constant Void Ratio

95. In practice it very seldom happens that the load is applied to a cohesive soil at such a slow rate that the void ratio always corresponds to the stress conditions. Usually, the total additional load is applied before the void ratio changes at all, particularly in the deeper layers. Therefore, the cohesion remains constant, whereas the hydrostatic pressure of the pore water varies. For a given point with a void ratio ϵ, the following relationship is obtained according to equation (30):

$$c = \nu e^{-B\epsilon} \tag{56}$$

In this case Coulomb's condition can be used when it is applied to the effective stresses and to the angle of effective internal friction ϕ_o. From Mohr's diagram (fig. 52C) the following general failure condition

is obtained for the zone with a void ratio ϵ :

$$\sigma_1 - \sigma_3 = 2 \sin \phi_o \left[\frac{\nu_e^{-B\epsilon}}{\tan \phi_o} + \frac{1}{2} (\sigma_1 + \sigma_3) - p_h \right] \qquad (57a)$$

In this case the hydrostatic pressure of the pore water is different from the static pressure head. Through equation (5) we obtain:

$$\sigma_1'' - \sigma_3'' = 2 \sin \phi_o \left[\frac{\nu_e^{-B\epsilon}}{\tan \phi_o} + \frac{1}{2} (\sigma_1 + \sigma_3) - p_u \right] \qquad (57b)$$

in which the excess hydrostatic pore-water pressure p_u differs from zero.

However, experimental data for determination of the changes in pore-water pressure are not yet available. In practice, equation (57) can be used for ascertaining whether or not failure will occur at a given point of the subsoil. For the determination of failure surfaces in general it can only be used in the cases where the void ratio and hence the cohesion can be considered constant within the entire soil layer to be investigated.

96. In a normally consolidated or slightly overconsolidated soil, a sudden load application initially produces a hydrostatic excess pressure in the pore water which gradually disappears as the void ratio decreases and the cohesion increases. Consequently, the most unfavorable stress conditions occur immediately after loading and the angle of effective internal friction must be applied in equation (57).

97. If the soil is highly overconsolidated and the load suddenly is applied to it, the opposite may occur because a negative pressure initially develops in the pore water and gradually disappears as the void ratio increases and the cohesion decreases. Hence the state of stress that eventually leads to failure may not develop until sometime after the load is applied. This fact can, among other things, explain the delayed failure of the soil observed below foundations of existing structures.

In such cases the stress condition at a completed adjustment of the void ratio is controlling, and the corresponding failure condition, equation (55), should be applied.

Effect of the Intermediate Principal Stress

98. In the preceding considerations the effect of the intermediate principal stress upon the failure conditions was apparently disregarded as is customary. Actually, however, the effect of the intermediate principal stress upon the cohesion is taken into account in equation (57) through its effect upon the void ratio. In $\sigma_1 = \sigma_2 > \sigma_3$ (case I), the void ratio is smaller and the cohesion greater than in $\sigma_1 > \sigma_2 = \sigma_3$ (case II). Undoubtedly the frictional resistance is also affected by the intermediate principal stress.

Only a few test results have thus far been published concerning the effect of the principal stress relations upon the void ratio and the failure conditions, the most important ones being those by Kjellman (27) and Rendulic (38). For normal sand, Kjellman found in case I an apparent angle of internal friction $\phi = 43^\circ$ and in case II $\phi = 35^\circ$. For Vienna clay Rendulic found in case I a substantially greater compressive strength than in case II. However, it is not possible to determine accurately from these test data which part of the difference in the compressive strength is caused by differences in the frictional resistance and which part by differences in cohesion.

Von Mises (32) has proposed the following general failure condition for solid materials:

$$(\sigma_1 - \sigma_2)^2 + (\sigma_2 - \sigma_1)^2 + (\sigma_3 - \sigma_2)^2 = f(\sigma_1 + \sigma_2 + \sigma_3)$$

This failure condition can probably also be used for cohesionless soils without stratification. However, in view of the preferred orientation of the flaky particles of cohesive soils, it is an open question whether this failure condition can also be applied to such soils.

A theoretical treatment of the problem similar to the one developed by Brandtzaeg (5) for solids can be successfully applied to uniform soils, as shown by Terzaghi. On the other hand, it is doubtful whether the application of this theory to cohesive soils will lead to reliable results since the assumption of a macroscopic isotropy does not appear to be justified in this case.

XI. RAPID TESTS AND HYDROSTATIC EXCESS PORE-WATER PRESSURE

Results of Rapid Shear Tests

99. In order to eliminate the difficult determination of the pore-water pressure, shear tests are often made as rapidly as practically feasible. In this way a change in the void ratio is avoided, and the effect of the variations in the pore-water pressure caused by shear stress is included in the test results. The question now arises whether the results of such tests can be used in the design of structures that are completed before the void ratio of the soil has adjusted itself noticeably to the new stress conditions.

100. Such rapid shear tests were made with both Vienna clay and Little Belt clay. The specimens were prepared in the normally consolidated as well as in the simple and cyclic overconsolidated state, just as in the case of slow shear tests. On the other hand, during the actual shear test the time intervals between individual load increments were kept constant at five seconds, whereas at the start of the test the load increments amounted to approximately 10 percent of the ultimate load, and were gradually reduced to 2 percent of the ultimate load in the course of the test. The total test duration ranged from two to three minutes.

The results of these tests are shown in fig. 53, where the shearing resistance curves of the standard tests, discussed earlier, also are shown by dashed lines. In the case of Vienna clay, the rapid and standard tests were not made with the same batch, however, and in the case of Little Belt clay there was a shortage of material so that the rapid tests had to be made with a clay which had already been used for the standard tests.

In accordance with previously discussed tests (fig. 32), the values obtained for the shearing resistance by means of rapid tests are lower for normal consolidation and higher for strong overconsolidation than those obtained by means of the corresponding standard tests. As explained earlier, the causes of these differences are the hydrostatic over- or underpressures in the pore water, the change in the void ratio and hence in cohesion, and the effect of viscosity. For Little Belt clay in a normal and cyclic

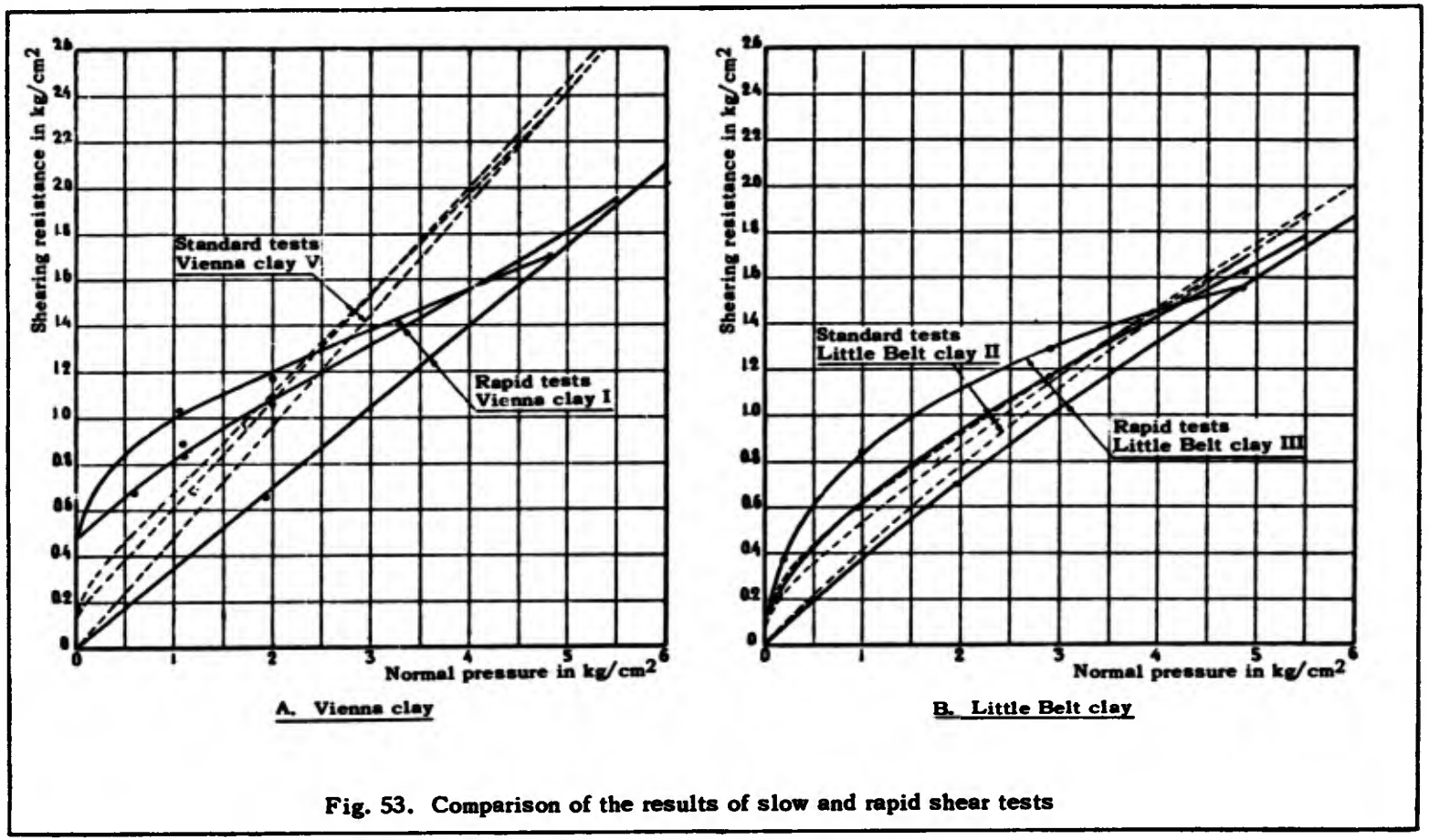

Fig. 53. Comparison of the results of slow and rapid shear tests

overconsolidated state, the differences between the test results of the rapid and standard tests are very small compared with the corresponding differences for Vienna clay.

101. The difference between the results of rapid and standard tests becomes even more pronounced when the Krey-Tiedemann coefficients of friction (μ_r) and cohesion (μ_c) are evaluated. The determination of these coefficients is shown in fig. 54A for tests that were all made with the

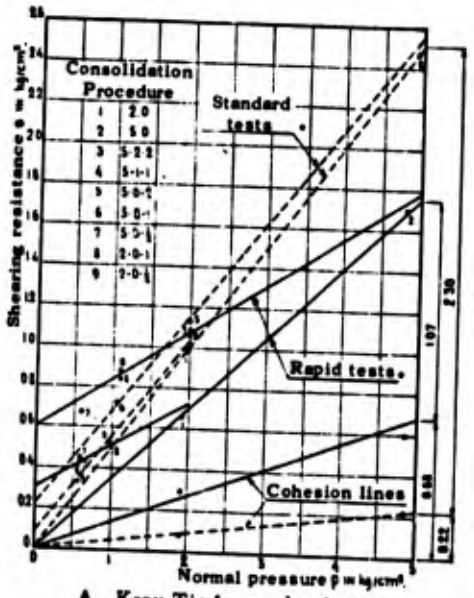

A. Krey-Tiedemann's shearing resistance lines

Standard Tests t_v > 600 MIN.		Rapid Tests t_v < 5 MIN.		$\frac{\mu_{Rapid}}{\mu_{Norm}}$
μ_b = 0.504	β_b = 26°45'	μ_b = 0.350	β_b = 19°17'	0.69
μ_r = 0.460	β_r = 24°42'	μ_r = 0.214	β_r = 12°05'	0.46
μ_c = 0.044	β_c = 2°31'	μ_c = 0.136	β_c = 7°45'	3.10

B. Coefficients of friction and cohesion

MATERIAL		p $\frac{kg}{cm^2}$	Shearing Resistance Standard Tests s_v	Shearing Resistance Rapid Tests s_v	$\frac{s_v}{s_v}$
Vienna clay (5-0-p) Fig. 54A	ΔH=0	1.0	0.66	0.82	1.20
	$\Delta\beta$=0	1.5	0.82	0.90	1.10
Vienna clay (5-p-p) Fig. 53A	ΔH=0	1.85	1.04	1.17	1.12
	$\Delta\beta$=0	1.85	1.04	1.17	1.12
Little Belt clay (5-p-p) Fig. 53B	ΔH=0	2.55	1.07	1.23	1.15
	$\Delta\beta$=0	3.20	1.24	1.34	1.09

C. Effect of thixotropy and viscosity

Fig. 54. Slow and rapid shear tests with Vienna clay I

same batch of Vienna clay. However, in the standard tests the complete shearing resistance-hysteresis loops could not be determined because of a shortage of test material from the same batch. For this reason, tests with normally consolidated and cyclic overconsolidated specimens were used as a basis of comparison. Consolidation procedures (5-0-p) as well as (2-0-p) were used.

The table of the coefficients of friction and cohesion in fig. 54B shows that rapid tests yield coefficients of friction (μ_r) which are less than half as large and coefficients of cohesion (μ_c) more than three times as large as those obtained in standard tests. Actually, however, the coefficient of internal friction remains constant, whereas the void ratio and hydrostatic excess pressures of the pore water and hence the cohesion and

effective normal pressures vary in accordance with the test conditions. To this must be added a difference in the thixotropic softening of the material in standard versus rapid tests, and further the effect of viscosity in the case of rapid tests.

For Vienna clay I, the coefficients of the proposed failure condition, equation (29), obtained by means of standard tests, are $\mu_o = 0.330$ and $\kappa = 0.097$. The corresponding values for rapid tests could not be obtained with the desired accuracy, since in this case only the water content at the center of the specimen was determined. Hence reliable mean values of the water content of the entire failure zone could not be established.*

Effect of Viscosity

102. The difference in the effect of such thixotropic changes, increased by the influence of viscosity, may be determined as the difference in the results of a rapid and a standard test. To do this the soil must be overconsolidated to such an extent that a change in volume and creation of a hydrostatic excess pressure in the pore water do not occur during the test. As previously indicated, this degree of overconsolidation can only be determined in an approximate manner by means of the tests described here, because of small changes in the physical properties of the various test specimens and because use of the different test procedures (shear box and consolidometer).

According to fig. 40, the specimen thickness of Vienna clay does not change, $\Delta H = 0$, during the test for the consolidation procedure (5-0-p) for $p = 1.0$ kg/cm^2, whereas curves representing the equivalent pressures before and after the test intersect at $p = 1.3$ kg/cm^2 ($\Delta p_e = 0$) . For the consolidation procedure (5-p-p), both ΔH and Δp_e are equal to zero for $p = 1.85$ kg/cm^2. From fig. 41 for Little Belt clay and the consolidation

---

* Translator/author note: This paragraph is incomplete; it refers to unsuccessful attempts to evaluate results of rapid shear tests by use of equivalent pressures, p_e .

procedure (5-p-p) is obtained; $\Delta H = 0$ for $p = 2.55$ kg/cm^2 and $\Delta p_e = 0$ for $p = 3.20$ kg/cm^2. Values of the shearing resistances determined by standard and rapid tests corresponding to these values of p are obtained from figs. 53 and 54A and are summarized in the table of fig. 54C.

According to this tabulation, rapid tests yield 10 to 20 percent higher values for the shearing resistance than standard tests. This difference represents the effect of viscosity, increased by the differences in the thixotropic softening. Because of uncertainty in the determination of the exact values of p, for which no volume change occurs during the shear test, the above figures can, of course, only serve as a guide. Furthermore, whether this effect, expressed in percent of the true shearing resistance, becomes greater or smaller for other states of consolidation is not known. Even though the influence of viscosity produces an appreciable increase of the shearing resistance in all rapid tests, it is likely that the rate of displacement in case of actual foundations is so small that this influence must be disregarded.

Practical Application of Rapid Tests

103. On the basis of these results and the final conclusions of the preceding section, the practical applicability of rapid tests can be summarized as follows:

When normally consolidated or slightly overconsolidated cohesive soils are involved, a rapid test furnishes a measure of the decrease in shearing resistance by hydrostatic excess pressure in the pore water (caused by the sudden application of shear stress). Moreover, an increase in the cohesion, noted in most standard tests, does not occur in rapid tests. The effect of viscosity must always be subtracted from the shearing resistance obtained by means of a rapid test. Furthermore, consideration must be given to the fact that the stress conditions and consequently the hydrostatic excess pressure of the pore water below the actual foundation and in a rapid test may be different.

104. In addition to the viscosity, a temporary negative hydrostatic pressure in the pore water and an increase in the effective normal

pressures and in the shearing resistance resulting therefrom must be taken into account in rapid tests with strongly overconsolidated cohesive soils. In a real foundation the change in stress conditions seldom represents that of a pure shear stress. It is more likely that all principal stresses are increased, which may cause an excess overpressure in the pore water. Moreover, in cases where pure shear stress and a negative pressure in the pore water occur, this negative pressure is equalized in the course of time. At the same time the effective normal stresses are reduced, the void ratio increases, and the cohesion decreases. Therefore, in this case the results of rapid tests should not be used as a basis for the design of structures.

105. In practical rapid tests, the effect of viscosity can probably be disregarded when very thick and properly sealed specimens are used and the test duration is increased from a few minutes to one hour. However, a reliable seal is difficult to attain. Moreover, when only rapid tests with an undisturbed soil are performed, it is not known whether the shear stress produces an over- or an underpressure in the pore water. In order to ascertain this, the same soil must also be subjected to slow tests, and the settlement or rise of the specimen surface must be observed.

Undisturbed cohesive soils usually have a very complex structure that is disturbed by displacements. It is therefore possible that a shear stress in such soils nearly always produces an overpressure in the pore water. In this case the great danger of overestimating the shearing resistance by use of rapid tests would be eliminated. The above-mentioned results of rapid tests with remolded soils are a warning against indiscriminate use of such tests.

Determination of Pore-Water Pressures

106. Because of the difficulty in determining the effect of viscosity, the results of rapid tests are of somewhat doubtful value, even in the case of normally consolidated soils. A great improvement would be achieved if the excess pressure p_u in the pore water, caused by the shear load, could be determined separately. The original shearing resistance could

then be obtained by means of standard tests and from equation (28), replacing p by the difference $(p - p_u)$ and using p_e corresponding to the void ratio at the start of the test.

In a few cases the pore-water pressure has been measured directly, not only during compression tests in the laboratory (Rendulic (37)), but also in the foundation soil (Biemond (4), Broekman-Buisman (8)). The greatest difficulty encountered in such direct measurements of the pore-water pressure is that no water can be removed or added in order to avoid development of a flow with a gradient and a consequent change in the pore-water pressure.

107. In the absence of appropriate and reliable devices for a direct measurement of the pore-water pressures, these pressures could be determined from the time-settlement curves for the various load increments in case the coefficient of permeability k is known. For this purpose the shear test must be made with fairly large load increments and with time intervals of at least 24 hours. Also, the filter paper (see fig. 22) must be left out, and it would be preferable to replace the dentated porous stones by rough stones. This does not alter the results of shear tests with cohesive soils as shown in the tests by Jürgenson (26) and by the author. When the time intervals are large enough to achieve an almost complete equalization of the excess pore-water pressures produced by the load increment, the initial value of these pressures can be determined with the aid of the formulas and tables contained in Terzaghi-Fröhlich's book entitled, "Theorie der Setzungen von Tonschichten" (Theory of Settlement of Clay Strata) (53) in the following manner (the notations in this book are used here in order to facilitate comparison).

108. Because of the nonuniform distribution of the shear stresses in a vertical cross section, the initial pore-water pressure will also be distributed nonuniformly. A trapezoidal distribution of the pressure may be assumed as the first approximation. Furthermore, the ratio between the mean pressure and the pressure in the failure zone will be equal to the ratio between the corresponding void ratio changes. The latter ratio k_e is given by equation (39). According to fig. 55, in which q_u and q_o

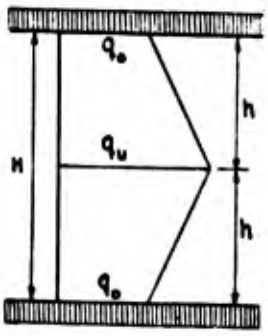

Fig. 55. Pore-water pressure during a shear test

are the excess hydrostatic pressure at the center and at the surface, respectively,

$$\frac{\frac{1}{2}(q_u + q_o)}{q_u} = k_e \tag{58}$$

or

$$\upsilon = \frac{q_u}{q_o} = \frac{1}{2k_e - 1} \tag{59}$$

When υ has been determined, a table can be prepared with the aid of equation (13) in section 23 and table 4 in reference (53) which indicates the relationship between the degree of consolidation μ_T and the time factor τ for a given specimen thickness H. The value of μ_T is then determined from the time-settlement curve, for a given time t after the load is applied, with the aid of the following equation:

$$\mu_T = \frac{s_t}{s_e} \tag{60}$$

in which s_t is the settlement at time t, and s_e the ultimate settlement produced by the load. The value of τ is determined from μ_T and the above-mentioned table whereupon, according to equation (15) in section 21 and equation (40) in section 15 of reference (53):

$$\tau = \frac{ct}{h^2} = \frac{kt}{\alpha\gamma}\frac{1 + \epsilon_o}{h^2} \tag{61}$$

Furthermore from equation (4) in section 17 of reference (53) and from the above equation (58),

$$\alpha = \frac{\Delta\epsilon}{\frac{1}{2}(q_u + q_o)} = \frac{\Delta\epsilon}{k_e q_u} \tag{62}$$

or

$$q_u = \tau\frac{\Delta\epsilon}{1 + \epsilon_o}\cdot\frac{\gamma h^2}{ktk_e}$$

and with

$$\Delta\epsilon = \frac{s_e}{2h}(1 + \epsilon_o)\frac{1}{k_e} \tag{63}$$

yields

$$q_u = \frac{\tau}{t} \cdot \frac{s_e \gamma h}{2k\, k_e^2} \tag{64}$$

Meaning of above symbols:

q_u = initial hydrostatic excess pressure at the center, g/cm^2
s_e = ultimate settlement for a load increment, cm
γ = specific gravity of the pore water, g/cm^3
$2h = H$ = specimen thickness, cm
k = coefficient of permeability, cm/sec
t = time after application of load, sec
τ = time factor (see reference (53)), dimensionless
k_e = effectiveness (equation (39)), dimensionless

109. The proposed method furnishes the initial values of the hydrostatic pore-water pressures or of their variations, with respect not only to the load increment but also to the stress conditions prevailing at the time the particular load increment is applied. However, it will of course be necessary to verify the method experimentally and to establish the most favorable test conditions before it can be universally applied.

Preliminary tests show that the hydrostatic pressure of the pore water also depends on the magnitude, direction, and velocity of the displacement, i.e., that this pressure can be increased or decreased by thixotropic changes of the material. When these effects are relatively important, equation (64) gives only an approximate value of q_u. In such a case it is better to use other equations that take the changes of q_u during the test into account (see Chapter IX, section 31, in reference (53)).

XII. CHANGES IN THE SHEARING RESISTANCE AFTER FAILURE

Stress Deformation Curves After Failure

110. Experienced engineers have known for a long time that undisturbed cohesive soils lose part of their strength at failure. The fact that the shearing resistance of a remolded, reconsolidated clay also is reduced after failure as a result of rapid, plastic flow was, among others, observed in the soils laboratory of the Hanover Institute of Technology and also by Gruner and Haefeli (25). However, more detailed data concerning this reduction in shearing resistance have thus far not been published.

In some soils the minimum value of the shearing resistance after failure is not reached until relatively large displacements have taken place. In conventional shear devices where failure is produced by a straight parallel displacement, the cross section of the specimen changes during the test, and the extent of the displacement is limited. In a ring shear apparatus, however, the test can be continued after failure as long as desired without a change in the cross section, and the complete stress-displacement curves for shear can be obtained.

Examples of the test procedure and the evaluation of the data for determining such complete stress-displacement curves for shear are given in the appendix, and some examples of evaluated test data are shown in fig. 56. Because of the relatively high rates of flow after failure, it is difficult to determine displacements corresponding to values of the shearing resistance in an accurate manner. Moreover, the position of the curves after failure is somewhat affected by the maximum rate of flow. The higher the rate of flow, the greater is the reduction in the shearing resistance. The stress-displacement curves after failure can therefore be determined only in an approximate manner and are represented by dashed lines in fig. 56.

111. After failure, the shearing resistance of Vienna clay in a normally consolidated state (fig. 55A) decreases rapidly to 73 percent of its maximum value, whereupon it slowly increases again to 83 percent. At the same time a slight additional consolidation occurs, which means that

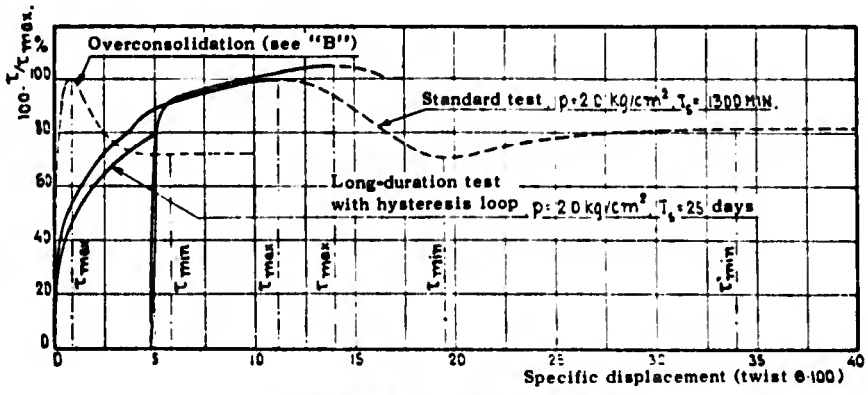

A. Vienna clay – normal consolidation

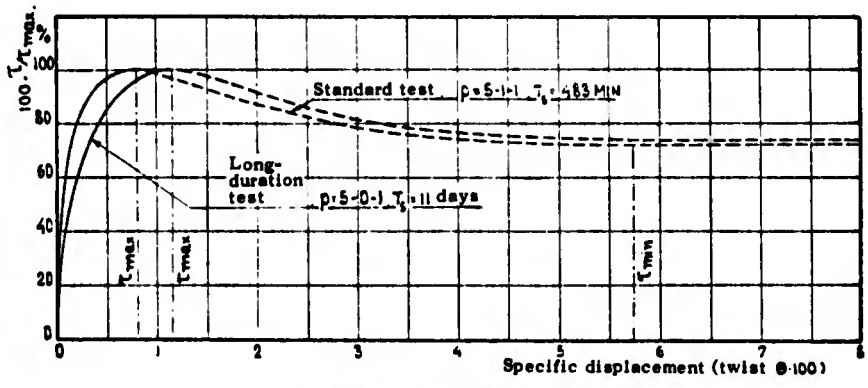

B. Vienna clay – overconsolidation

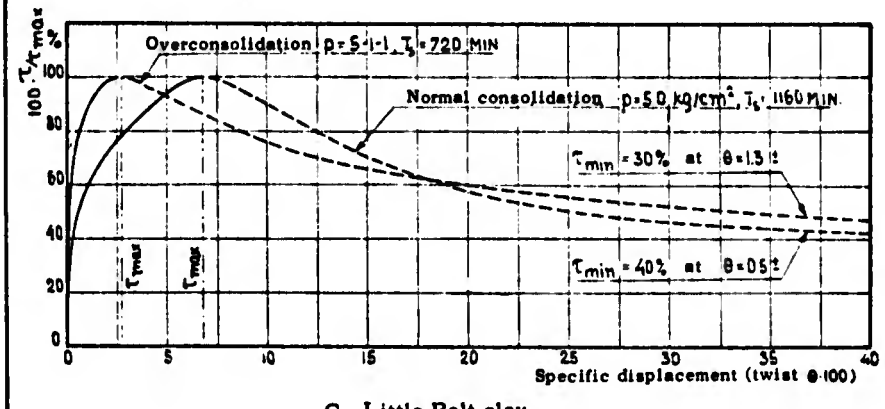

C. Little Belt clay

Fig. 56. Stress-displacement curves for shear before and after failure

after failure a temporary excess pressure is again produced in the pore water. The increase in the shearing resistance from 73 to 83 percent is probably caused by an equalization of this excess pressure and by the increase in the cohesion corresponding to the additional consolidation.

Vienna clay in a strongly overconsolidated state (p = 5-1-1) likewise shows a minimum value of the shearing resistance of approximately 72 percent of the maximum value determined by means of Krey's shear apparatus; but in this case an ultimate increase of the minimum value does not occur. However, in strongly overconsolidated soils a slight additional swelling occurs also after failure (as in the case of dense sands). Here both the maximum and minimum values of the shearing resistance are attained at relatively small displacements, and the stress-displacement curves are therefore shown in an enlarged scale in fig. 56B.

In Little Belt clay (fig. 56C), the decrease in the shearing resistance occurs at a slower rate, but it is surprisingly large. For normally consolidated Little Belt clay, the minimum value amounts to only 40 percent of the maximum value and is not reached until the angle of twist θ has a value of about 0.5 radians, i.e., at a displacement of approximately 3 cm (see fig. 72 in the appendix). At strong overconsolidation (p = 5-1-1) the maximum value is reached sooner, and after failure the shearing resistance first decreases more rapidly and then more slowly than for normal consolidation. The minimum value of about 30 percent is not reached until the angle of twist θ is approximately 1.3 radians. In tests of long duration (shear time T_s = 2 months), however, the minimum value appears to be somewhat higher, namely 38 percent of the maximum value. Neither in normally consolidated nor in overconsolidated Little Belt clay was an ultimate increase of the minimum value observed.

Change in the Friction and Cohesion After Failure

112. The shearing resistance diagrams corresponding to the minimum values of the shearing resistance are shown in fig. 57 and compared with the maximum values obtained with Krey's shear apparatus. For Vienna clay, both the temporary and the ultimate minimum values are plotted. The

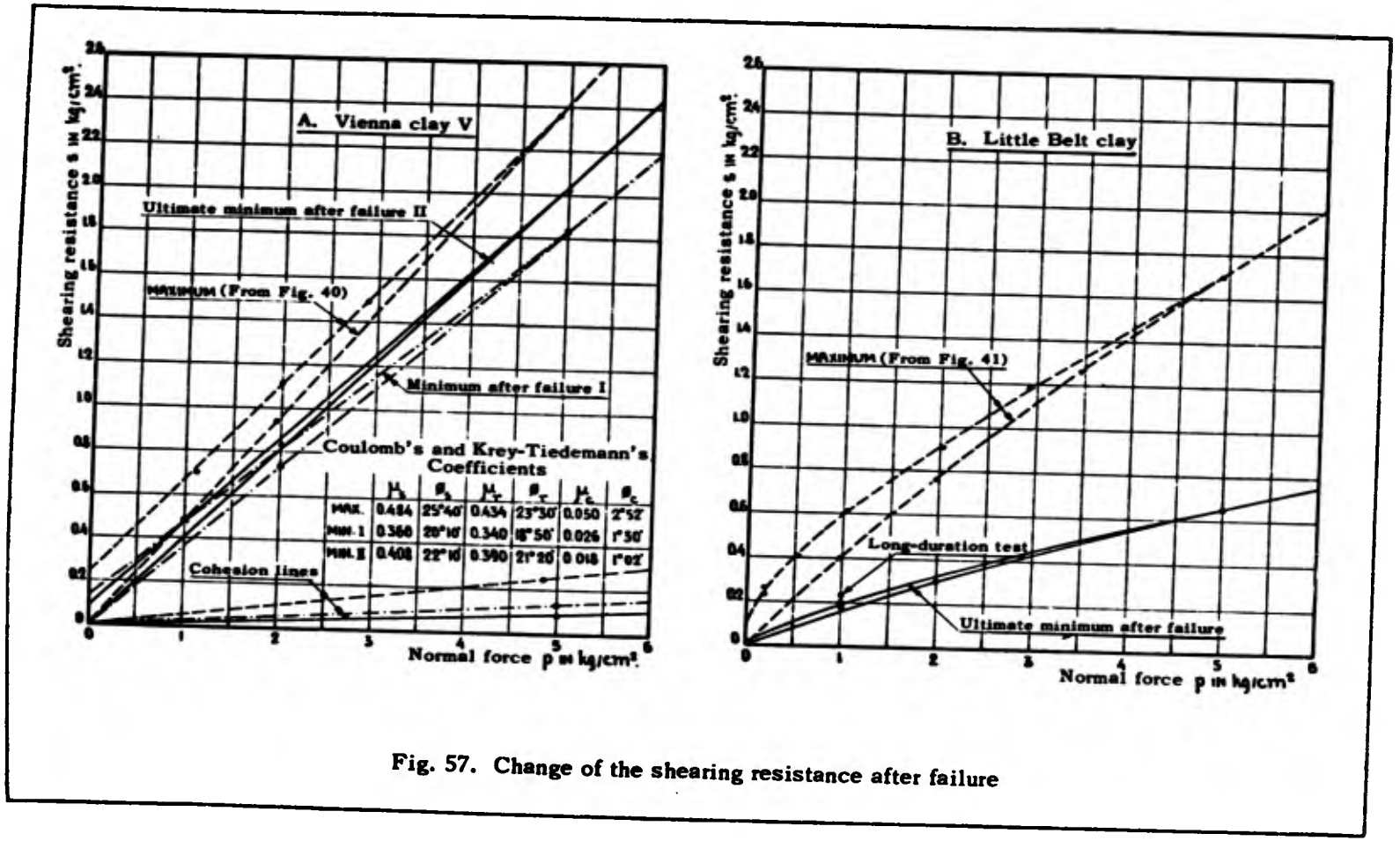

MAX.	0.484	25°40'	0.434	23°30'	0.050	2°52'
MIN. I	0.368	20°10'	0.340	18°58'	0.026	1°30'
MIN. II	0.408	22°10'	0.390	21°26'	0.048	1°92'

Fig. 57. Change of the shearing resistance after failure

question now arises whether the decrease of the shearing resistance is caused by the decrease of the cohesion alone or by a decrease of the friction in addition to the decrease of the cohesion.

For Vienna clay, the minimum values of Krey-Tiedemann's coefficients, μ_r and μ_c, can be determined as shown in fig. 57A. The coefficients corresponding to the temporary minimum show that μ_r is reduced by 22 percent and μ_c by 48 percent. The ultimate minimum values correspond to a reduction by 13 percent (μ_r) and 60 percent (μ_c). A similar evaluation of the tests with Little Belt clay cannot be made because of the curvature of the shearing resistance lines.

Under the assumption that the proposed failure condition, equation (29), also applies to minimum values of the shearing resistance, the plotted points $\left(\frac{p}{p_e}, \frac{s_{min}}{p_e}\right)$ show the minimum values of the coefficients of effective internal friction (μ_o) and of the cohesion (κ), as shown in fig. 58. The values of the equivalent pressures p_e respectively correspond to the void ratios at failure (temporary minimum) and to the ultimate void ratios (ultimate minimum) of the failure zone. The table in fig. 58A shows that in Vienna clay the coefficient of friction is

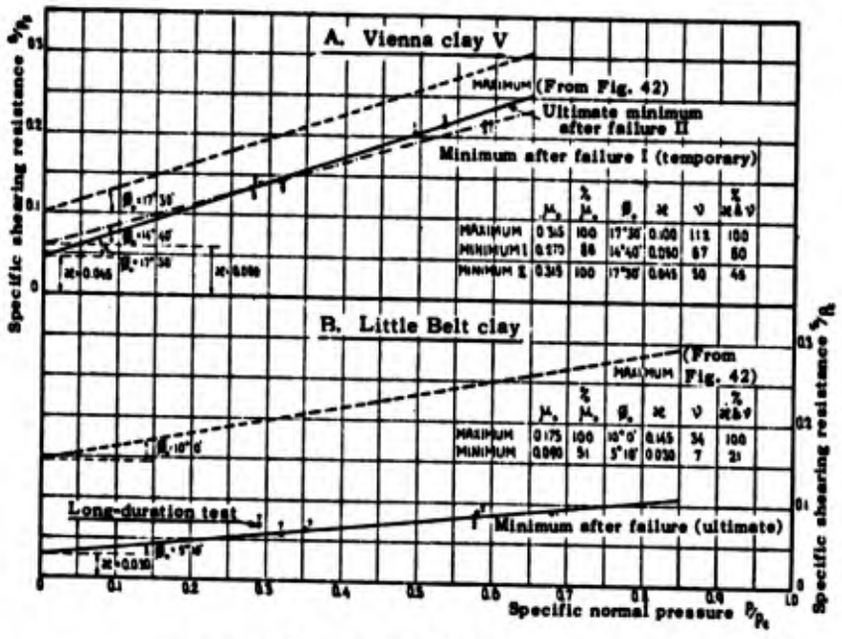

Fig. 58. Change of the shearing resistance coefficients after failure

temporarily reduced by 16 percent and the coefficient of cohesion by 40 percent. This decrease of the coefficient of friction is only apparent, however, and is caused by the previously mentioned excess pressure of the pore water occurring after failure. The coefficients corresponding to the ultimate minimum show that the coefficient of friction is not changed by failure, whereas the coefficient of cohesion is reduced by 55 percent. In the case of Little Belt clay, on the other hand, the coefficient of friction is reduced by 49 percent (fig. 58B, ultimate minimum) and the simultaneous reduction in the coefficient of cohesion amounts to 79 percent.

The number of the tests discussed above is insufficient to draw final conclusions concerning the change in the coefficients of friction and cohesion after failure. According to communications from Dr. B. Tiedemann and Dipl. Ing. J. Ohde, the decrease of the shearing resistance after failure has lately been investigated by means of a ring shear apparatus at the "Preussische Versuchsanstalt für Wasserbau und Schiffbau" in Berlin. These tests were made with a larger number of different soils, and the results seem to be quite similar to those mentioned above.

Recovery of the Shearing Resistance

113. When the rapid, plastic flow is arrested by a further decrease of the shear load after the ultimate minimum value of the shearing resistance has been reached, a recovery of shearing resistance occurs in the course of time. This recovery was observed in all tests and was especially pronounced in the case of Vienna clay in a normally consolidated state.

The results of a test with normally consolidated Vienna clay ($p = 2.0$ kg/cm^2), made for the purpose of investigating these processes, are shown in fig. 59. The original maximum value s_{max} and minimum value s_{min} of the shearing resistance amounted to 1.00 and 0.73 kg/cm^2, respectively. At the time of failure the water content of the shear zone was approximately 25 percent. In the course of time and progressive plastic flow, the water content decreases and s_{min} increases until eventually a stationary condition is attained at a water content of approximately 24 percent and a value

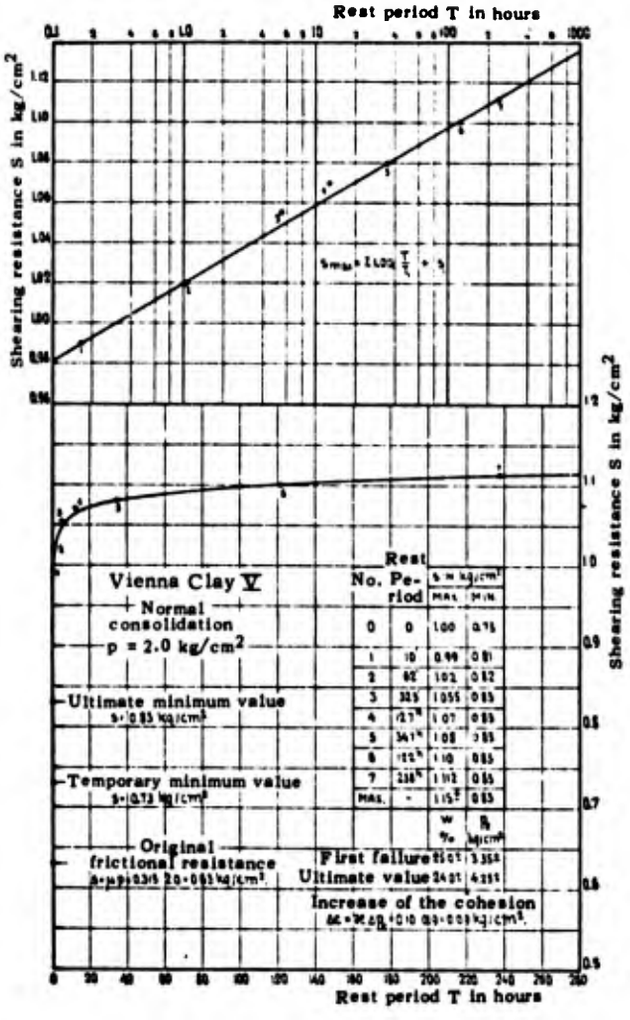

Fig. 59. Recovery of the shearing resistance in Vienna clay

s_{min} = 0.83 kg/cm^2. The ultimate minimum value of the shearing resistance has been reached at this point. When the flow is interrupted and the specimen again is brought to failure after a certain period of time, the rest period T , by increasing the shear load, the new values of s_{max} appear to depend on the duration of the rest period, whereas the water content and s_{min} remain constant.

As can be seen in fig. 59, s_{max} first increases very rapidly with the duration of the rest period. It takes only about one hour for the shearing resistance to reach its original maximum value, but further increase occurs very slowly. When plotted in a simple logarithmic manner,

points (T, s_{max}) form approximately a straight line or, expressed analytically:

$$s_{max} = Z \log \frac{T}{T_1} + s_1 \tag{65}$$

in which Z and s_1 are coefficients. However, there must be a lower as well as an upper boundary value. Since the results of only one test are available, it is not possible to draw general conclusions for the time being.

For normally consolidated Vienna clay, the time interval between the placement of the thoroughly remolded specimen in the shear box and the beginning of the shear test amounts to approximately 150 hours. After a corresponding period of rest T = 150 hours, s_{max} = 1.10 kg/cm^2, which represents an increase of 0.10 kg/cm^2 over the original shearing resistance. However, during the plastic flow the water content decreased from 25 percent to 24 percent, and this corresponds to an increase in the cohesion of 0.09 kg/cm^2, as shown in fig. 59.

A very rapid recovery of the shearing resistance could also be observed in strongly overconsolidated Vienna clay. Whether the original maximum value (obtained with Krey's shear apparatus) is reached again could not be determined with certainty, since a ring shear apparatus does not furnish accurate maximum values of the shearing resistance in the case of strongly overconsolidated soils.

114. In contrast to Vienna clay, Little Belt clay shows a very slow recovery of the shearing resistance. In normally consolidated Little Belt clay the shearing resistance increases from 40 percent minimum value to 45-50 percent of the maximum value during a rest period of four to five days. A strongly overconsolidated specimen having a minimum value of 30 percent, after a rest period of four days, indicated an increase to 37 percent, and after 60 days an increase to 55 percent of the maximum value of the shearing resistance, determined with the Krey-Terzaghi shear apparatus. It is therefore an open question whether the original shearing resistance is ever again attained.

115. The decrease and subsequent recovery of the shearing resistance

of Vienna clay is doubtless caused by a thixotropic change of properties. However, the recovery curve in fig. 59 is quite different from the curves determined by means of Swedish cone tests (fig. 21). An explanation of this difference cannot be given at this time. Temporarily it can only be emphasized that the test conditions are different. Because of the small weight of the cone, the cone tests were made with a soil batch having a water content much higher than that of the softest specimens tested in the shear apparatus. In cone tests the effect of viscosity probably plays a more important part than in the slow shear tests discussed here. Moreover, in the latter considerable deformations and hence a thixotropic disturbance occur before failure. Furthermore, the thixotropic disturbance caused by remolding is different from the disturbance occurring in the planes of failure of the shear test specimens. In the latter case the flaky particles are oriented more or less in a specific direction even before failure, and the plastic flow after failure occurs in this direction. It is known from the field of colloid chemistry (Freundlich (19, 20)) that such an orientation of the particles of the solid phase has a considerable effect on the thixotropic properties.

Both the large decrease and the very slow and incomplete recovery of the shearing resistance of Little Belt clay indicate that in this case not only a thixotropic but also a more profound permanent change of the internal structure has taken place in the planes of failure. After the shear tests were completed and the test specimens had been removed from the shear box, planes of failure could not be detected with the naked eye in the case of Vienna clay. On the other hand, in the case of Little Belt clay, the test specimens split readily along the planes of failure, which had a semimat appearance.

APPENDIX - THE RING SHEAR APPARATUS

Advantages and Disadvantages of Shear Devices

116. Compared with conventional shear devices where failure is produced by a horizontal parallel displacement, an apparatus in which the test specimen is subjected to rotation offers the advantages that this type of loading is better suited for a theoretical treatment of the stress distribution and that the shear plane does not change during the test. This makes it possible to continue the test as long as desired, even after the shear strength has been attained, and to determine the decrease of the shearing resistance after failure or a possible recovery of the shearing resistance. Furthermore, conditions governing the slow, plastic flow before failure and the rapid, plastic flow after failure can also be investigated with this equipment.

This type of shear apparatus, in which the shear plane is a full circular cross section, has been used for many years both in America (15) and in Europe (Streck (44)). In addition, Dr. Tiedemann, at the Preussische Versuchsanstalt für Wasserbau and Schiffbau in Berlin, built an apparatus in which test specimen and cylinder have a full circular cross section. However, the bottom of the cylindrical vessel is subdivided in such a manner that a ring equipped with radial ribs is formed and can be rotated. But the full circular cross section of the test specimen has the disadvantage that the shear stresses and deformations caused by rotations decrease to zero toward the center. Under certain assumptions it is nevertheless possible to compute the highest shear stress of the cross section, as will be shown later. Difficulties will be encountered, however, in an attempt to determine the relationships between these shear stresses on the one hand and the actual normal stresses, the start and rate of the slow plastic flow, or the vertical settlements on the other hand.

In most cases, soils, and particularly cohesive soils, are subject to considerable volume changes by a pure shear load. Now when the shear stresses are unevenly distributed over the cross section of the test specimen there will also be differences in the volume changes. However, these

differences are partly equalized by a radial flow caused by an uneven distribution of the vertical normal stresses. This means that, in the case where the shear stresses cause a decrease in volume, the danger exists that the vertical load will be partly concentrated at the center of the specimen. This results in a decrease of the torsional resistance and hence in a decrease of the coefficient of internal friction, which is computed on the basis of uniform distribution of the vertical load.

117. The following advantages are obtained when the full circular cross section is replaced by an annular cross section:

1. A better agreement between the actual conditions and the assumptions required for the evaluation, particularly with respect to the distribution of the normal stresses in the shear plane.

2. The difference between the maximum and minimum shear stresses in the cross section is reduced, which facilitates the investigation of preliminary plastic flow phenomena and volume changes caused by pure shear stresses.

3. A condition of general flow and an even stress distribution are attained for a finite rotation, not only in theory but also in practice. This makes it possible to determine the decrease and eventual recovery of the shearing resistance after failure.

If the test specimen is confined between rigid annular sidewalls, these advantages will nevertheless be somewhat reduced by the friction between specimen and sidewalls. The influence of friction increases as the width of the ring decreases. Hence, when no provision is made to eliminate this friction, there exists a certain most favorable relationship between the inside and outside diameters of the ring.

An annular cross section also possesses several construction advantages over a full circular cross section, but the disadvantage is that it is difficult to install specimens of undisturbed soil. However, in tests with undisturbed cohesive soils this difficulty can be avoided by eliminating the horizontal confinement of the specimen by rigid rings. Such a test arrangement is used by the Building Research Station in Watford, England (Cooling-Smith (16)). In this case the soil is subjected to capillary pressure, and the magnitude and change of these pressures during the test

cannot yet be determined accurately, exactly as in unconfined compression tests. For this reason neither the true cohesion nor the coefficient of effective internal friction can be obtained from such tests. However, useful values are obtained for the sum of the true and apparent cohesion, and furthermore, this test arrangement offers good possibilities for checking the results of unconfined compression tests.

The theory, design, and calibration of a ring shear apparatus designed by the author and constructed in the soils laboratory of the Vienna Institute of Technology will be discussed in the following sections. Concurrently with the design and construction of this apparatus, similar testing equipment was proposed by Gruner and Haefeli (25).

Theory of the Apparatus

118. On the assumption that all normal cross sections remain plane and that the displacement in such cross sections is proportional to the distance from the center, Duguet, Ludwik, and Prandtl showed (Nadai (33)) that the displacement-shear stress function can be determined for a full circular cross section with a torsional load by differentiation of the moment-twist curve. This method can be extended to an annular cross section and to shear tests with soils in the manner described below.

Such a test specimen, of a thickness H, is shown in fig. 60. In soil tests the specimen is usually confined between rigid walls and subjected to a normal pressure p producing the lateral pressure p_s. In addition to the assumptions mentioned in the preceding paragraph it is also assumed that p and p_s are uniformly distributed and remain constant during the test, and that the friction between specimen and sidewalls produced by p_s can be disregarded. Further, the shear strain γ is assumed to be the same for the entire thickness H at a distance r from the center. To what extent these assumptions agree with the actual conditions will be discussed later.

119. If the moment M produces a total twist θ, the shear strain at a distance r from the center is given by

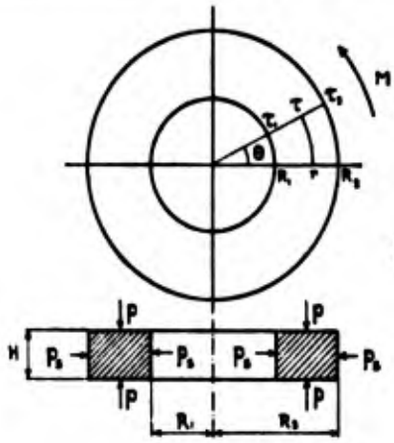

Fig. 60. Annular cylinder in torsion

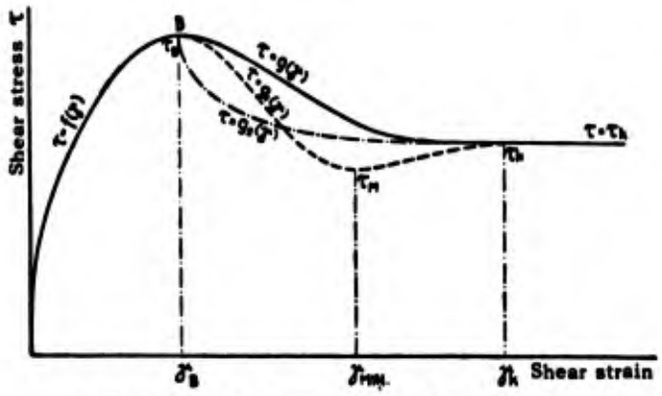

Fig. 61. Displacement curve for pure shear

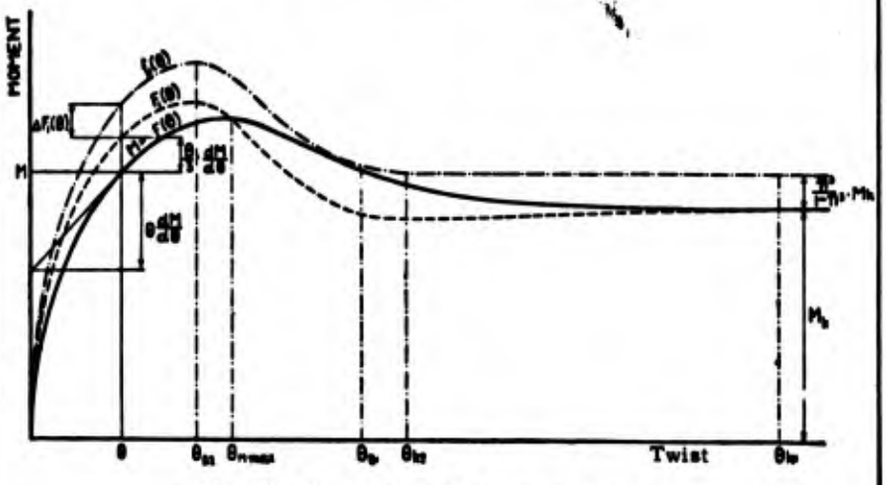

Fig. 62. Evaluation of the moment curve

$$\gamma = \frac{\theta}{H} r \tag{66}$$

Furthermore, if the stress-displacement curve for pure shear (fig. 61) before failure is represented by

$$\tau = f(\gamma) \tag{67}$$

and provided the failure stress nowhere is exceeded $\left(\theta < \gamma_B \frac{H}{R_2}\right)$, the moment can be expressed by

$$M = 2\pi \int_{R_1}^{R_2} \tau\, r^2 dr = \frac{2\pi H^3}{\theta^3} \int_{\gamma_{R_1}}^{\gamma_{R_2}} f(\gamma)\gamma^2 d\gamma \tag{68}$$

Since $\gamma_{R_1} = \frac{\theta}{H} R_1$ and $\gamma_{R_2} = \frac{\theta}{H} R_2$, the integral is also a function of θ, and because $f(\gamma)$ is independent of θ, differentiation of the moment with respect to θ yields:

$$\frac{dM}{d\theta} = -\frac{3}{\theta} \frac{2\pi H^3}{\theta^3} \int_{\gamma_{R_1}}^{\gamma_{R_2}} f(\gamma)\gamma^2 d\gamma + \frac{2\pi H^3}{\theta^3} \left(\frac{\theta}{H} R_2\right)^2 \frac{R_2}{H} f\left(\frac{\theta}{H} R_2\right)$$

$$- \frac{2\pi H^3}{\theta^3} \left(\frac{\theta}{H} R_1\right)^2 \frac{R_1}{H} f\left(\frac{\theta}{H} R_1\right)$$

Here, $f\left(\frac{\theta}{H} R_1\right)$ and $f\left(\frac{\theta}{H} R_2\right)$ are the shear stresses τ_1 and τ_2 at the inner and outer edges of the ring, and further simplification by means of equation (68) produces:

$$\tau_2 - \left(\frac{R_1}{R_2}\right)^3 \tau_1 = \frac{3}{2\pi R_2^3} \left(M + \frac{\theta}{3} \frac{dM}{d\theta}\right) \tag{69}$$

The right side of this equation has the same form as Duguet-Ludwik-Prandtl's equation, but on the left side, instead of one there are two unknowns τ_1 and τ_2. They are related to each other through equations

(66) and (67), however. In order to solve equation (69) the following curve is constructed from the experimentally obtained moment-twist curve, $M = F(\theta)$, and by means of the graphical procedure shown in fig. 62.

$$F_1(\theta) = M + \frac{\theta}{3}\frac{dM}{d\theta} \tag{70}$$

With $\frac{R_1}{R_3} = n$, equation (69) can be written in the following form:

$$\tau_2 = \frac{3}{2\pi R_2^3} F_1(\theta) + n^3 \tau_1$$

and

$$\tau_1 = \frac{3}{2\pi R_2^3} F_1(n\theta) + n^3 \tau_1(n\theta)$$

and further

$$\tau_1(n\theta) = \frac{3}{2\pi R_2^3} F_1(n^2\theta) + n^3 \tau_1(n^2\theta)$$

etc.

By addition the following expression is obtained:

$$\tau_2 = \frac{3}{2\pi R_2^3}\left[F_1(\theta) + n^3 F_1(n\theta) + n^6 F_1(n^2\theta) + n^9 F_1(n^3\theta) + \ldots \right. \tag{71}$$

and with

$$f_1(\theta) = F_1(\theta) + n^3 F_1(n\theta) + n^6 F_1(n^2\theta) + n^9 F_1(n^3\theta) + \ldots \tag{72}$$

$$\tau_2 = \frac{3}{2\pi R_2^3} f_1(\theta) \tag{73}$$

and

$$\tau_1 = \frac{3}{2\pi R_2^3} f_1(n\theta) \tag{74}$$

To the ordinates of the $F_1(\theta)$ curve is added:

$$\Delta F_1(\theta) = n^3 F_1(n\theta) + n^6 F_1(n^2\theta) + n^9 F_1(n^3\theta) + \ldots \tag{75}$$

and thus the $f_1(\theta)$ curve is obtained from which the shear stresses τ_1 and τ_2 at the inner and outer edges of the specimen can be computed by means of equations (73) and (74). Series (75) converges very well, and the first two or three terms suffice. Moreover, equation (75) needs to be evaluated for only one or two small values of θ, since equation (75) can be replaced by

$$\Delta F_1(\theta) = n^3 f_1(n\theta) \tag{76}$$

for larger values.

120. With $\tau_1 = \tau_2 = \tau_a$, in which τ_a represents a mean (average) shear stress, the well-known formula:

$$\tau_a = \frac{3M}{2\pi\left(R_2^3 - R_1^3\right)} \tag{77}$$

is obtained. In fig. 62 the ordinates respectively represent the values of function $f_1(\theta)$ and of moment curve $F_1(\theta)$, which in turn correspond to the values τ_2 and τ_a. However, the scales of the ordinates of the two functions are different.

As shown earlier for the soils investigated and for the conventional test procedure, the stress-strain curve for shear can approximately be represented by equation (25) up to the vicinity of failure or

$$\tau = \beta\gamma^m$$

In this case it is easy to prove that the ratio τ_2/τ_a is constant and is determined by the following equation:

$$\frac{\tau_2}{\tau_a} = \left(1 + \frac{m}{3}\right)\frac{1 - n^3}{1 - n^{3+m}} = k_a \tag{78}$$

Since the exponent m can be determined directly from the moment curve $M = F(\theta)$, the relationship (78) facilitates the determination of the stress-deformation curve. Near the failure, stress k_a decreases somewhat and differs but little from $k_a = 1$, as will be shown later.

121. After failure, the stress-displacement curve changes its form and may assume various shapes as shown in fig. 61. In some cases the value of τ decreases steadily as γ increases, until the terminal value τ_k is attained, whereas in other cases the stress passes a temporary minimum value before the terminal value τ_k is reached. In case τ_1 has not yet exceeded the failure stress, or $\frac{\theta}{H} R_2 > \gamma_B > \frac{\theta}{H} R_1$, the moment produced by the internal forces becomes:

$$M = \frac{2\pi H^3}{\theta^3} \int_{\gamma_{R_1}}^{\gamma_B} f(\gamma)\gamma^2 d\gamma + \frac{2\pi H^3}{\theta^3} \int_{\gamma_B}^{\gamma_{R_1}} g(\gamma)\gamma^2 d\gamma$$

If no discontinuities occur in the function $M = F(\theta)$ and its first derivative, there results:

$$\frac{dM}{d\theta} = -\frac{3}{\theta} \frac{2\pi H^3}{\theta^3} \int_{\gamma_{R_1}}^{\gamma_B} f(\gamma)\gamma^2 d\gamma - \frac{3}{\theta} \frac{2\pi H^3}{\theta^3} \int_{\gamma_B}^{\gamma_{R_2}} g(\gamma)\gamma^2 d\gamma$$

$$+ \frac{2\pi H^3}{\theta^3} \left[f(\gamma_B)\gamma_B^2 \frac{d\gamma_B}{d\theta} - f\left(\frac{\theta}{H} R_1\right)\left(\frac{\theta}{H} R_1\right)^2 \frac{R_1}{H} \right.$$

$$\left. + g\left(\frac{\theta}{H} R_2\right)\left(\frac{\theta}{H} R_2\right)^2 \frac{R_2}{H} - g(\gamma_B)\gamma_B^2 \frac{d\gamma_B}{d\theta} \right]$$

and since γ_B is independent of θ, that is $\frac{d\gamma_B}{d\theta} = 0$,

$$\frac{dM}{d\theta} = -\frac{3}{\theta} M + \frac{2\pi}{\theta} \left(\tau_2 R_2^3 - \tau_1 R_1^3\right)$$

$$\tau_2 - \left(\frac{R_1}{R_2}\right)^3 \tau_1 = \frac{3}{2\pi R_2^3}\left(M + \frac{\theta}{3}\frac{dM}{d\theta}\right)$$

Because $\tau_1 = f\left(\frac{\theta}{H} R_1\right)$, the above-mentioned graphical procedure can also be used when $\frac{\theta}{H} R_2 > \gamma_B > \frac{\theta}{H} R_1$. On the other hand, if a discontinuity occurs in $\frac{dM}{d\theta}$ when the failure stress is exceeded or somewhat later (in accordance with $\tau = g_2(\gamma)$ in fig. 61), the graphical procedure cannot be applied at this point. However, the points of the stress-displacement curves can be determined with sufficient accuracy up to the immediate vicinity of the failure stress and hence also the failure stress itself can be determined from the general shape of the curves.

122. The evaluation procedure in fig. 62 is based on the assumption that the stress-displacement curve does not have a temporary minimum value after failure ($\tau = g(\gamma)$). In this case the configuration of the curves and stresses is as follows: τ_2 reaches the failure stress at $\theta = \theta_{B_2}$ and the minimum value for $\theta = \theta_{k_2}$, while τ_1 reaches the same limits for $\theta = \theta_{B_1} = \frac{1}{n}\theta_{B_2}$ and $\theta = \theta_{k_1} = \frac{1}{n}\theta_{k_2}$. At θ_{k_2} the curve $f_1(\theta)$ changes to a straight line; at θ_{k_1} the curve $F_1(\theta)$ joins the moment curve, and together they form a straight line $M = M_k$. For $\theta > \theta_{k_1}$ equation (76) yields $f_1(\theta) = M_k + \frac{n^3}{1 - n^3} M_k$. If the moment curve between θ_{B_2} and θ_{k_1} is not accurately determined experimentally, the above relationships can furnish guiding points for estimation.

When the displacement is arrested by partial unloading to M_o, and M_o differs but little from M_k, it may be assumed that a uniform shear stress τ_o prevails in the shear plane. If, starting from this state, further tests are made (either unloading tests or, in the case of a strength recovery, reloading tests), the additional stresses can be determined by exactly the same procedure as above, since only the additional moments and twists are plotted.

On the other hand, if a hysteresis loop is introduced before failure,

the described evaluation procedure can be used only on the assumption that the stress-displacement curve for unloading is independent of the stress at reversal. This is probably not correct, and some internal stresses remain even at complete unloading.

Design of the Apparatus

123. The ring shear apparatus was designed with the objective of producing an apparatus by means of which various testing arrangements could be investigated in order to arrive at the best possible agreement between testing conditions and theoretical assumptions.

The details of this apparatus are shown in figs. 63, 64, and 65. It consists of a base D with an annular recess in which dentated porous stones B are fitted. The bottom surface of these stones is provided with grooves which engage the ribs C. In the bottom of the recess there is a small channel which is connected with drain Q and the glass standpipe R. The center of the base is shaped like a tubular pivot that serves as a guide for inner ring F. This ring can be held in a given position by the two setscrews N. In the pivot, several small holes Y are drilled which prevent the development of an excess pressure in the water that has penetrated from test specimen A into the space between ring and pivot. The outer ring G is held in the initial position by the temporarily raised clamping ring Z and locking pins O.

The material to be tested is now placed between the rings and well molded with a segmental spatula in order to expel the inclosed air. Finally the material is leveled off at the exact height desired, whereupon the annular piston E is carefully placed. This piston is equipped with dentated porous stones, just like the base. The annular drain P is located above the stones. It is connected to four large holes that serve as water reservoirs in case the soil is subject to swelling. The torque wheel H is screwed onto the top of the piston. The vertical load is transmitted through the screw and cable I, and the torque through two very flexible steel cables with adjustable wire clamps J.

The vertical movements of the test specimen are measured by the Zeiss

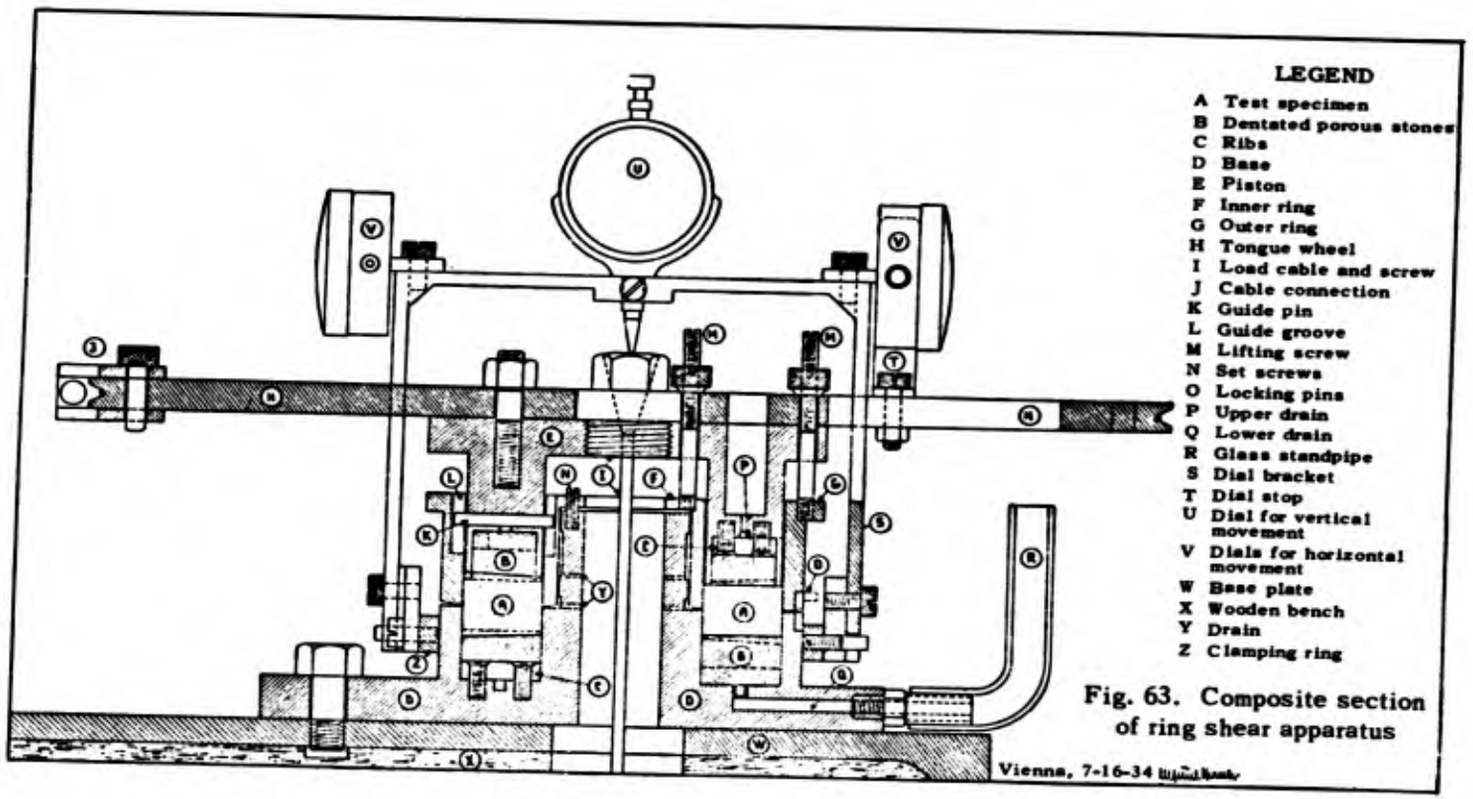

Fig. 63. Composite section of ring shear apparatus

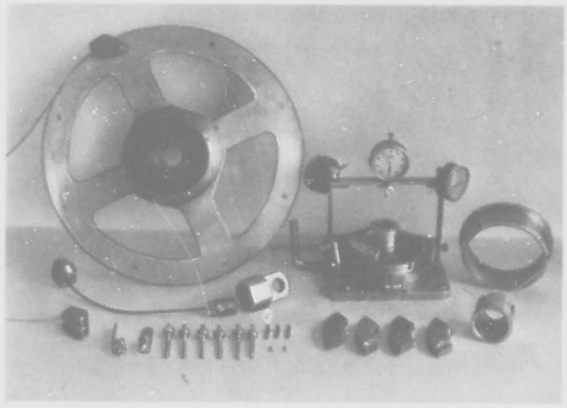

Fig. 64. Elements of the ring shear apparatus

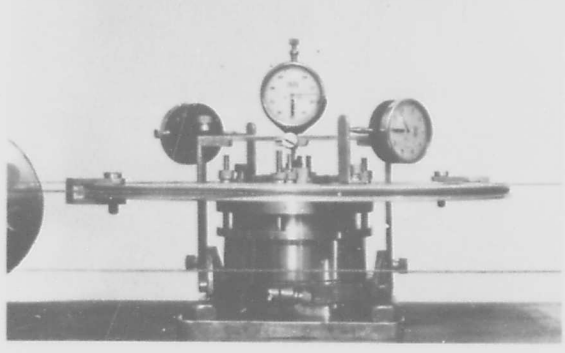

Fig. 65. Ring shear apparatus, free rings

dial U and the twists by the two dials V. The dial bracket S is attached to the adjustable clamping ring Z.

124. The shear test can be performed with the three following arrangements:

I. Fixed Rings.

The setscrews and locking pins are not released but the lift screws M are removed. The shear zone will then occur slightly below the teeth of the piston.

II. Free Rings.

The setscrews and locking pins are removed and the clamping ring is moved downward so that the rings can move freely and the shear plane is free to develop anywhere. In order to eliminate the friction between the rings and the base, the rings are raised 1 to 2 mm (depending on the soil) before the test by means of lifting screws M.

III. Restrained Rings.

Also in this case the setscrews and locking pins are removed and the rings raised. In addition, guide pins K are pushed into the piston. The projecting ends of these pins slide in grooves L of the outer and inner rings and thus do not affect the vertical movement of the test specimen. On the other hand, during shear the rings are forced to participate in the rotation of the piston, and failure must occur in the dividing plane between rings and base.

125. The complete apparatus with loading bench is shown in figs. 66 and 24. The apparatus can also be mounted, together with Casagrande's shear device, on a common testing bench. Up to a pressure of 2.0 kg/cm^2 the normal load can be applied directly, but at higher pressures it is transmitted through a lever arm. Although the flexibility of loading cable D is such that its torsional resistance can be disregarded, a turnbuckle E with ball bearing is attached to its end so that the lever arm may always be kept in a horizontal position.

Torque is produced by the two steel cables H. In order to maintain exactly the same tension in the two wires, they are carried over the same number of ball-bearing sheaves and are attached to beam M. The balanced load scale L for the shear load is suspended from the center of this beam.

Sheaves I are adjustable, so that the wires can always be kept in the plane of the torque wheel.

Calibration of the Apparatus

126. The inside diameter of the shear apparatus is $2R_1 = 5.95$ cm, the outside diameter $2R_2 = 11.95$ cm, so that $R_1/R_2 = n = 1/2$ and the cross-sectional area A is $84.25\ cm^2$. The diameter of the torque wheel between centers of cables is 39.7 cm. The flexural resistance of the wires and the friction of the sheaves amounts to $0.0134S$, in which S is the shear load placed on the scale. Hence the following value is obtained for the moment actually acting upon the test specimen:

$$M = 1/2 \cdot 39.7(1 - 0.0134)S = 19.64S \text{ kg/cm}$$

In the practical evaluation of the shear tests it is expedient to introduce the shear load S instead of the moment M into the formulas. Then for this apparatus equation (69):

$$\tau_2 - \frac{1}{8}\tau_1 = \frac{1}{22.8}\left(S + \frac{\theta}{3}\frac{dS}{d\theta}\right) \tag{79}$$

and with

$$F_1(\theta) = S + \frac{\theta}{3} \cdot \frac{dS}{d\theta} \tag{80}$$

there results

$$\tau_2 = \frac{1}{22.8}\left[F_1(\theta) + \frac{1}{8}F_1\left(\frac{\theta}{2}\right) + \frac{1}{64}F_1\left(\frac{\theta}{4}\right) + \frac{1}{512}F_1\left(\frac{\theta}{8}\right) + \ldots\right] = \frac{1}{22.8}f_1(\theta) \tag{81}$$

$$\tau_1 = \frac{1}{22.8}f_1\left(\frac{\theta}{2}\right) \tag{82}$$

and for the mean shear stress τ_a :

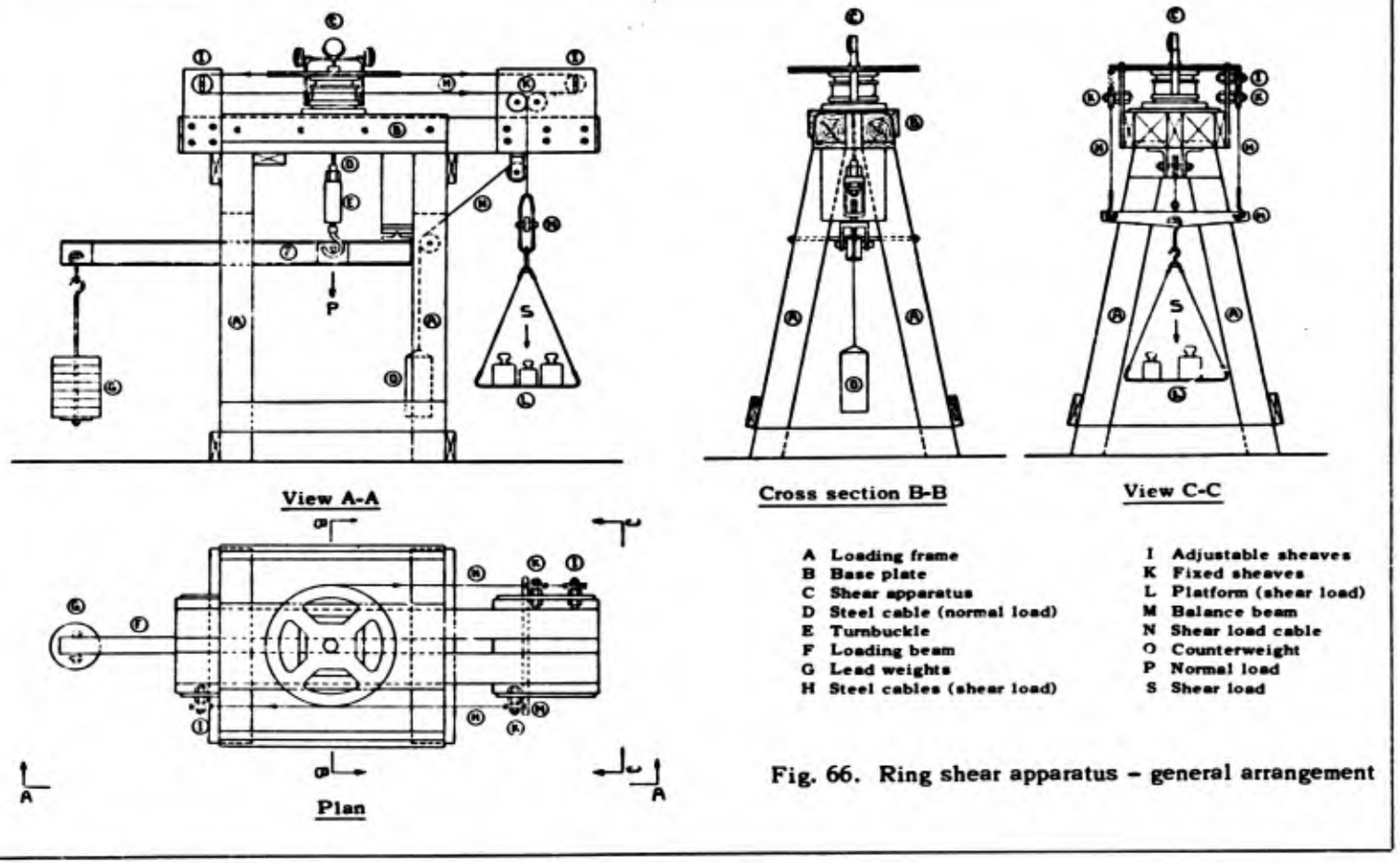

Fig. 66. Ring shear apparatus – general arrangement

$$\tau_a = \frac{S}{20} \tag{83}$$

In all equations the values of S are expressed in kilograms (kg) and those of τ_1, τ_2, and τ_a in kg/cm^2. Because of the great simplicity of equation (83), the τ_a curve can be obtained from the S curve by simply changing the scale.

127. The results of comparative tests with the three previously described testing arrangements show that arrangements II and III yield almost the same results, but a lower maximum shear stress, a smaller total twist, and larger settlements than arrangement I. The larger settlement is caused by the fact that test material is squeezed out between the raised rings. This is, to a certain extent, also the cause of the lower maximum shear stress, since part of the vertical load is transmitted through the rings to the squeezed out soil. The resulting friction between clay and bronze is less than the internal friction of clay. This friction cannot be eliminated by a repeated raising of the rings during the test, since this would lead to a disturbance of the clay structure and failure of the test specimen, even when the shear stress only amounts to two-thirds of the maximum shear strength.

The main reason that a lower maximum shear stress (failure stress) is obtained in the case of experimental arrangements II and III lies in the local concentration of the stresses at the outer edge of the test specimen between the raised rings, as shown by Filon (18) in torsion tests with conventional solid materials. This concentration of the stresses, which was not taken into account in the above formulas, causes premature failure and a subsequent decrease of the shearing resistance in a small zone at the outer face of the specimen. After general failure the shear stresses become the same over the entire plane of failure. When the rings are now raised, experimental arrangements II and III yield exactly the same values for the minimum shearing resistance as arrangement I.

128. The displacements inside the test specimen can be determined by coloring of thin, vertical strips. Figs. 67 and 68 show the results of such tests. In order to make the zones of plastic flow clearly visible, the apparatus was allowed to rotate until twice the amount of twist θ_{B_2},

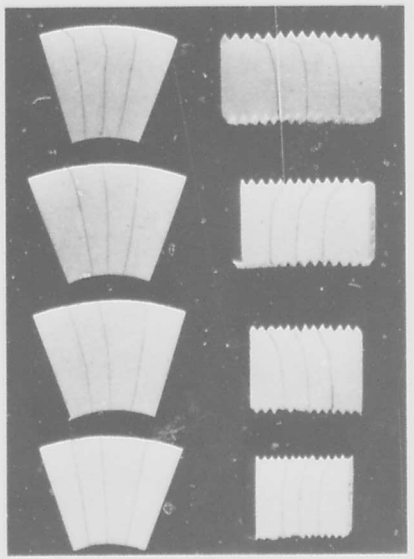

Fig. 67. Internal deformations of test specimen with fixed rings

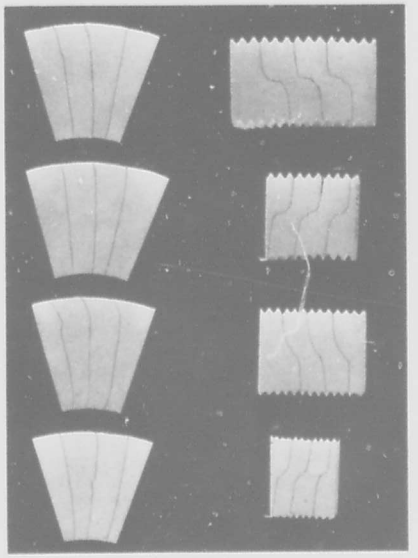

Fig. 68. Internal deformations of test specimen with free rings

fig. 62, was reached, at which failure occurred at the outer face of the ring. However, from the displacement diagrams thus obtained, a reconstruction can be made of the probable state of displacement at the moment failure occurred at the outer face.

Fig. 69 is a schematic representation of such a reconstruction. The results of similar tests with arrangement III are not shown because they practically agree with those of arrangement II. It should be noted that in the case of the fixed rings failure does not occur right at the dentated porous stones but a little lower.

The displacement diagrams clearly show the effect of lateral friction in that the originally straight radial rays become curved during the test. However, this curvature is very small at the moment of failure, particularly in arrangement I. The curvature has less influence after occurrence of failure because the shearing resistance changes but very slowly with respect to the rate of the displacement.

129. The diagrams of displacements along vertical cylindrical surfaces show that the shear strains decrease with the distance from the surface, or that equation (66) does not apply. However, as long as this equation can be replaced by

$$\gamma = \frac{\theta}{H_e} r \qquad (84)$$

in the failure zone, the above formulas and graphical procedures can also be used for the determination of the stresses in the failure zone. The relationship between H_e and H can be obtained approximately from shear tests that only differ from each other with respect to the specimen thickness. Four of such parallel tests were made with Vienna clay in a normally consolidated state $p = 2.0$ kg/cm^2 and T_s approximately equal to 1000 minutes. The principal result of these tests is shown in fig. 70. Curve A-B-C represents the displacements θ at $\tau_a = 0.875$ kg/cm^2, or approximately 92 percent of the shearing resistance. For lower values of τ_a the ratio between the twists is approximately the same as for $\tau_a = 0.875$ kg/cm^2. At higher values of τ_a the ratio changes somewhat because of the transient plastic flow. As in fig. 33B, the height

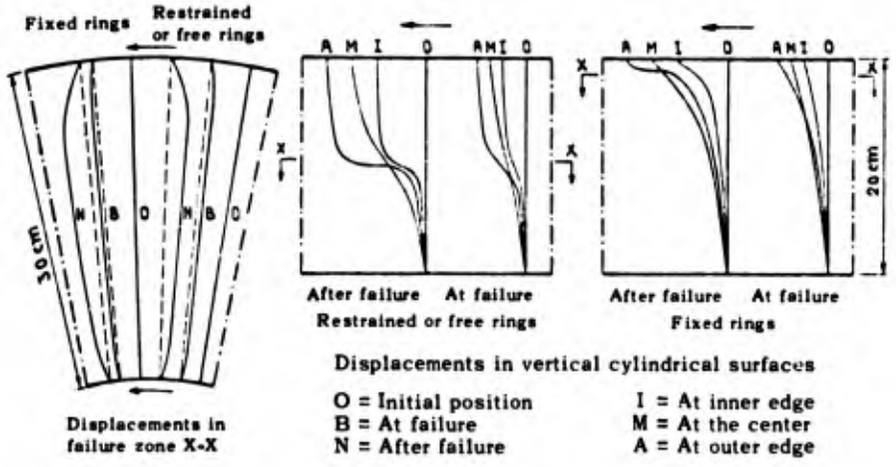

Fig. 69. Internal displacements of test specimen in ring shear apparatus

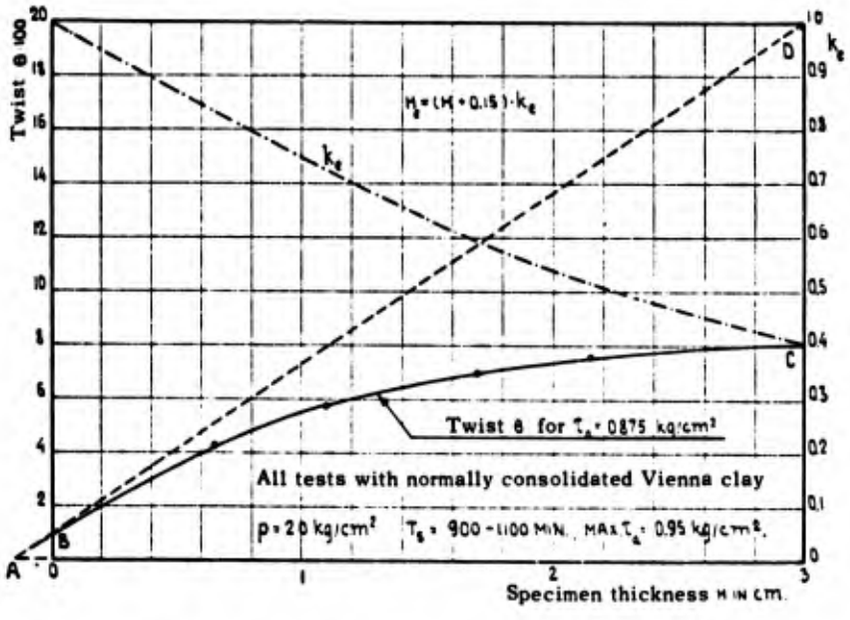

Fig. 70. Ring shear apparatus, fixed rings. Effect of specimen thickness on displacements.

O-A = 0.15 cm represents the effect of the material between the teeth of the porous stones. The active specimen thickness is then:

$$H_e = (H + 0.15) \cdot k_e \qquad (H \text{ in cm}) \tag{85}$$

in which k_e is the ratio between the ordinates of curve A-B-C and tangent A-D. Since there are not enough test results to determine the shape of the curve and the position of the tangent with certainty, the values of k_e obtained from fig. 70 must be regarded as rough approximate values only.

In the ring shear apparatus used here the clearance between piston and rings is a little too large so that some clay is forced into this clearance during the shear test, which causes slightly excessive settlements (see fig. 33A). Therefore, the effect of the specimen thickness upon the settlements could in this case not be determined with certainty.

130. In accordance with the results obtained from this investigation, testing arrangement I should, in general, be given preference. However, this arrangement has the disadvantage that the failure zone is too close to the surface. During the time required for removing the test specimen the water content in the failure zone changes somewhat because of the absorption of water. It is therefore difficult to determine the water content at the moment of failure with a sufficient degree of accuracy. Moreover, the values of the shearing resistance of highly overconsolidated soils obtained with this testing arrangement appear to be too low compared with those obtained with the Krey-Terzaghi apparatus, as will be shown later. The reason for this must probably be sought in the effect of the teeth of the porous stones. According to the results of tests with the Krey-Terzaghi apparatus, the small distance between the teeth and the shear plane does not appear to affect the magnitude of the shearing resistance in the case where the tests were made with normally consolidated or slightly overconsolidated soils. However, in the case of strongly overconsolidated soils, this small distance causes a slight decrease of the shearing resistance. For this reason the suitability of testing arrangement II should be investigated further, even though it will be difficult to take account of the aforementioned local concentration of stresses and

effect of test material squeezed out between the rings. Anyway, testing arrangement III can be discarded as being unnecessary,* which means a considerable simplification in the use of the apparatus.

Examples of the Test Evaluation and Comparison with Krey's Shear Apparatus

131. The following examples and analyses are only concerned with tests that were made with experimental arrangement I. In all these tests the load increments amounted to approximately 2 percent of the greatest shear load, while the corresponding time intervals varied from 5 minutes at the start to 30 to 60 minutes at the end of the test. The total duration of a test ranged from 10 to 14 hours, which corresponds to a value T_s = 17 to 22 hours at a uniform load increase.

Fig. 71 shows an example of the tests with Vienna clay. Because of the rapid recovery of internal strength after failure and of the thixotropic properties of the soil, the moment curve can only be determined in an approximate manner after failure, the best way being by comparing the results of a few tests that were interrupted at various values of θ. The curve for τ_2 was derived from the $f_1(\theta)$ curve and plotted on the same scale as the τ_a curve. Before the start of failure, the relationship between the two curves is accurately given by equation (78). After failure, the difference between the two curves is greater until the equalization of the stresses becomes effective. The maximum values of τ_2 and τ_a are almost the same, even though they are not attained at the same values of θ. The temporary minimum values of the stresses differ considerably, whereas the ultimate minimum values of τ_a and τ_2 are the same.

Fig. 72 shows a similar example of the evaluation of tests with normally consolidated Little Belt clay. In this soil the decrease of the shearing resistance occurs at a much slower rate, and a temporary minimum could not be observed. For this reason the minimum values of τ_a and τ_2

---

* Translator/author note: This applies only to remolded and reconsolidated soils.

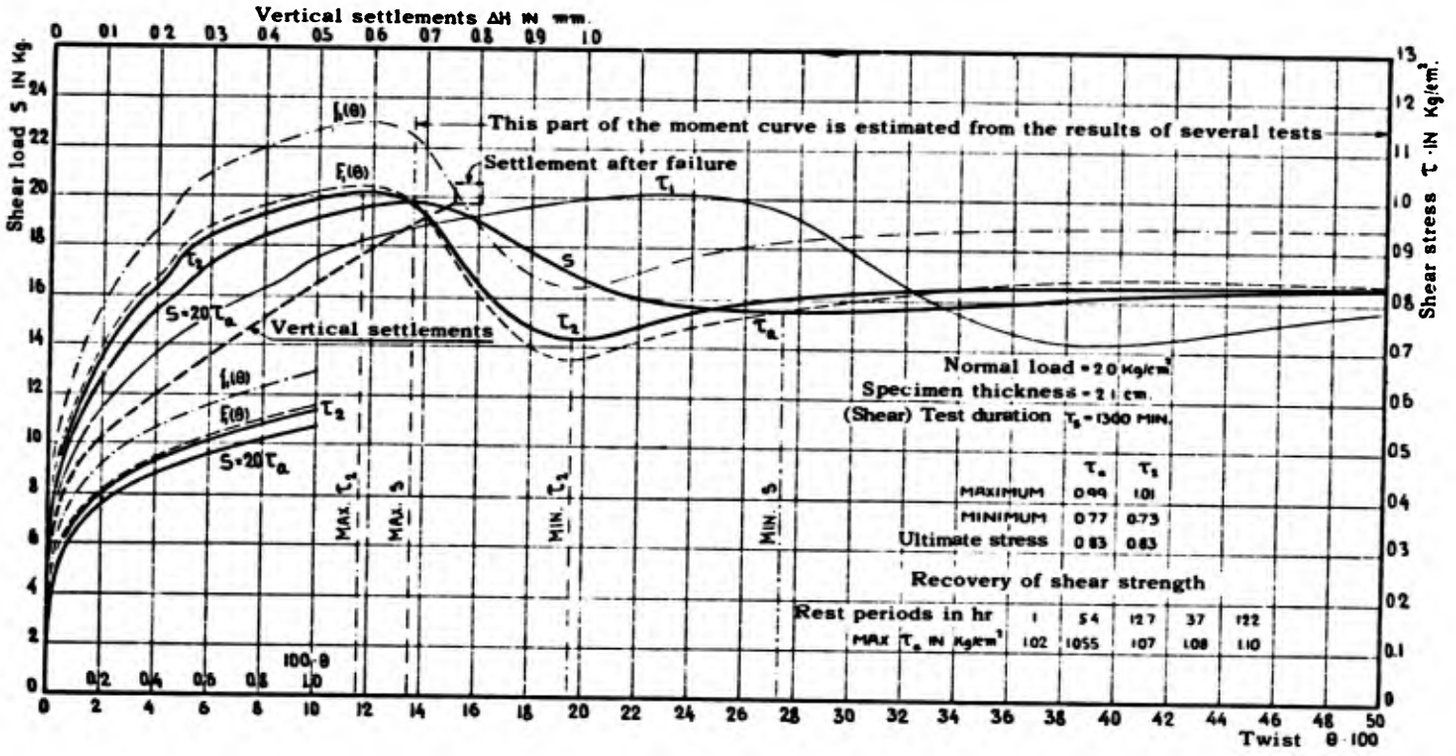

Fig. 71. Shearing Resistance of Vienna clay determined with the ring shear apparatus

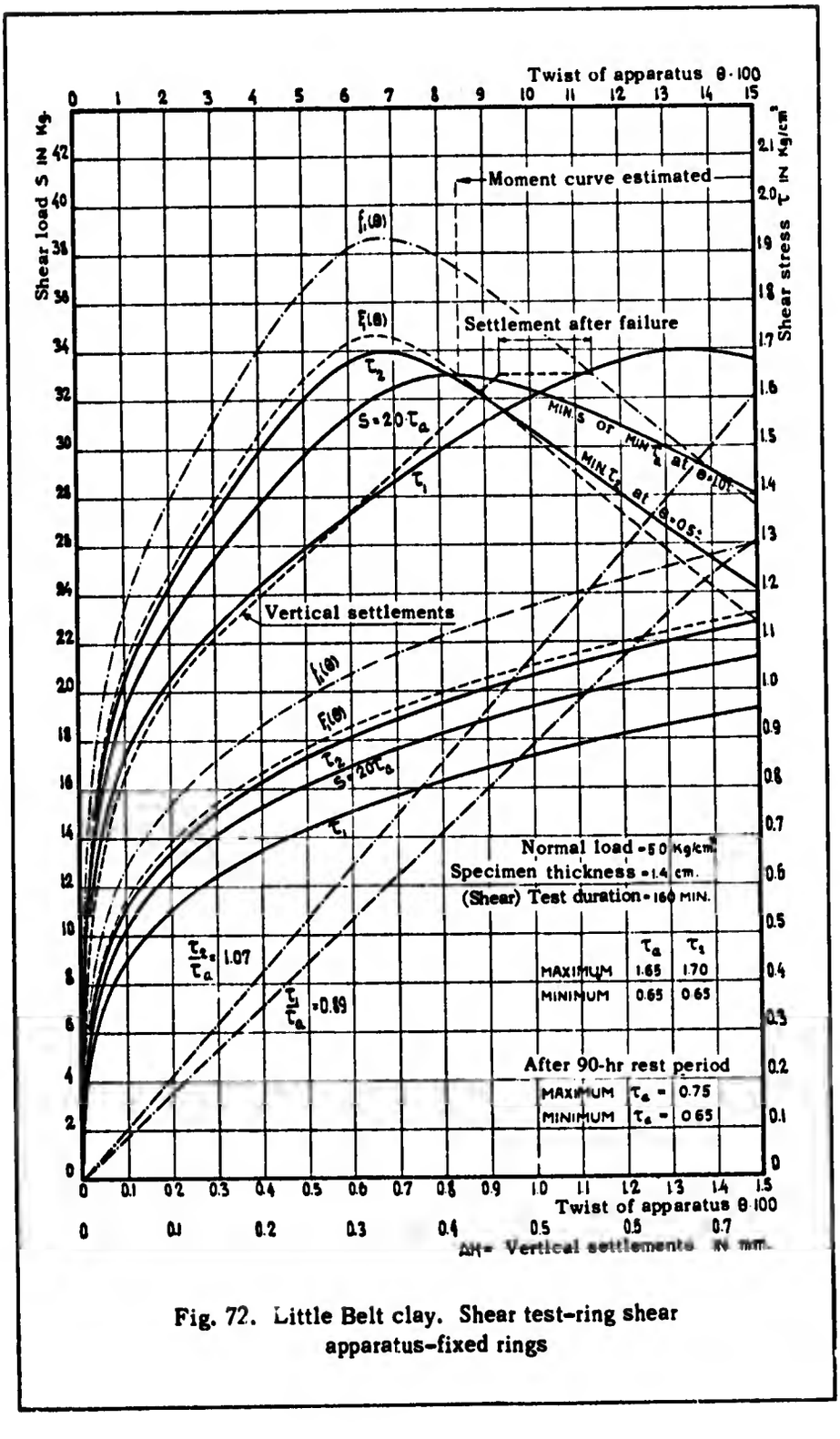

Fig. 72. Little Belt clay. Shear test-ring shear apparatus-fixed rings

are the same, but they are reached at different twists (see fig. 62). The complete displacement curve could not be plotted in fig. 72 but is shown in fig. 56C. The two dot-dash lines through the origin (fig. 72) represent the relationships between τ_a (abscissa) and τ_2 or τ_1 (ordinate). The lines are straight up to the vicinity of failure, i.e., equation (78) also applies to Little Belt clay.

132. Table 6 contains a summary of the test data and furnishes a comparison between the results of shear tests performed with the ring shear apparatus and with Krey's shear apparatus.

Table 6

Comparison of the Results Obtained with Krey's Shear Apparatus and the Ring Shear Apparatus

Ring Shear Apparatus Fixed Rings	Vienna Clay		Little Belt Clay	
	Normal Consolidation	Overconsolidation	Normal Consolidation	Overconsolidation
$k_a = \tau_2/\tau_a$ (before failure)	1.06-1.07	1.07-1.11	1.07-1.08	1.08-1.09
$k' = \max \tau_2/\max \tau_a$	1.02-1.03	1.00-1.01	1.02-1.03	1.00-1.01
$k'' = \min \tau_2/\min \tau_a$	0.92	1.00	1.00	1.00
s max s min } first test	101-105 69-75	88-90 70-74	98-100 38-40	87-90 33-37
s' max s' min } after several tests and a rest period of 4 to 5 days	109-115 80-85	93-97 70-74	45-50 38-40	37 30-40
Krey-Terzaghi apparatus				
s max s min } first test	100% 83-87	100% (80-90)	100% 70-75	100% 70-74

As a basis of comparison for the various values of the shearing resistance, the peak values of the shearing resistance obtained with Krey's shear apparatus were used and set equal to 100 percent. The notation "overconsolidation" refers to the consolidation procedure (5-1-1).

This table shows that the maximum and minimum values of τ_a are almost equal to those of τ_2, except where a temporary minimum is involved as in the case of Vienna clay. Since such a temporary minimum is primarily of theoretical importance, the much simpler determination of τ_a is sufficient in most practical cases. Before failure, τ_2 can be obtained through $\tau_2 = k_a \tau_a$ with a sufficient degree of accuracy. It must be pointed out, however, that the maximum and minimum values of τ_a and τ_2 are not attained at the same angle of twist θ.

Compared to the Krey-Terzaghi shear apparatus, the ring shear apparatus yields almost the same results for s_{max} in the case of a normal consolidation of the test specimen, but 12 percent lower values in the case of considerable overconsolidation. The probable causes of this difference have already been mentioned. Hence the maximum values of the shearing resistance obtained with Krey-Terzaghi's shear apparatus were assumed to be correct. On the other hand, the difference between the minimum values of the shearing resistance determined by means of the two types of devices may be very large. The reason is that these minimum values cannot be reached with Krey's apparatus or similar shear devices because of their limited horizontal movement. Since in addition the minimum values of the shearing resistance determined by means of the three different test arrangements of the ring shear apparatus are exactly the same, these minimum values were assumed to be correct.

As mentioned before, the settlements of the specimen surface observed in tests with the ring shear apparatus are somewhat greater than those obtained from tests with Terzaghi's shear boxes, because of the squeezing out of clay in the case of the ring shear apparatus. However, the rises of the specimen surface observed in tests with strongly overconsolidated specimens are exactly the same in both cases.

Closing Remarks

Usually, reliable final conclusions concerning the physical properties of a large group of soils cannot be drawn from tests made with only two soils of this group. However, the investigations discussed here deal

with soils which were so different in character that they represented opposite limits of real cohesive soils. It is therefore quite possible that other cohesive soils will likewise conform to the common physical laws found for these two soils. On the other hand, the probability that these laws also apply outside the void-ratio ranges investigated, i.e., to very soft or very stiff conditions of the soils, is much more remote.

Generally acceptable final conclusions could not be formulated in case of some specific problems. This must be attributed partly to the inadequacy of the tests or the varying behavior of the two types of soil and in part to the unknown variations in the pore-water pressure. The last problem causes many difficulties, particularly in the application of the test results to practical foundation problems. It is therefore a pressing task of research in this field to establish the basic laws for the changes in the pore-water pressure and void ratio caused by arbitrary changes in the general stress condition.

PHYSICAL PROPERTIES OF REMOLDED COHESIVE SOILS

SUMMARY

The commonly used conditions of failure for remolded, cohesive soils are based on the assumptions that the cohesion is either constant (Coulomb's law, $s = \mu p + c$) or proportional to the maximum preconsolidation pressure (Krey-Tiedemann's condition of failure, $s = \mu_r p + \mu_c p_m$). However, neither of these conditions of failure is in complete agreement with the results of shear and compression tests. Furthermore, until recently the slow plastic flow before failure, the decrease of the shearing resistance after failure, and the eventual thixotropic regain of the original shearing resistance have not been subjected to systematic research in the soil-mechanics laboratories. The investigations described in this paper are a contribution to the filling of these voids in our knowledge of the physical properties of cohesive soils.

In the interpretation of the results of physical tests on soils and by the practical application of these results, it must be borne in mind that the ultimate deformations and the failure of soils are governed not by the total, but by the effective stresses in the soil. The effective normal stress is defined as the difference between the total normal stress and the hydrostatic pressure in the pore water, while the effective shear stress is consequently equal to the total shear stress. Moreover, the influence of volume changes, thixotropic change , and the viscosity must be taken into consideration, as well as the stratification arising from a definite orientation of the flaky mineral soil particles during the reconsolidation process of a remolded soil (figs. 1 and 2).

In the tests to be described in this paper, the shearing resistance at failure was determined by means of the Krey shear apparatus with Terzaghi shear boxes (fig. 22). This apparatus was thoroughly investigated for the influence of the external deformations of the test specimen and of external, secondary forces caused by friction and movements of various parts of the apparatus and shear boxes. The internal displacements in the test specimen and the influence of the dentated, porous stones on the stress

distribution were studied by coloring thin, vertical sections of the test specimen and by determining the variations of the water content (figs. 26 to 30). The study of the influence of the loading procedure and the duration of the shear test is facilitated by introducing the equivalent shear time T_s (fig. 31). It was found that, while the shearing resistance of soils in a state of normal consolidation increases with T_s, the shearing resistance of soils in a state of strong overconsolidation decreases with T_s (fig. 32). The vertical and horizontal deformations are not uniformly distributed over the height of the specimen; curves and formulas for the equivalent thickness H_e of a specimen with uniform deformations are given in fig. 33.

The true form of the stress-strain curves before and after failure, the slow plastic flow before failure, and the permanent and thixotropic variations of the shearing resistance after failure were investigated by means of a new shear apparatus, wherein the specimen is brought to failure through rotation. By this means it becomes possible to extend the test at will after failure, and by choosing a circular ring as cross section of the specimen, a more uniform distribution of vertical and horizontal stresses and deformations and of the velocities of the plastic flow is obtained. The theory and construction details of this ring shear apparatus, together with a discussion of various testing arrangements and sources of error, are given in the appendix.

The tests were carried out with two entirely different clays--the silty Vienna clay and the plastic Little Belt clay. The grain-size distribution and the Atterberg limits were first of all determined (fig. 13). It was found that the liquid and shrinkage limits are influenced by the water content at the start of the test and by the testing procedure (fig. 14 and table 1). The pressure-void ratio diagrams were determined both by the Terzaghi Oedometer (figs. 15 and 16) and by the shear boxes (fig. 17), and the virgin consolidation curves were found to conform satisfactorily with the simplified Terzaghi equation (equation 11). Furthermore, the thixotropic regain of strength as a function of the length of time after remolding was investigated by determination of the Casagrande flow curves and by the Swedish cone tests (figs. 19 to 21).

From the thoroughly remolded and mixed stock material with a water content close to the liquid limit, specimens for the shear tests were reconsolidated in three different ways, so that the soil at the start of the shear test was in a state of either normal consolidation (virgin compression curve), simple overconsolidation (rebound curve), or cyclic overconsolidation (recompression curve). For a certain, final, vertical pressure specimens were thereby obtained with three different void ratios, although in each instance the hydrostatic excess pressure in the pore water is zero. During the shear tests the specimens undergo further volume changes; as first shown by A. Casagrande, the void ratio of cohesive soils in a state of normal consolidation is decreased. Conversely to this, the author found that the void ratio of cohesive soils in a state of strong overconsolidation is increased during the shear test (figs. 40 and 41). This indicates that the shear load will call forth a positive or negative excess pressure in the pore water, by Terzaghi called the hydrodynamic stress, according to the state of consolidation of the soil. In this case, however, the shear load was applied at such a slow rate that the hydrostatic excess pressures in the pore water were practically equalized at the moment of failure, and the measured stresses therefore equal to the effective stresses.

According to A. Casagrande, a cohesionless soil has a certain critical void ratio, and a material with this void ratio, when subjected to pure shear, will not undergo changes in void ratio or pore-water pressure (fig. 43). The author found that in the case of cohesive soils such a definite critical void ratio does not exist, and that any void ratio can become critical if it is produced by a critical consolidation procedure.

Examples of stress-strain curves before failure are given in figs. 35 and 36. The effect of a decrease and subsequent increase of the shear stresses is shown in fig. 37. A stiffening of the material and an increase of the shearing resistance is hereby produced. The stress-strain curve forms a perfect hysteresis loop, while the settlement curve has the shape of a zigzag line. This means that a decrease of the shear stresses can produce changes in the void ratio and pore-water pressure of the same sign, although not of the same magnitude, as those caused by an increase of the shear stresses.

In the case of Little Belt clay in a state of strong overconsolidation it was found that a continuous, slow, plastic flow starts at a shear stress, by Terzaghi called the "bond resistance," which in this case is close to one-third of the shearing resistance. It was furthermore found that in the stress interval between the bond resistance and the shearing resistance the velocity of this slow plastic flow increases more or less linearly with the increase of the shear stress (fig. 38). At stresses close to the shearing resistance a rapid plastic flow often begins; the velocity of this flow increases for some time, and then decreases to the velocity of the above-mentioned slow plastic flow. At the shearing resistance, however, the velocity of the rapid plastic flow will increase to a certain value and thereafter remain constant. It was found that over 20 hours may pass between the last load application and the actual failure (fig. 39).

To facilitate the analytical expression and graphical representation of the influence of the void ratio on the shearing resistance, the equivalent consolidation pressure p_e was introduced, defined as the pressure in the virgin pressure-void ratio diagram, which corresponds to the actual void ratio ϵ of the soil. By means of Terzaghi's simplified equation for virgin consolidation (equation 11),

$$p_e = p_1 e^{B(\epsilon_1 - \epsilon)}$$

By plotting the shearing resistance and the corresponding values of the equivalent consolidation pressure at failure, similar curves are obtained (figs. 40 and 41), which suggest the following condition of failure:

$$\frac{s}{p_e} = \mu_o \frac{p}{p_e} + \kappa$$

As will be seen in fig. 42, the points $(p/p_e, s/p_e)$ lie almost exactly in a straight line, which gives directly the values of the coefficient of effective internal friction $\mu_o = \tan \phi_o$ and the coefficient of effective cohesion κ. By means of the relation between p_e and ϵ, and by introducing the coefficient $\nu = \kappa p_1 e^{B\epsilon_1}$,

$$s = \mu_o p + \nu e^{-B\epsilon}$$

or, expressed in words, the shearing resistance is a function of the effective normal stress on and the void ratio in the plane of and at the moment of failure, and this function is independent of the stress history of the specimen.

This condition of failure takes into consideration the effect of volume changes by rebound and recompression and by the shear test, and it explains the shearing resistance hysteresis loop and the curved shearing resistance lines of Little Belt clay. The angles of effective internal friction ϕ_o are considerably smaller than the corresponding angles of internal friction ϕ_s and ϕ_r obtained by Coulomb's and Krey-Tiedemann's conditions of failure (fig. 49), but they are in almost complete agreement with the angles of internal friction $\phi = 90 - 2\alpha$, obtained by means of unconfined compression tests.

The proposed condition of failure applies only to saturated cohesive soils and is to be considered only as an approximation of the actual conditions, as the shearing resistance is dependent on several other factors than those included in the equation. The cohesion, for example, is influenced not only by the total water content, but also by the ratio between the adsorbed and free water in the soil. Therefore, the condition of failure cannot be expected to apply for states of consolidation with either a higher or a lower water content than those investigated.

In cases where the shearing resistance line of a cohesive soil in the state of normal consolidation is straight (figs. 40 and 44), the increase of cohesion, Δc, during the shear test can be expressed by

$$\Delta c = \kappa(n_c - 1)p$$

and the change in void ratio by

$$\Delta\epsilon = -\frac{\ln n_c}{B}$$

wherein $n_c = p_e/p$ is a constant for the particular soil.

By shear tests, the friction and cohesion is only determined for planes parallel to the planes of orientation of the flaky mineral soil particles. In order to investigate possible changes of the friction and cohesion with respect to the orientation of these particles, three series of unconfined compression tests were carried out. The specimens for these tests were prepared in such a manner that the angle β between the direction of the compressive force and the principal plane of orientation of the flaky mineral particles was 0°, 45°, and 90°, respectively (fig. 45).

The compressive strength is a function of the coefficient of effective internal friction and the effective cohesion in the plane of failure and of the capillary pressure. The capillary pressure p_k decreases during the test (fig. 47), but in the case of anisotropic materials this decrease, as well as the angle of inclination α between the direction of the compressive force and the plane of failure, may vary with the angle β.

The results of the tests show that for specimens of the same material in a state of normal consolidation and with the same angle β the ratio between the compressive strength q and the equivalent consolidation pressure p_e is a constant (fig. 48). The ratio q/p_e varies with the material and with the value of β (fig. 49). For the same material this variation amounts to ± 10 percent from the average value, which is obtained for $\beta = 45^{\circ}$. The angle of inclination α also varies with β, but due to differences in the behavior of the two clays used for the tests and to the indeterminable changes in the capillary pressure, it was not possible to arrive at any definite conclusions concerning the variation of the friction and the cohesion, with respect to the direction of the planes of orientation of the flaky mineral particles. For comparison of the results of shear tests and unconfined compression tests, the specimens for the latter should be prepared in such a way that the planes of stratification will as nearly as possible be parallel to the planes of failure. In this case the angle of inclination α will correspond to an angle of internal friction ($\phi = 90 - 2\alpha$), which agrees very closely with the angle of effective internal friction ϕ_o determined by the shear tests.

In the practical application of the conditions of failure we must distinguish between three cases, where the hydrostatic excess pressure in

the pore water immediately after application of the full load is negative (I), zero (II), or positive (III). In case I, the most dangerous stress condition will not be reached until the negative excess pressure in the pore water has been fully equalized, while in II and III the most dangerous stress condition obtains immediately after application of the full load. In practice, therefore, case I must be treated as case II, and according to fig. 52, it is immaterial if Coulomb's, Krey-Tiedemann's, or the above proposed condition of failure is used. On the other hand, in case III it is necessary to determine the actual value of the angle of effective internal friction and the value of the effective cohesion corresponding to the actual void ratio. Furthermore, in order that the effective stresses may be computed, means to determine the value of the excess pressure in the pore water must be available.

Our knowledge of the physical properties of cohesive soils is still so limited that in most cases it is very difficult to determine the hydrostatic excess pressure in the pore water with satisfactory accuracy. To avoid this difficulty, it has been the practice to determine the shearing resistance by means of rapid shear tests. In this way, changes in the void ratio are avoided and the influence of changes of the hydrostatic pressure in the pore water will be directly included in the test results. The question now arises as to whether the results of such tests may be directly and safely used for the design of such structures, which will be fully erected before the void ratio of the soil in the foundation has undergone a material change.

A comparison of the results of slow and rapid shear tests (figs. 53 and 54) shows that, in the case of rapid shear tests, the viscosity of the soil will cause an apparent increase of the shearing resistance. The actual value of this increase (10 to 20 percent) is difficult to determine, but it is so large that it cannot safely be neglected. Furthermore, with clays in a state of strong overconsolidation, the rapid shear test will call forth a negative, hydrostatic excess pressure in the pore water and thereby a very appreciable increase of the shearing resistance. Neither the increase due to viscosity nor the increase due to the negative excess pressure can be relied upon in the design of the actual foundation

structures. These facts are a warning against the indiscriminate use of the results of rapid shear tests.

A reliable and practical method for the determination of the hydrostatic excess pressure in the pore water is to be preferred to rapid shear tests. Direct measurements of these excess pressures have been made by various investigators, but the methods used need improvement, the difficulty being that no quantity of water must be carried to, or away from, the place of measurement. In this paper an indirect method is outlined whereby the excess pressure in the pore water can be determined by means of time-settlement curves, observed during slow shear tests. However, by whatever means the influence of the hydrostatic excess pressure in the pore water is determined, it must be borne in mind that the stress conditions, and thereby the excess pressures in the pore water in the actual foundation, may be entirely different from those existing in the shear boxes.

In such practical cases, wherein a progressive failure of the soil takes place, it is essential to know the laws governing the decrease of the shearing resistance after failure. The tests with the ring shear apparatus show that this decrease depends mostly on the total displacement of, and to a lesser degree on the velocity of the rapid plastic flow after failure. Examples of stress-strain curves before and after failure are shown in fig. 56, and in fig. 57 are plotted the shearing resistance lines, which correspond to the minimum values of the shearing resistance. For Vienna clay these minimum values vary between 70 and 75 percent of the maximum values. In the case of specimens in a state of normal consolidation, however, an additional decrease of the void ratio takes place after failure, and the minimum value of the shearing resistance is ultimately increased to 80-85 percent of the original, maximum value of the shearing resistance. The coefficient of effective internal friction is not changed by failure, but the coefficient of effective cohesion is decreased by 55 percent (fig. 58). For Little Belt clay the minimum values of the shearing resistance are only reached after very large displacements, and they vary between 30 and 40 percent of the maximum values. In this case the coefficient of effective internal friction is decreased by 49 percent and the coefficient of effective cohesion by 79 percent. If the shear load is decreased until

the plastic flow stops, the shearing resistance of Vienna clay will be rapidly regained and may ultimately even exceed its original maximum value (fig. 59), while this recovery in the case of Little Belt clay is very slow and probably also incomplete.

The conclusions drawn from the results of these investigations are in some cases to be regarded only as tentative, as the number of tests is insufficient for final conclusions. In other cases no conclusions can be drawn; this is due partly to a difference in behavior of the two soils and partly to unknown changes of the hydrostatic pressure in the pore water. Difficulties from the last-mentioned source will be encountered to an even larger degree by the application of the test results to practical problems. There is, therefore, an urgent need for research with the object of establishing the fundamental laws governing the initial change of the hydrostatic pressure in the pore water and the ultimate change of the void ratio, which will occur when a soil, acted upon by an arbitrary system of stresses, is subjected to an arbitrary change of these stresses.

NOTATION

The meaning of the various symbols used in this paper is explained in the following table. The terminology of soil mechanics has not yet been fully standardized and there exist, therefore, certain differences in the names given to the various stresses and coefficients. Whenever possible, firmly established names have been used, but as a whole, the table only represents the terminology and notation used in this paper. In the discussion of the hydrostatic excess pressure in the pore water caused by shear tests (Chapter XI-4), the symbols have another meaning than that given in the table. To facilitate the comparison of the formulas and the use of tables, the notation in Terzaghi-Fröhlich: "Theorie der Setzung von Tonschichten" was adopted.

NOTATION

Symbol	Dimension	Definition
A	cm^2	Area
A	0	Coefficient of swelling
B	0	Coefficient of virgin consolidation
c	kg/cm^2	Cohesion
$c_{(index)}$	0	Various coefficients
e	0	Basis of natural (napierian) logarithms
e	0	Vertical strain (simple compression)
H	cm	Thickness of test specimen
ΔH	cm	Change in thickness of specimen (settlement or swelling)
H_e	cm	Effective thickness of test specimen
h	cm	Height of specimen over plane of failure
h	cm	Pressure head
h	cm	Depth below water surface
Δh	cm	Change in pressure head
h_o	cm	Reduced thickness of test specimen (solid phase)
i	0	Hydraulic gradient
K	g	Consistency factor (Swedish "Hallfasthetstall")
K'	$1/cm^2$	Relative consistency factor ($K' = 1/t^2$)
$k_{(index)}$	0	Various coefficients
k_e	0	Coefficient of effective thickness of test specimen
k_o	cm/min	Reduced coefficient of permeability (referred to h_o)
L, ℓ	cm	Length
ΔL	cm	Horizontal displacement of test specimen
ln	0	Natural (napierian) logarithms
M	kgcm	Moment
m	0	Poisson's ratio
m	0	Exponent (stress strain curves for shear)
n	0	Porosity $\left(n = \frac{\epsilon}{1 + \epsilon}\right)$
n	0	Ratio R_1/R_2

Symbol	Dimension	Definition
n_c	0	Degree of overconsolidation ($n_c = p_e/p$)
P	kg	Vertical normal load (shearing tests)
p	kg/cm^2	Effective consolidation pressure
p	kg/cm^2	Effective normal pressure in shear tests
p_0	kg/cm^2	Zero pressure (consolidation tests)
p_1	kg/cm^2	Unit of pressure ($p_1 = 1$) (consolidation tests)
p_e	kg/cm^2	Equivalent consolidation pressure
p_h	kg/cm^2	Hydrostatic pressure in pore water
p_k	kg/cm^2	Capillary pressure
p'_k	kg/cm^2	Reduced capillary pressure (simple compression test)
p_m	kg/cm^2	Maximum preconsolidation pressure
p_n	kg/cm^2	Natural hydrostatic pressure in pore water ($p_n = h \cdot \gamma_w$)
p_s	kg/cm^2	Earth pressure at rest
p_s	kg/cm^2	Flow pressure
p_u	kg/cm^2	Hydrostatic excess pressure in the pore water
Q	kg	Compressive force (simple compression)
Q	kg	Weight of cone (Swedish cone tests)
q	kg/cm^2	Compressive strength
q	kg/cm^2	Equivalent surface pressure (Swedish cone tests)
R_1, R_2	cm	Internal and external radius (ring shear apparatus)
r	cm	Radius
S	kg	Shear load
ΔS	kg	Load increment (shear tests)
S_r	kg	Frictional force (caused by the lateral pressure p_s)
s	kg/cm^2	Shearing resistance (shear strength)
s_r	kg/cm^2	Frictional stress (caused by the lateral pressure p_s)
T	min-h	Time (rest period after remolding)
T	min	Actual duration of shear test
ΔT	min	The time interval between load applications
T_s	min	Equivalent duration of shear test (see fig. 31)

Symbol	Dimension	Definition
t	cm	Cone penetration
v	cm/sec	Velocity
v_a	cm/sec	Average or rate of displacement due to shear
v_γ	1/h	Velocity of increase in shear strain (see γ)
v_θ	1/h	Velocity of twist (see θ)
w	0	Moisture content (water content) (in percentage of dry weight)
w_a	0	Plastic limit
w_f	0	Liquid limit
w_n	0	Normal moisture content (Swedish "Finlekstal")
w_p	0	Plasticity index
w_s	0	Shrinkage limit
α	0	Angle between the first principal stress and the plane of failure
β	0	Angle between the first principal stress and the plane of stratification
β	0	Coefficient (stress-strain curves for shear)
γ	0	Shear strain (angular displacement by shear)
γ	g/cm^3	Specific gravity (unit weight)
γ_f	g/cm^3	Average unit weight of solid phase
γ_r	g/cm^3	Total unit weight of soil (including water)
γ_s	g/cm^3	Apparent unit weight of earth in water
γ_w	g/cm^3	Unit weight of water ($\gamma_w = 1$) (metric system)
ϵ	0	Void ratio
ϵ_1	0	Void ratio for $p + p_o = p_1$ (consolidation test)
ζ	0	Coefficient of earth pressure at rest ($\zeta = p_s/p$)
η	$g \cdot sec/cm^2$	Coefficient of viscosity
θ	0	Angle of twist (ring shear apparatus)
κ	0	Coefficient of effective cohesion
μ	0	Coefficient of internal friction
μ_o	0	Coefficient of effective internal friction
μ_c	0	Krey-Tiedemann's coefficient of cohesion
μ_r	0	Krey-Tiedemann's coefficient of internal friction

Symbol	Dimension	Definition
μ_s	0	Coefficient of apparent internal friction
ν	kg/cm^2	Specific coefficient of effective cohesion
σ	kg/cm^2	Total normal stress
σ_z	kg/cm^2	Total perpendicular stress
σ_1, σ_2, σ_3	kg/cm^2	Principal stresses
σ'	kg/cm^2	Effective normal stress ($\sigma' = \sigma - p_h$)
σ''	kg/cm^2	Total normal stress computed by use of γ_s
$\tau = \tau' = \tau''$	kg/cm^2	Shear stresses
τ_1, τ_2	kg/cm^2	Shear stress at intrados and extrados of ring
ϕ	0	Angle of internal friction (index as by μ)

BIBLIOGRAPHY

In this bibliography, the "Proceedings of the International Conference on Soil Mechanics and Foundation Engineering, June 22 to 26, 1936, Harvard University, Cambridge, Mass." are designated as follows: Proc. Int. Conf. Soil Mech. and Found. Eng., 1936.

(1) Alenius, Per. "Byggnadsteknisk undersökning av en lerjord fra Halikko" (Geotechnical Investigation of a Clay from Halikko). Tekniska Foreningens i Finland Forhandlingar, 1936, No. 12.

(2) Atterberg, Alb. "Die Plastizität und Bindigkeit liefernde Bestandteile der Tone" (The Plasticity and Cohesion Producing Components of Clays). Int. Mitt. f. Bodenkunde, Vol. III, 1913.

(3) Bernatzik, W. "Versuche über Festigkeitseigenschaften von Sand im dreiachsigen Spannungszustand" (Tests Concerning Physical Properties of Sand in a Triaxial Stress Condition). Die Wasserwirtschaft, 1935, Nos. 16, 17.

(4) Biemond, C. "Direct Measuring of Internal Water Pressures in Clay." Proc. Int. Conf. Soil Mech. and Found. Eng., 1936, Vol. I.

(5) Brandtzaeg, A. "Failure of a Material Composed of Isotropic Elements." Det kgl. Norske Videnskabers Selskabs Skrifter, 1927, No. 2.

(6) Brenner, Thor. "Mineraljordarternes Fysikaliska Egenskaper" (Physical Properties of Mineral Soils). Helsingfors, 1931.

(7) Bretting, A. E. "Soil Studies for the Storström Bridge, Denmark." Proc. Int. Conf. Soil Mech. and Found. Eng., 1936, Vol. I.

(8) Broekman and Buisman. "Determination of Ground-Water Tensions." Proc. Int. Conf. Soil Mech. and Found. Eng., 1936, Vol. I.

(9) Buisman, Keverling. "De Weerstand van paalpunten in zand" (Point Resistance of Piles in Sand). De Ingenieur, 1935, Nos. 14, 18.

(10) Casagrande, A. "Research on Atterberg Limits of Soils." Public Roads, Dec. 1929.

(11) Casagrande, A. "The Structure of Clay and Its Importance in Foundation Engineering." Journal Boston Society of Civil Engineers, Vol. 19, 1932.

(12) Casagrande, A. "Die Aräometermethode zur Bestimmung der Kornverteilung" (The Hydrometer Method for Determining the Grain Distribution). Jul. Springer, Berlin, 1934.

(13) Casagrande, A. "Characteristics of Cohesionless Soils Affecting the Stability of Slopes." Journal Boston Society of Civil Engineers, Jan. 1936.

(14) Casagrande and Albert. "Research on the Shearing Resistance of Soils." Massachusetts Institute of Technology, 1930. Report not published.

(15) Committee on Earths and Foundations. American Society of Civil Engineers. Papers and Discussions, Jan. 1917.

(16) Cooling and Smith. "The Shearing Resistance of Soils." Proc. Int. Conf. Soil Mech. Found. Eng., 1936, Vol. I.

(17) Endell and Hoffman. "The Chemical Nature of Clays." Proc. Int. Conf. Soil Mech. Found. Eng., 1936, Vol. I.

(18) Filon, L. N. G. "On the Elastic Equilibrium of Circular Cylinders Under Certain Practical Systems of Load." Philosophic Transactions of the Royal Society of London, May 1902.

(19) Freundlich, H. "Kapillarchemie" (Capillary Chemistry). Vol. II. Akademische Verlagsgesellschaft, Leipzig, 1932.

(20) Freundlich, H. "The Colloidal State - I - Thixotropy." Herman & Cie, Paris, 1935.

(21) Fröhlich, O. K. "Druckverteilung im Baugrunde" (Pressure Distribution in Foundation Soils). Julius Springer, Vienna, 1934.

(22) Gilboy, Glennon. "Soil Mechanics Research." Transactions, Am. Soc. Civ. Eng., Vol. 98, 1933.

(23) Goldschmidt, V. M. "Undersökelser over lersidimenter" (Investigations of Sedimentary Clays). Nordisk Jordbrugforskning, No. 1, Oslo, 1926.

(24) Gruner and Haefeli. "Untersuchungsmethoden um festzustellen, ob sich ein gegebenes Baumaterial für den Bau eines Erddammes eignet" (Methods of Investigation for Determining Whether a Given Building Material Is Suitable for the Construction of an Earth Dam). First Congress on Large Dams, Stockholm, 1933.

(25) Gruner and Haefeli. "Beitrag zur Untersuchung des physikalischen und statischen Verhaltens Rohärenter Böden" (Contribution to the Investigation of the Physical and Static Behavior of Cohesive Soils). Schweizer. Bauzeitung, April 1934.

(26) Jürgenson, Leo. "The Shearing Resistance of Soils." Journal Boston Society of Civil Engineers, July 1934.

(27) Kjellman, Walter. "Om undersökning av jordarters deformationsegenskaper" (Investigation of Deformation Characteristics of Soils). Teknisk Tidskrift, Aug. 1936.

(28) Krey, H. D. "Rutschgefährliche und fliessende Bodenarten" (Soils with a Tendency to Slide and Flow). Die Bautechnik, 1927, Vol. 5, pp. 279-283.

(29) Krey and Ehrenberg. "Erddruck, Erdwiderstand und Tragfähigkeit des Baugrundes" (Earth Pressure, Passive Earth Pressure, and Bearing Capacity of Foundation Soils). Wilhelm Ernst & Son, Berlin, 1932.

(30) Langer, Karl. "The Influence of the Speed of the Loading Increment on the Pressure-Voids-Ratio Diagram of Undisturbed Soil Samples." Proc. Int. Conf. Soil Mech. Found. Eng., 1936, Vol. II.

(31) Mertz, Ellen Louise. "Lillebältsler og London Clay" (Little Belt Clay and London Clay). Danmarks Geologiske Undersøgelse, Series II, No. 51, Copenhagen, 1928.

(32) Mises, R. von. "Mechanik der plastischen Formänderungen von Kristallen" (Mechanics of the Plastic Deformations of Crystals). Zeitschrift für angew. Math. u. Mech., 1928, No. 3.

(33) Nadai, A. "Plasticity." McGraw-Hill Co., New York, 1931.

(34) Prandtl, L. "Über die Eindringungsfestigkeit plastischer Baustoffe und die Festigkeit der Schneiden" (Penetration Strength of Plastic Building Materials and Strength of Wedges). Zeitschr. f. angew. Mat. u. Mech., Feb. 1927.

(35) Redlich, Terzaghi, and Kampe. "Ingenieurgeologie" (Engineering Geology). Julius Springer, Vienna and Berlin, 1929.

(36) Rendulic, Leo. "Porenziffer und Porenwasserdruck" (Void Ratio and Pore Water Pressure). Der Bauingenieur, 1936, Nos. 51, 52.

(37) Rendulic, Leo. "Ein Grundgesetz der Tonmechanik und sein experimenteller Beweis" (A Basic Law of Clay Mechanics and Its Experimental Proof). Der Bauingenieur, 1937, Vol. 18, pp. 459-467.

(38) Rendulic, Leo. "Relation Between Voids Ratio and Effective Principal Stresses for a Remolded Silty Clay." Proc. Int. Conf. Soil Mech. Found. Eng., 1936, Vol. III.

(39) Samsioë, A. Frey. "Über die Beziehung zwischen Deformation und Spannung" (The Relationship Between Deformation and Stress). Ph. D. Dissertation, Stockholm, 1935.

(40) Samsioë, A. Frey. "Report on the Investigation of the Compressibility of the Ground at the Hydroelectric Power Plant at Svir 3." Proc. Int. Conf. Soil Mech. Found. Eng., 1936, Vol. I.

(41) Seifert, R. "Untersuchungsmethoden um festzustellen, ob sich ein gegebenes Baumaterial für den Bau eines Erddammes eignet" (Methods of Investigation for Determining Whether a Given Building Material Is Suitable for the Construction of an Earth Dam). First Congress on Large Dams, Stockholm, 1933.

(42) Seifert, Ehrenberg, Tiedemann, Endell, Hoffmann, Wilm. "Bestehen Zusammenhänge zwischen Rutschneigung und Chemie von Tonböden?" (Is There Any Connection Between the Tendency of Sliding and the Chemistry of Clayey Soils?). Communications of the Preuss. Versuchsanstalt für Wasserbau und Schiffbau, No. 20, Berlin, 1935.

(43) Statens Järnvägers geotekniske Kommission: "Sluttbetänkende" (Geotechnical Commission of the State Railways: Final Report). Stockholm, 1922.

(44) Streck, O. "Fortschritte auf dem Gebiet der Baugrundforschung" (Progress Made in the Field of Foundation Soil Research). Zentralblatt der Bauverwaltung, 1928, No. 9.

(45) Terzaghi, K. von. "Erdbaumechanik auf bodenphysikalischer Grundlage" (Soil Mechanics Based on Physical Properties of Soils). Franz Deuticke, Vienna, 1925.

(46) Terzaghi, K. von. "Determination of the Consistency of Soils by Means of Penetration Tests." Public Roads, Feb. 1927.

(47) Terzaghi, K. von. "The Mechanics of Shear Failures on Clay Slopes and the Creep on Retaining Walls." Public Roads, Dec. 1929.

(48) Terzaghi, K. von. "The Science of Foundations." Proc. Am. Soc. Civ. Eng., 1927, and Trans. Vol. 93, 1929.

(49) Terzaghi, K. von. "The Static Rigidity of Plastic Clays." Journal of Rheology, 1931.

(50) Terzaghi, K. von. "Festigkeitseigenschaften der Sedimente, Schüttungen und Gele" (Physical Properties of Sediments, Fills, and Gels). In Auerbach and Hort's "Handbuch der physikalischen und technischen Mechanik," Vol. 4, Barth, Leipzig, 1931.

(51) Terzaghi, K. von. "Die Oedometerbeobachtung als Hilfsmittel zur Erforschung der Gelstruktur" (Consolidometer Observations as Aid in the Investigation of the Gel Structure). Kolloid Zeitschrift, Vol. 65, No. 2, 1933.

(52) Terzaghi, Ruth von. "Thixotropic Properties of Clays." Not published.

(53) Terzaghi and Fröhlich. "Theorie der Setzung von Tonschichten" (Theory of the Settlement of Clay Layers). Franz Deuticke, Vienna, 1936.

(54) Winterkorn, H. F. "The Chemical Nature of Clays." Discussion. Proc. Int. Conf. Soil Mech. Found. Eng., 1936, Vol III.